

EXTENDED RELATIVISTIC CONFIGURATION INTERACTION AND MANY-BODY PERTURBATION CALCULATIONS OF SPECTROSCOPIC DATA FOR THE $N \leq 6$ CONFIGURATIONS IN NE-LIKE IONS BETWEEN CR XV AND KR XXVII

K. WANG^{1,2,3}, Z.B. CHEN⁴, R. SI³, P. JÖNSSON⁵, J. EKMAN⁵, X.L. GUO^{6,3}, S. LI², F.Y. LONG², W. DANG¹, X.H. ZHAO¹, R. HUTTON³, C.Y. CHEN³, J. YAN^{2,7,8}, AND X. YANG⁹

¹Hebei Key Lab of Optic-electronic Information and Materials, The College of Physics Science and Technology, Hebei University, Baoding 071002, China

²Institute of Applied Physics and Computational Mathematics, Beijing 100088, China

³Shanghai EBIT Lab, Institute of Modern Physics, Department of Nuclear Science and Technology, Fudan University, Shanghai 200433, China

⁴College of Science, National University of Defense Technology, Changsha 410073, China

⁵Group for Materials Science and Applied Mathematics, Malmö University, SE-20506, Malmö, Sweden

⁶Department of Radiotherapy, Shanghai Changha Hospital, Second Military Medical University, Shanghai 200433, China

⁷Center for Applied Physics and Technology, Peking University, Beijing 100871, China

⁸Collaborative Innovation Center of IFSA (CICIFSA), Shanghai Jiao Tong University, Shanghai 200240, China

⁹The Third Institute of Surveying and Mapping of Hebei Province, Hebei Bureau of Geoinformation, Shijiazhuang 050000, China

ABSTRACT

Level energies, wavelengths, electric dipole, magnetic dipole, electric quadrupole, and magnetic quadrupole transition rates, oscillator strengths, and line strengths from combined relativistic configuration interaction and many-body perturbation calculations are reported for the 201 fine-structure states of the $2s^22p^6$, $2s^22p^53l$, $2s2p^63l$, $2s^22p^54l$, $2s2p^64l$, $2s^22p^55l$, and $2s^22p^56l$ configurations in all Ne-like ions between Cr XV and Kr XXVII. Calculated level energies and transition data are compared with experiments from the NIST and CHIANTI databases, and other recent benchmark calculations. The mean energy difference with the NIST experiments is only 0.05%. The present calculations significantly increase the amount of accurate spectroscopic data for the $n > 3$ states in a number of Ne-like ions of astrophysics interest. A complete dataset should be helpful in analyzing new observations from the solar and other astrophysical sources, and is also likely to be useful for modeling and diagnosing a variety of plasmas including astronomical and fusion plasma.

Keywords: atomic data - atomic processes

1. INTRODUCTION

The rapid advance of astronomical observations requires more extensive accurate spectroscopic data. This paper is a continuation of our recent work of providing the data of energy levels and transition characteristics for L-shell ions to the accuracy needed to exploit the high quality of observations from space- and ground-based telescopes. Systematic calculations for the beryllium, carbon and nitrogen isoelectronic sequences have already been performed (Wang et al. 2014, 2015, 2016). In this paper, we report accurate data for the neon isoelectronic sequence between Cr XV and Kr XXVII.

In view of a stable closed L-shell ground state, Ne-like ions show high abundance over a wide range of

temperatures in ionization equilibrium (Mazzotta et al. 1998; Bryans et al. 2006, 2009; Liang & Badnell 2010). A wealth of emission lines in a wide wavelength range are frequently observed in astrophysics (Feldman et al. 2000; Behar et al. 2001; Mewe et al. 2001; Kaastra et al. 2002; Ko et al. 2002; Raassen et al. 2002; Ness et al. 2003; Curdt et al. 2004; Holczer et al. 2005; Landi & Phillips 2005; Brown et al. 2008; Del Zanna 2008; Shestov et al. 2008; Warren et al. 2008; Raassen & Pollock 2013; Del Zanna & Mason 2014; Shestov et al. 2014). These observations constitute an important tool for obtaining useful information of the physical conditions, chemical abundances, and evolution of the astrophysical objects. For example, in high-resolution observations with the *Chandra* and *XMM-Newton* X-ray observatories, the Fe XVII spectrum dominated the X-ray emission in the 700-1000 eV range of a large number of as-

trophysical objects. Thus these spectral lines were used for diagnostics (Paerels & Kahn 2003; Del Zanna 2011). The Fe XVII EUV lines were measured by the *Hinode* Imaging Spectrometer and provided useful information about the nature of the heating in the solar corona (Culhane et al. 2007; Del Zanna & Ishikawa 2009). The Ni XIX lines have been identified in the spectra of solar flares (Phillips et al. 1982; Landi & Phillips 2005), the Capella (Behar et al. 2001), and the supergiant star (Raassen & Pollock 2013), and offer an opportunity for determining elemental abundances and physical conditions of astrophysical objects.

Using various methods a number of calculations have been carried out to provide datasets of energy structures and transition rates for the Ne-like sequence (Cogordan et al. 1985; Quinet et al. 1991; Hibbert et al. 1993; Dong et al. 2003; Dong et al. 2003; Froese Fischer & Tachiev 2004; Gu 2005b; Ishikawa et al. 2009; Del Zanna & Ishikawa 2009; Jönsson et al. 2014). However, in these studies the calculations were restricted to the $n \leq 3$ states (the 37 fine-structure states of the $(1s^2)2s^22p^6$, $2s^22p^53l$, and $2s2p^63l$ configurations).

Atomic data involving higher-lying states of the $n > 3$ configurations are also urgently demanded because of their wide applications for line identifications and plasma diagnostics in solar physics and astrophysics (Phillips et al. 1982; Acton et al. 1985; Del Zanna 2008; Del Zanna & Ishikawa 2009; Raassen & Pollock 2013; Del Zanna & Mason 2014). Calculations were performed for the $n > 3$ states in Fe XVII using various methods, including the calculations of Chen et al. (2003) and Nahar et al. (2003) using the configuration interaction (CI) method of the code SUPERSTRUCTURE (Eissner et al. 1974), and the calculation by Aggarwal et al. (2004) utilizing the GRASP code of Dyall et al. (1989). Relativistic perturbation theory with a model potential was used to calculate transitions probabilities of the lowest 72 excited energy to the ground state for ions up to $Z = 66$ (Ivanova & Gulov 1991). Using mixed CI and perturbation theory, energies and oscillator strengths for the seven lowest $J = 1$ odd excited states of neon-like ions with $Z = 11 - 18$ were calculated by Savukov (2003). Relativistic combined configuration interaction (RCI) and many-body perturbation theory (MBPT) calculations were carried out for wavelengths of $n \rightarrow 2$ ($3 \leq n \leq 7$) transitions in Fe XVII and Ni XIX (Gu 2007). Liang & Badnell (2010) reported the results for the energy levels, and transition data among the 209 states of the $2s^22p^6$, $(2s, 2p)^7nl$ ($n \leq 5$ and $l \leq n - 1$), and $2s^22p^5n'l'$ ($6 \leq n' \leq 7$ and $l' \leq 2$) configurations in Ne-like ions from Na II to Kr XXVII using the AUTOSTRUCTURE code (Badnell 1986). Among the above $n > 3$ calculations, the MBPT

results of Gu (2007) in Fe XVII and Ni XIX are sufficiently accurate to identify observed spectra. In this work, however, transition properties were not computed. The other mentioned calculations are not adequate to meet the accuracy requirements of line identification and interpretation in astrophysics.

The present work aims at extending the accurate calculations for Fe XVII and Ni XIX by Gu (2007), providing the energy data of spectroscopic accuracy and transition rates for the $n \leq 6$ states in a number of Ne-like ions of astrophysics interest. By using a combined RCI and MBPT approach in the FAC code (Gu 2003, 2005a,b; Gu et al. 2006), we present data for the lowest 201 bound energy states arising from the $2s^22p^6$, $(2s, 2p)^7nl$ ($3 \leq n \leq 4$ and $l \leq n - 1$), and $2s^22p^5n'l'$ ($5 \leq n' \leq 6$ and $l' \leq n' - 1$) configurations in Ne-like ions from Cr XV to Kr XXVII, as well as the electric-dipole (E1), electric-quadrupole (E2), magnetic-dipole (M1), and magnetic-quadrupole (M2) transition rates among these states. To assess the accuracy of the MBPT data, the multiconfiguration Dirac-Hartree-Fock (MCDHF) and RCI method has been used to calculate the data for Fe XVII (hereafter referred to as MCDHF/RCI). The MBPT energies in Fe XVII agree well with the MCDHF/RCI values, as well as the experimental energies from the Atomic Spectra Database (ASD) of the National Institute of Standards and Technology (NIST) (Kramida et al. 2015). The energy differences between the calculated MBPT and MCDHF/RCI level energies are within 0.07% for all 201 states in Fe XVII, and the mean difference of the NIST and MBPT values is 0.05% for the 425 states listed in the NIST ASD. Compared with the recent systematic MCDHF and RCI calculations by Jönsson et al. (2014), in which both accurate energy levels and transition rates were given, the present calculations are extended to report the data for additional 174 levels of the $2s2p^63l$, $2s^22p^54l$, $2s2p^64l$, $2s^22p^55l$, and $2s^22p^56l$ configurations. The calculations also extend the elaborate work by Gu (2005b, 2007) to include data of additional eleven neon-like ions between Cr XV and Kr XXVII. The excellent description of the energy separations along the sequence makes it possible to point out a number of lines for which the experimental identifications can be questioned. A complete dataset including energy levels and transition data should be helpful in analyzing new data from the solar and other astrophysical sources.

2. THEORY

2.1. The MBPT method

According to the Rayleigh-Schrödinger perturbation theory, the no-pair Dirac-Coulomb-Breit (DCB) Hamiltonian H_{DCB} for an N -electron ionic system can

be written as (Sucher 1980; Gu 2005a,b):

$$H_{\text{DCB}} = \sum_i^N [h_d(i) - \frac{Z}{r_i}] + \sum_{i < j}^N (\frac{1}{r_{ij}} + B_{ij}), \quad (1)$$

where $h_d(i)$ and Z are the free-electron Dirac Hamiltonian and the nuclear charge, respectively. r_i and r_{ij} are the radial coordinate of electron i , and the distance between the electrons i and j , respectively. B_{ij} is the frequency independent Breit interaction, given by

$$B_{ij} = -\frac{1}{2r_{ij}} [\boldsymbol{\alpha}_i \cdot \boldsymbol{\alpha}_j + \frac{(\boldsymbol{\alpha}_i \cdot \mathbf{r}_{ij})(\boldsymbol{\alpha}_j \cdot \mathbf{r}_{ij})}{r_{ij}^2}]. \quad (2)$$

where $\boldsymbol{\alpha}_i$ is a matrix vector constructed from Pauli spin matrices. H_{DCB} is divided into two parts, namely, a model Hamiltonian H_0 and a perturbation V , given by

$$H_0 = \sum_i [h_d(i) + U(r_i)], \quad (3)$$

$$V = -\sum_i \left[\frac{Z}{r_i} + U(r_i) \right] + \sum_{i < j} \left(\frac{1}{r_{ij}} + B_{ij} \right), \quad (4)$$

where $U(r)$ is a model potential including the screening effects of all electrons, whose appropriate choice makes V as small as possible.

For calculations:

(a). The approximated local central potential $U(r)$ and eigenfunctions Φ_k of H_0 are obtained by the Dirac-Fock-Slater self-consistent field calculations.

(b). The Hilbert space of the Hamiltonian is divided into two parts, namely, a model space M , and the orthogonal space O . A subset of Φ_k will define the space M , and the remaining states belong to the space O .

(c). The second order eigenvalues are obtained through solving the generalized eigenvalue problem for the first-order effective Hamiltonian.

2.2. The MCDHF method

The MCDHF method was described in detail by Grant (2007), and here we just give a brief outline. The atomic state function (ASF) is given as an expansion over configuration state functions (CSFs)

$$\Psi(\gamma J\pi) = \sum_j c_j \Phi(\gamma_j J\pi). \quad (5)$$

where J and π are the total angular momentum and parity of the system, respectively, γ_j is a set of quantum numbers, additional to $J\pi$, to specify a CSF, and c_j is the mixing coefficient.

For calculations:

(a). A CSF $\Phi(\gamma_j J\pi)$ is constructed from a product of single-electron wave functions through a proper angular momentum coupling and antisymmetrization.

(b). The self-consistent iteration method is used to obtain simultaneously the Dirac orbitals and the expansion coefficients.

(c). When the radial orbitals are obtained, RCI calculations are performed, which include the Breit interaction and first-order Quantum Electrodynamics (QED) corrections (self-energy and vacuum polarization).

3. CALCULATIONS AND RESULTS

In the MBPT calculations, the model space M contains the configurations $2s^22p^6$, $(2s, 2p)^7nl$ ($3 \leq n \leq 4$ and $l \leq n-1$), and $2s^22p^5n'l'$ ($5 \leq n' \leq 6$ and $l' \leq n'-1$). The N space contains all configurations formed by single and double (SD) virtual excitations of the M space. For single/double excitations, configurations with $n \leq 200$ and $l \leq \min(n-1, 25)$ /the inner electron promotion up to $n=65$ and promotion of the outer electron up to $n'=200$ are considered. For level energy and radiative transition calculations, some corrections such as finite nuclear size, nuclear recoil, and QED are also included. A more detailed description of the MBPT calculations procedure could be found in our recent work (Wang et al. 2014, 2015, 2016).

Table 1 displays the computed excitation energies of 201 fine structure levels in Ne-like ions ($Z = 24-36$) obtained from the MBPT method. Also listed in the table are the experimental energy levels recommended by the NIST ASD. Among the 2613 energy levels in the 13 ions given by the MBPT method, 443 experimental results are available. The wavelengths (λ_{ji} in Å), line strengths (S_{ji} in atomic units, 1 AU = 6.460×10^{-36} cm² esu²), weighted oscillator strengths (gf_{ji} dimensionless) and radiative rates (A_{ji} in s⁻¹) for the E1, M1, E2, and M2 transitions among the 201 levels for each ion, are listed in Table 2.

For assessing the accuracy of the MBPT results, the MCDHF and subsequent RCI calculations are carried out for Fe XVII. Separate calculations are performed for the even and odd states belonging to the M space of the above MBPT calculations, which are considered as the multi-reference configurations. The CSFs expansions are obtained through single and double excitations of the orbitals in the multi-reference configurations with orbitals in an active set with principal quantum numbers $n = 3, \dots, 8$ and angular symmetries s, p, d, f, g, h , and i . To monitor the convergence of the calculated energies and transition parameters, the active sets were increased in a systematic way by adding layers of orbitals. For the $n=8$ expansion this resulted in 3034729 CSFs with even parity and 3009779 CSFs with odd parity. The self-consistent field calculations for each layer of orbitals are followed by RCI calculations. A more detailed description of the MCDHF/RCI calculations procedure could be found in our recent work (Jönsson et al. 2013; Jönsson et al. 2014; Si et al. 2015a,b).

4. EVALUATION OF DATA

4.1. Energy Levels

Up to now, with regard to experimental data and elaborate computed results along the isoelectronic sequence, the Fe XVII spectrum is the most studied in astrophysics. For example, many Fe XVII EUV lines observed by the Hinode EUV Imaging Spectrometer were identified by [Del Zanna & Ishikawa \(2009\)](#). These Fe XVII lines provide useful information about the nature of the heating in the solar corona. In Table 3, the MBPT energy results for the 201 levels in Fe XIX are compared with experimental values of [Del Zanna & Ishikawa \(2009\)](#), who reviewed the Fe XVII spectrum in the 30–450 Å range, and provided accurate results for the $n = 3 - 5$ states, which have been included in the CHIANTI database ([Del Zanna et al. 2015](#); [Dere et al. 1997](#)). The present MCDHF/RCI values, the previous results for the $2s^22p^6$ and $2s^22p^53l$ levels ([Jönsson et al. 2014](#), MCDHF/RCI2) and the relativistic multireference Möller-Plesset results for the $2s^22p^6$ and $2l^73l'$ states ([Ishikawa et al. 2009](#), MR-MP), as well as the experimental values from the NIST ASD, are also given in the table for comparison. Compared with the present MBPT calculations, [Gu \(2005b\)](#) adopted the same method, and reported similar results which are not shown in this table.

Compared with the previous elaborate computed results (MCHDF/RCI2 and MR-MP) for the $n = 3$ levels, the present MBPT and MCDHF/RCI calculations give very consistent results. The experimental values from the NIST and CHIANTI databases and the four theoretical datasets also show good agreement (within 0.1%) for the $n = 3$ states, except for the $2s2p^63s\ ^1S_0$ state. For this level, the NIST value 869.1 eV is observed at a considerably higher energy (about 4 eV) than the CHIANTI experimental value 865.266 eV and the MBPT, MCHDF/RCI and MR-MP theoretical values (864.8332, 865.2301 and 865.146 eV).

Observed energies are scarce and the identification of some states becomes questionable for the $n > 3$ states. The $2s^22p^54d\ ^1D_2$ (1010.682 eV), and $2s^22p^54f\ ^1G_4$ (1017.9 eV) and $2s^22p^54f\ ^3G_4$ (1014.2 eV) states in the NIST ASD do not have any obvious counterparts in the Chianti database or in calculated energies, and misidentification can not be ruled out. As an example, we analyze the $2s^22p^54f\ ^1G_4$ (1017.9 eV) state in more detail. By means of the $2s^22p^53d\ ^3D_3$ level energy, the observed wavelength 58.98 Å ($2s^22p^53d\ ^3D_3 - 2s^22p^54f\ ^1G_4$) is utilized to extract the $2s^22p^54f\ ^1G_4$ level energy ([Shirai et al. 2000](#)). This NIST wavelength is about 1.4% lower than the CHIANTI, MBPT, and MCDHF/RCI values (59.776, 59.821, and 58.856 Å), but is very close to the CHIANTI, MBPT, and MCDHF/RCI values (58.980, 58.026, and 59.057 Å)

for the $2s^22p^53d\ ^3F_3 - 2s^22p^54f\ ^1G_4$ transition, whose the lower state is $2s^22p^53d\ ^3F_3$, but not $2s^22p^53d\ ^3D_3$. And the transition rate is $1.075 \times 10^{12} \text{ s}^{-1}$ for the $2s^22p^53d\ ^3F_3 - 2s^22p^54f\ ^1G_4$ ($\Delta L = 1$) transition, which is indeed larger by over one order of magnitude than the $8.8 \times 10^{10} \text{ s}^{-1}$ for the $2s^22p^53d\ ^3D_3 - 2s^22p^54f\ ^1G_4$ ($\Delta L = 2$) transition. Therefore, we conclude that the $\Delta L = 1$ transition is more likely to be observed than the $\Delta L = 2$ transition, and the NIST wavelength 58.98 Å should be assigned to the $2s^22p^53d\ ^3F_3 - 2s^22p^54f\ ^1G_4$ transition. By means of this wavelength and the NIST energy 805.0331 eV of the $2s^22p^53d\ ^3F_3$ states, the NIST value for $2s^22p^54f\ ^1G_4$ should be changed to 1015.3 eV, which agrees with the CHIANTI, MBPT, and MCDHF/RCI (1015.96, 1015.255, and 1015.461 eV) to within 0.1%. Based on the above argument, a misidentification for this NIST level cannot be ruled out. Together with the $2s^22p^54f\ ^1G_4$ (1017.9 eV) energy, all the other NIST values for the $2s2p^63s\ ^1S_0$, $2s^22p^54d\ ^1D_2$, and $2s^22p^54f\ ^3G_4$ states in Fe XVII, for which the NIST results differ from the MBPT values by more than 0.2%, are tabulated in Table 4.

The agreement of the CHIANTI experimental energies and the MBPT results is better. Deviations are less than 0.2% for all 30 $n = 4, 5$ states listed in the CHIANTI database, and are within 0.1% for 28 states. We can also see from Table 3 that the present MBPT and MCDHF/RCI calculations give very consistent results for all the 201 $n \leq 6$ levels, and the deviation of the two datasets are within 0.07% for all levels. The calculations predict energy levels with such a high precision that the results can be utilized to analyze the new observations from space- and ground- based telescopes.

For further assessing the accuracy of the MBPT energies, we compare them with the NIST experimental values for all the 13 Ne-like ions. Among the 2613 energy levels in 13 ions given by the MBPT method, the 443 NIST results are available. The computed energies agree very well with the NIST values. The differences between experimental and calculated energies are less than 0.1% for 393 states, and are within 0.2% for another 32 states. The remaining 18 states including four levels in Fe XVII discussed in detail above, for which the deviations are larger than 0.2%, are listed in Table 4. We cannot find any obvious duplicate energies in the present MBPT calculations, and these NIST values should be carefully used. As an example, Figure 1 shows the energy deviations as functions of Z for the $2s^22p^54s\ ^3P_1$ and $2s2p^64p\ ^1P_1$ states. Some obvious anomalies are seen for the $2s^22p^54s\ ^3P_1$ state in Se XXV (the difference is about 1.3%), and the $2s2p^64p\ ^1P_1$ state (1.5%) in Ga XXII. The differences fall between 0.2%–0.3% for the $2s2p^64p\ ^1P_1$ state in Ge XXIII and Br XXVI. The misidentification, line blending, or large experimental

errors of the spectral observations could be responsible for the large uncertainty of the data compiled by the NIST ASD (Kramida et al. 2015). Apart from these irregularities, the two datasets agree well for most states along the sequence.

In short, apart from the 18 states included in Table 4, the mean energy deviation of the observed and computed values for the 425 states included in the NIST ASD is 0.05%. Seeing that the same computational procedure is adopted for each ion, which implies that the quality of the data should be consistent and systematic, we conclude that relatively large uncertainties of observed energies brings on the large deviations for these states, and these NIST values should be re-evaluated.

4.2. Radiative Rates

In Table 5, weighted oscillator strengths for the E1, M1, E2, and M2 transitions among the $n \leq 3$ levels of the $2s^22p^6$, $2s^22p^53s$, $3p$, and $3d$, and $2s2p^63s$, $3p$ and $3d$ configurations are shown. Our results, gf (MBPT) and gf (MCDHF/RCI), are compared for Fe XVII with the calculated values from Jönsson et al. (2014), gf (MCDHF/RCI2), and the NIST ASD (Kramida et al. 2015), gf (NIST). The overall agreement among the present MBPT and MCDHF/RCI values and the previous MCDHF/RCI2 results is good, and the relative deviations are within 10% for the most of transitions. The average differences (with standard deviations) are $3.1\% \pm 4.4\%$ between the MBPT and MCDHF/RCI values and $2.1\% \pm 3.1\%$ between the MBPT and MCDHF/RCI2 values, which are also satisfactory. Among the large number of the transitions listed in Table 5, the gf values for some transitions (20 transitions) are given by the NIST ASD. The NIST gf values for these 20 transitions are compared with the MBPT gf values in Figure 2 (a). The two datasets agree within 10% for 13 transitions, while differing from each other between 10% and 35% for the 7 transitions. Note that good agreement (within 6%) can be found between the MBPT and MCDHF/RCI gf values for all transitions in Figure 2 (a), and thus the NIST values for these 7 transitions, which are compiled by Fuhr et al. (1988), should be updated.

Weighted oscillator strengths among the $n \leq 3$ states in Fe XVII given by the CHIANTI database are also compared with the present MBPT gf values in Figure 2 (b). Many of the CHIANTI compilations differ from the present calculations by 10%-50%, and moreover, the deviations exceed 10% for many relatively strong transitions with gf values $\geq 10^{-2}$. The agreement of the present two calculations is within 10% for all strong transitions, and is no more than 15% for few weak transitions.

To further assess the accuracy of the present calcula-

tions, in Figure 3 the MCDHF/RCI weighted oscillator strengths are compared with the MBPT values for all the 1557 strong transitions ($gf \geq 10^{-2}$) among the $n \leq 6$ states in Fe XVII, and the comparison of the MBPT and MCDHF/RCI2 calculations for all the 675 strong transitions among the $n \leq 3$ states from Cr XV to Kr XXVII are shown in Figure 4. For 92% of the transitions in Fe XVII shown in Figure 3, the agreement of the present two calculations are within 10%, while they differ from each other by over 20% (but less than 40%) for only 29 transitions. The upper states of these 29 transitions mostly belong to the highest states of the $n = 6$ configurations. For such transitions, the present MCDHF/RCI calculations converge very slowly with increasing active sets. Nevertheless, the average difference with the standard deviation of the present two calculations for the 1557 transitions is only $3.0\% \pm 5.5\%$. In addition, as shown in Figure 4 the MBPT and MCDHF/RCI2 gf values for the 675 transitions among the $n \leq 3$ states from Cr XV to Kr XXVII agree within 10% for 672 transitions. The average difference with the standard deviation of the two calculations for all transitions is only $1.4\% \pm 1.2\%$, which is highly satisfactory.

Based on the above analysis we conclude that the present transitions data have better accuracy compared to the values from the NIST and CHIANTI databases. Using the part of transition values with insufficient accuracy, especially for the strong transitions, may lead to quite different, even wrong results when carrying out line identifications and plasma diagnostics in solar physics and astrophysics. Therefore, hopefully, it would be possible to replace the existing CHIANTI data, as well as the NIST values by the present MBPT and/or MCDHF/RCI results.

Del Zanna (2011) have pointed out that the Fe XVII lines in the X-rays range can be reliably used for the measurement of electron temperatures in the solar corona and other astrophysical sources. Using the MBPT radiative transition data, as well as the collisional atomic data recommended by the CHIANTI database, in conjunction with the statistical equilibrium code of Dufton (Dufton 1977), the synthetic Fe XVII spectra in the range of 10 – 20 Å are shown in Figure 5. The intensity of each transition is represented by a Gaussian distribution with a resolving power of 1000, corresponding to a temperature $T_e = 10^7$ K and a density $N_e = 10^{11} \text{ cm}^{-3}$, a typical solar flare condition. As shown in Figure 5, prominent transitions (with wavelengths and transition rates) in the 10 – 20 Å range are

$$\begin{aligned} & 2s^22p^6 \ ^1S_0 - 2s^22p^55d \ ^1P_1 \ (11.256 \text{ Å and } 3.07 \times 10^{12} \text{ s}^{-1}) \\ & 2s^22p^6 \ ^1S_0 - 2s^22p^54d \ ^1P_1 \ (12.130 \text{ Å and } 5.62 \times 10^{12} \text{ s}^{-1}) \\ & 2s^22p^6 \ ^1S_0 - 2s^22p^54d \ ^3D_1 \ (12.269 \text{ Å and } 5.08 \times 10^{12} \text{ s}^{-1}) \end{aligned}$$

$$\begin{aligned}
& 2s^22p^6 \ ^1S_0 - 2s2p^63p \ ^1P_1 \ (13.830 \text{ \AA} \text{ and } 3.33 \times 10^{12} \text{ s}^{-1}) \\
& 2s^22p^6 \ ^1S_0 - 2s^22p^53d \ ^3D_1 \ (15.268 \text{ \AA} \text{ and } 6.08 \times 10^{12} \text{ s}^{-1}) \\
& 2s^22p^6 \ ^1S_0 - 2s^22p^53d \ ^3P_1 \ (15.459 \text{ \AA} \text{ and } 9.04 \times 10^{10} \text{ s}^{-1}) \\
& 2s^22p^6 \ ^1S_0 - 2s^22p^53s \ ^3P_1 \ (16.784 \text{ \AA} \text{ and } 7.88 \times 10^{11} \text{ s}^{-1}) \\
& 2s^22p^6 \ ^1S_0 - 2s^22p^53s \ ^1P_1 \ (17.059 \text{ \AA} \text{ and } 9.34 \times 10^{11} \text{ s}^{-1}) \\
& 2s^22p^6 \ ^1S_0 - 2s^22p^53s \ ^3P_2 \ (17.103 \text{ \AA} \text{ and } 2.06 \times 10^5 \text{ s}^{-1})
\end{aligned}$$

The strongest resonance transition in the spectrum is

$$2s^22p^6 \ ^1S_0 - 2s^22p^53d \ ^1P_1 \ (15.021 \text{ \AA} \text{ and } 2.19 \times 10^{13} \text{ s}^{-1})$$

5. SUMMARY

Systematic and consistent MBPT calculations have been preformed in Ne-like ions with $Z = 24 - 36$ using the FAC code. A complete dataset with high accuracy, including energies, wavelengths, line strengths, oscillator strengths, and transition rates for the E1, M1, E2, and M2 transitions among the 201 states of the $2s^22p^6$, $(2s, 2p)^73l$, $(2s, 2p)^74l$, $2s^22p^55l$, and $2s^22p^56l$ configurations, have been deduced for each ion. The MBPT energy results are in excellent agreement with observations, and the mean energy deviation with the NIST observations is 0.05%. Compared with the elaborate MCDHF/RCI and MCDHF/RCI2 calculations, the accuracy of the MBPT transition data has been estimated to only 1.4% for transitions among the $n \leq 3$ states for all 13 ions, and 3.0% for transitions involving the higher states in Fe XVII. Because our calculations are systematic and consistent, reporting unified quality of data, we expect that the transition rates are highly accurate and may serve as benchmarks for other calculations.

The present calculations significantly increase the amount of accurate energy data for a number of Ne-like ions of astrophysics interest, as well as their highly accurate transition rates. A reanalysis of electron temperature and density in the solar or other astrophysical sources using the current extended dataset in high accuracy allows for a more thorough consistency check with the possibility to identify and include new lines of diagnostic value. Through the comparison, we can point out some observations that may have large errors or wrongly assigned, which have been included in Table 1. The high accuracy of the current data may rule out the possibility that wrongly identified lines enter the analysis.

The authors express their gratitude to Dr. MingFeng Gu for offering guidance in using his FAC code. We acknowledge the support from the National Natural Science Foundation of China (Grant No. 21503066, No. 11504421, and No. 11474034) and the support from the Foundation for the Development of Science and Technology of Chinese Academy

of Engineering Physics (Grant No. 2012B0102012). This work is also supported by NSAF under Grant No. 11076009, the Chinese Association of Atomic and Molecular Data, Chinese National Fusion Project for ITER No. 2015GB117000, and the Swedish Research Council under contract 2015-04842. One of the authors (KW) expresses his gratefully gratitude to the support from the visiting researcher program at the Fudan University.

REFERENCES

- Acton, L. W., Bruner, M. E., Brown, W. A., et al. 1985, ApJ, 291, 865
- Aggarwal, K. M., Keenan, F. P., & Kisielius, R. 2004, A&A, 420, 783
- Badnell, N. R. 1986, JPhB, 19, 3827
- Behar, E., Cottam, J., & Kahn, S. M. 2001, ApJ, 548, 966
- Brown, C. M., Feldman, U., Seely, J. F., Korendyke, C. M., & Hara, H. 2008, ApJS, 176, 511
- Bryans, P., Badnell, N. R., Gorczyca, T. W., et al. 2006, ApJS, 167, 343
- Bryans, P., Landi, E., & Savin, D. W. 2009, ApJ, 691, 1540
- Chen, G. X., Pradhan, A. K., & Eissner, W. 2003, JPhB, 36, 453
- Cogordan, J. A., Lunell, S., Jupén, C., & Litzén, U. 1985, PhysS, 31, 545
- Culhane, J. L., Harra, L. K., James, A. M., et al. 2007, Solar Physics, 243, 19
- Curdt, W., Landi, E., & Feldman, U. 2004, A&A, 427, 1045
- Del Zanna, G. 2008, A&A, 481, L69
- . 2011, A&A, 536, A59
- Del Zanna, G., Dere, K. P., Young, P. R., Landi, E., & Mason, H. E. 2015, A&A, 582, A56
- Del Zanna, G., & Ishikawa, Y. 2009, A&A, 508, 1517
- Del Zanna, G., & Mason, H. E. 2014, A&A, 565, A14
- Dere, K. P., Landi, E., Mason, H. E., Monsignori Fossi, B. C., & Young, P. R. 1997, A&AS, 125, 149
- Dong, C., Xie, L., Fritzsche, S., & Kato, T. 2003, Nuclear Instruments and Methods in Physics Research Section B: Beam Interactions with Materials and Atoms, 205, 87
- Dong, C. Z., Xie, L. Y., Zhou, X. X., Ma, X. W., & Fritzsche, S. 2003, Hyperfine Interactions, 146, 161
- Dufton, P. 1977, CoPhC, 13, 25
- Dyall, K., Grant, I., Johnson, C., Parpia, F., & Plummer, E. 1989, CoPhC, 55, 425
- Eissner, W., Jones, M., & Nussbaumer, H. 1974, CoPhC, 8, 270
- Feldman, U., Curdt, W., Landi, E., & Wilhelm, K. 2000, ApJ, 544, 508
- Froese Fischer, C., & Tachiev, G. 2004, ADNDT, 87, 1
- Führ, J. R., Martin, G. A., & Wiese, W. L. 1988, JPCRD, 17 (Supplement 4), 1
- Grant, I. P. 2007, Relativistic Quantum Theory of Atoms and Molecules
- Gu, M. F. 2003, ApJ, 582, 1241
- Gu, M. F. 2005a, ADNDT, 89, 267
- . 2005b, ApJS, 156, 105
- . 2007, ApJS, 169, 154
- Gu, M. F., Holczer, T., Behar, E., & Kahn, S. M. 2006, ApJ, 641, 1227
- Hibbert, A., Ledourneuf, M., & Mohan, M. 1993, ADNDT, 53, 23
- Holczer, T., Behar, E., & Kaspi, S. 2005, ApJ, 632, 788
- Ishikawa, Y., Encarnación, J. M. L., & Träbert, E. 2009, PhysS, 79, 025301
- Ivanova, E. P., & Gulov, A. V. 1991, ADNDT, 49, 1
- Jönsson, P., Gaigalas, G., Bieroń, J., Fischer, C. F., & Grant, I. P. 2013, CoPhC, 184, 2197
- Jönsson, P., Bengtsson, P., Ekman, J., et al. 2014, ADNDT, 100, 1
- Kaastra, J. S., Steenbrugge, K. C., Raassen, A. J. J., et al. 2002, A&A, 386, 427
- Ko, Y. K., Raymond, J. C., Li, J., et al. 2002, ApJ, 578, 979
- Kramida, A., Yu. Ralchenko, Reader, J., & and NIST ASD Team. 2015, NIST Atomic Spectra Database (ver. 5.3), [Online]. Available: <http://physics.nist.gov/asd> [2016, May 10]. National Institute of Standards and Technology, Gaithersburg, MD., ,
- Landi, E., & Phillips, K. J. H. 2005, ApJS, 160, 286
- Liang, G. Y., & Badnell, N. R. 2010, A&A, 518, A64
- Mazzotta, P., Mazzitelli, G., Colafrancesco, S., & Vittorio, N. 1998, A&AS, 133, 403
- Mewe, R., Raassen, A., Drake, J., & Kaastra, J. 2001, A&A, 368, 888
- Nahar, S. N., Eissner, W., Chen, G.-X., & Pradhan, A. K. 2003, A&A, 408, 789
- Ness, J.-U., Brickhouse, N. S., Drake, J. J., & Huenemoerder, D. P. 2003, ApJ, 598, 1277
- Paerels, F. B. S., & Kahn, S. M. 2003, ARA&A, 41, 291
- Phillips, K. J. H., Fawcett, B. C., Kent, B. J., et al. 1982, ApJ, 256, 774
- Quinet, P., Gorlia, T., & Biemont, E. 1991, PhysS, 44, 164
- Raassen, A. J. J., & Pollock, A. M. T. 2013, A&A, 550, A55
- Raassen, A. J. J., Mewe, R., Audard, M., et al. 2002, A&A, 389, 228
- Savukov, I. M. 2003, JPhB, 36, 4789
- Shestov, S., Reva, A., & Kuzin, S. 2014, ApJ, 780, 15
- Shestov, S. V., Bozhenkov, S. A., Zhitnik, I. A., et al. 2008, Astronomy Letters, 34, 33
- Shirai, T., Sugar, J., Musgrave, A., & Wiese, W. L. 2000, JPCRD
- Si, R., Guo, X. L., Yan, J., et al. 2015a, JPhB, 48, 175004
- Si, R., Guo, X., Yan, J., et al. 2015b, JQSRT, 163, 7
- Sucher, J. 1980, PhRvA, 22, 348
- Wang, K., Li, D. F., Liu, H. T., et al. 2014, ApJS, 215, 26
- Wang, K., Guo, X. L., Liu, H. T., et al. 2015, ApJS, 218, 16
- Wang, K., Si, R., Dang, W., et al. 2016, ApJS, 223, 3
- Warren, H. P., Feldman, U., & Brown, C. M. 2008, ApJ, 685, 1277

ALL AUTHORS AND AFFILIATIONS

AND

K. WANG^{1,2,3}, Z.B. CHEN⁴, R. SI³, P. JÖNSSON⁵, J. EKMAN⁵, X.L. GUO^{6,3}, S. LI², F.Y. LONG², W. DANG¹, X.H. ZHAO¹, R. HUTTON³, C.Y. CHEN³, J. YAN^{2,7,8}, AND X. YANG⁹.

¹Hebei Key Lab of Optic-electronic Information and Materials, The College of Physics Science and Technology, Hebei University, Baoding 071002, China

²Institute of Applied Physics and Computational Mathematics, Beijing 100088, China

³Shanghai EBIT Lab, Institute of Modern Physics, Department of Nuclear Science and Technology, Fudan University, Shanghai 200433, China

⁴College of Science, National University of Defense Technology, Changsha 410073, China

⁵Group for Materials Science and Applied Mathematics, Malmö University, SE-20506, Malmö, Sweden

⁶Department of Radiotherapy, Shanghai Changhai Hospital, Second Military Medical University, Shanghai 200433, China

⁷Center for Applied Physics and Technology, Peking University, Beijing 100871, China

⁸Collaborative Innovation Center of IFSA (CICIFSA), Shanghai Jiao Tong University, Shanghai 200240, China

⁹The Third Institute of Surveying and Mapping of Hebei Province, Hebei Bureau of Geoinformation, Shijiazhuang 050000, China

FIGURE AND TABLE

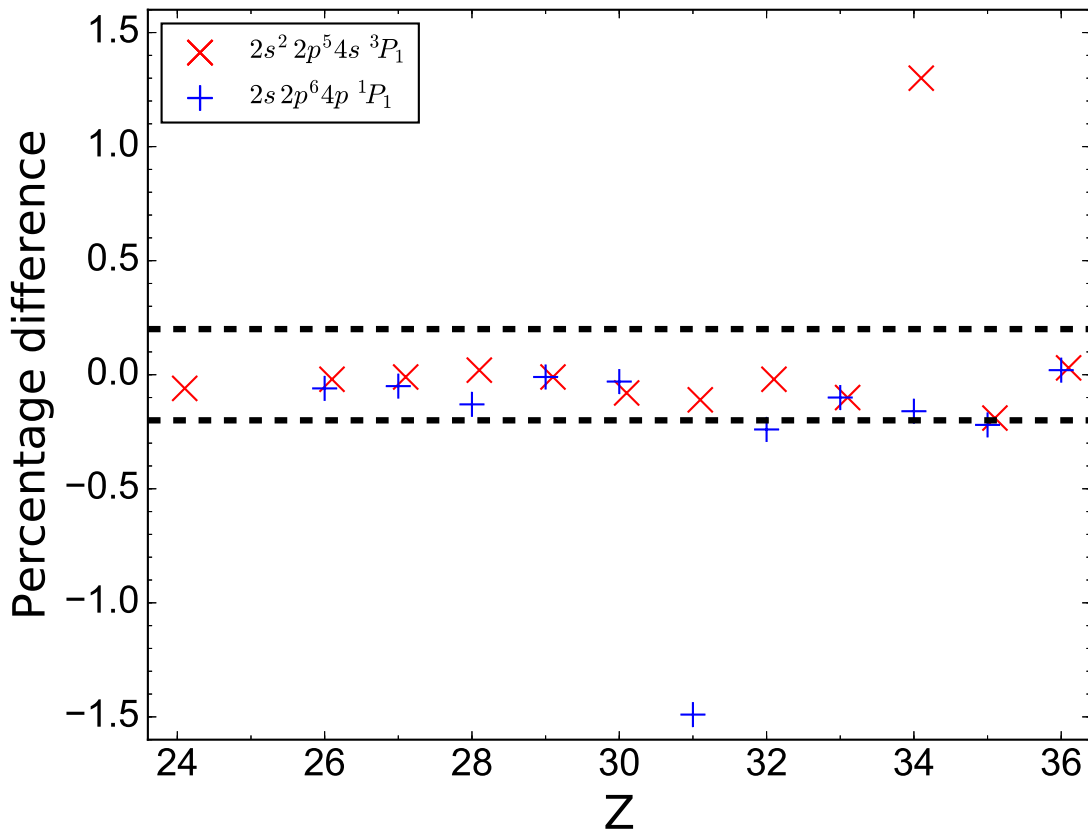


Figure 1. Percentage differences of the MBPT energies relative to the NIST observations for the $2s^2 2p^5 4s \ ^3P_1$ and $2s 2p^6 4p \ ^1P_1$ states along the sequence.

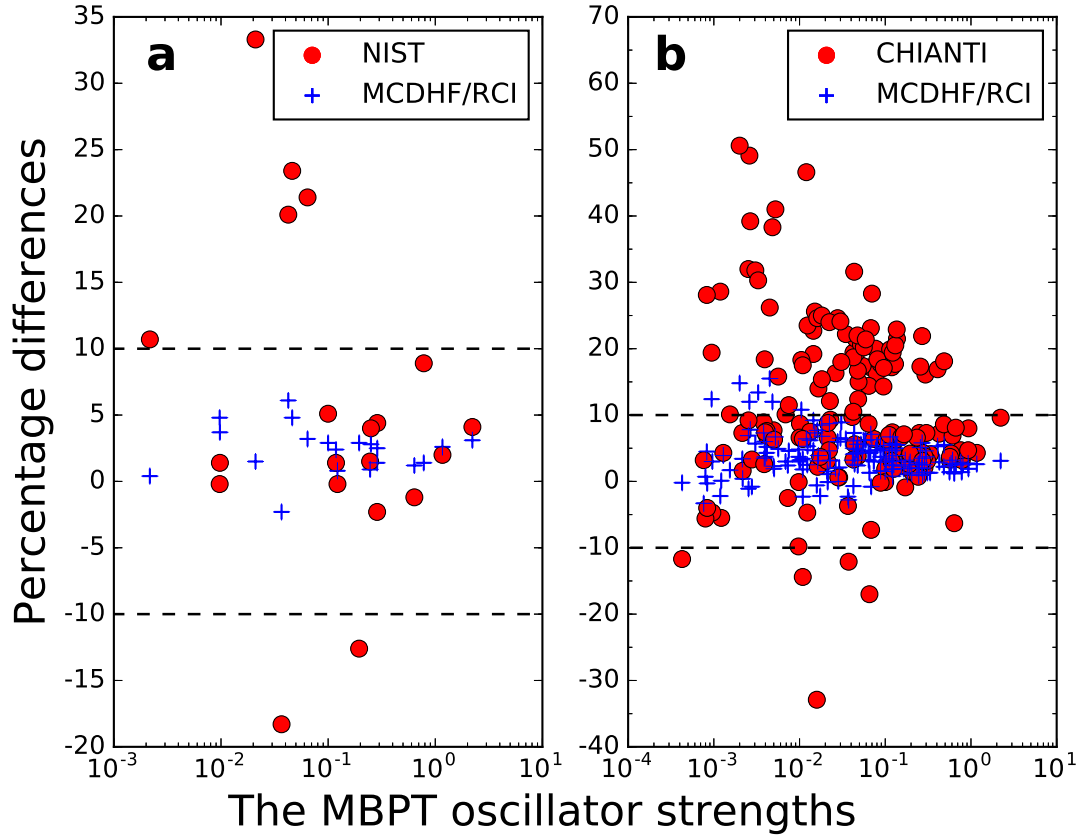


Figure 2. (a) Percentage differences of the NIST and MCDHF/RCI oscillator strengths relative to the present MBPT results for the transitions among the $n \leq 3$ states given by the NIST ASD. (b) Percentage differences of the CHIANTI and MCDHF/RCI oscillator strengths relative to the present MBPT results for the transitions among the $n \leq 3$ states given by the CHIANTI database. Dashed lines indicate the differences of $\pm 10\%$.

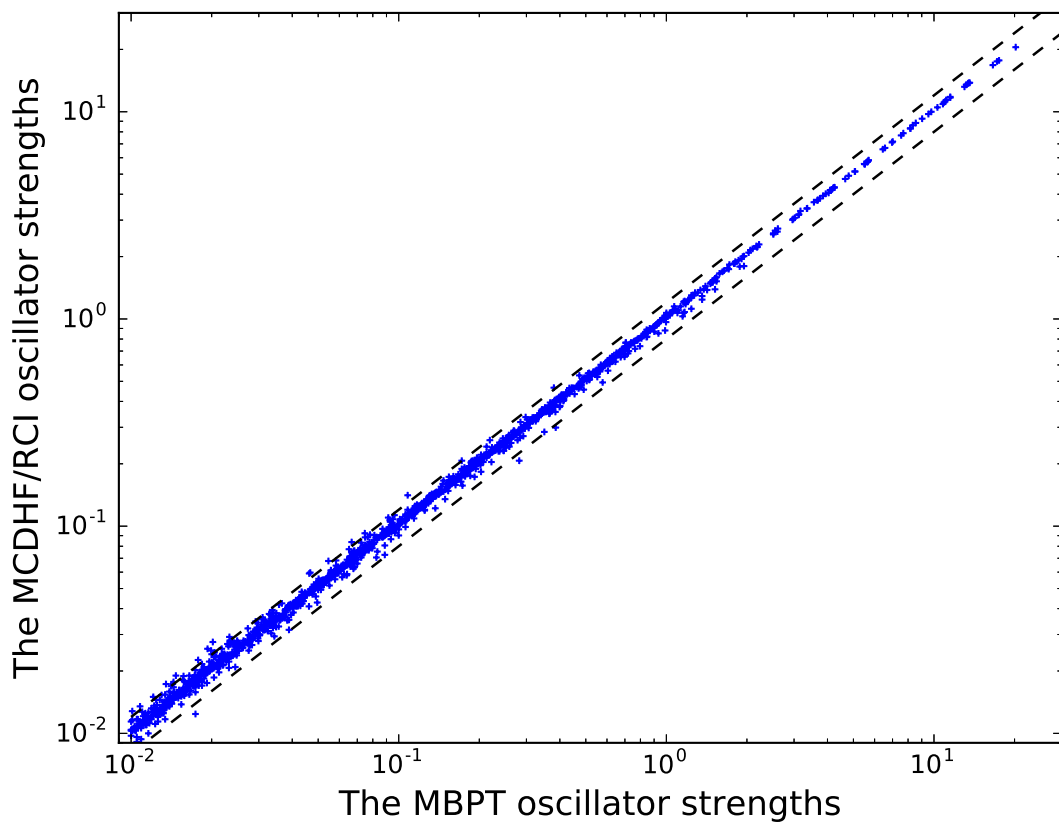


Figure 3. Comparison of the present MBPT oscillator strengths with the MCDHF/RCI results for the transitions with $gf \geq 0.01$ in Fe XVII. Dashed lines indicate the differences of $\pm 20\%$.

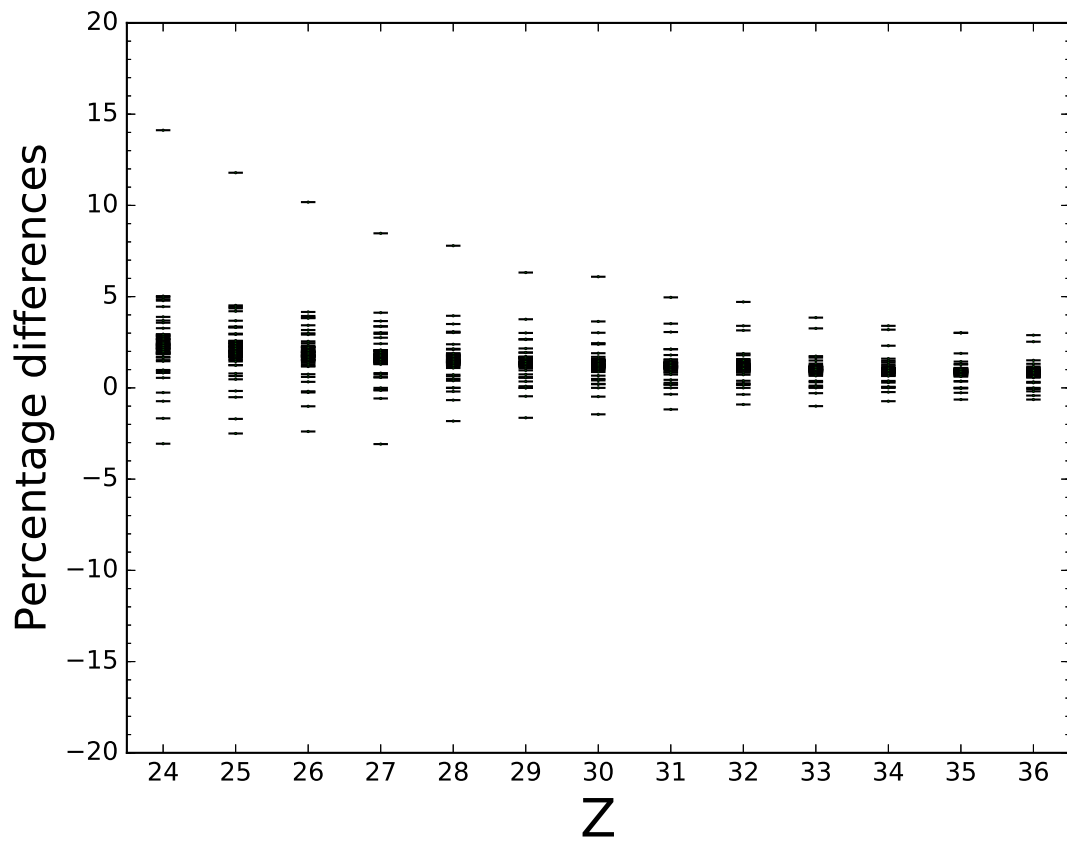


Figure 4. Comparison between the MCDHF/RCI2 and MBPT oscillator strengths for the $gf \geq 0.01$ transitions among the $n \leq 3$ states along the sequence.

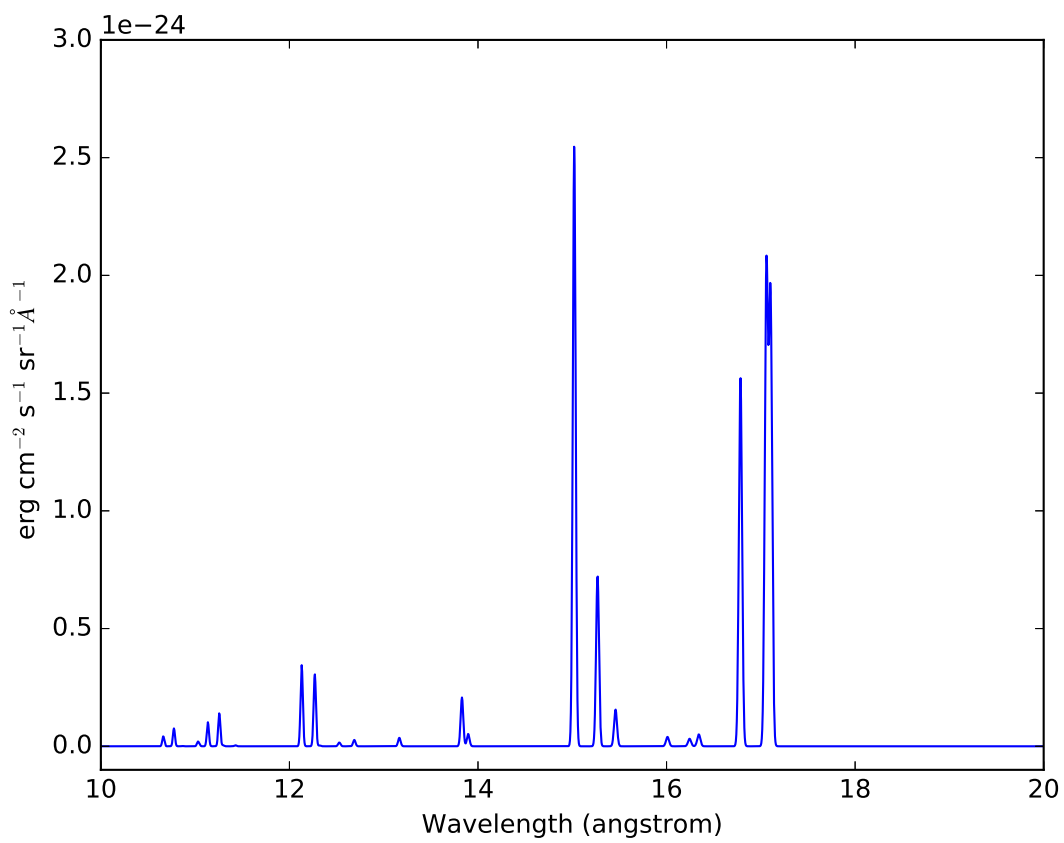


Figure 5. Synthetic Fe XXI spectrum containing transitions between 10 – 20 Å. See text for details.

Table 1. Level energies (in eV) of the states in Ne-like ions from Cr XV to Kr XXVII, as well as level designations in both the LSJ - and jj -coupling schemes, and the dominant mixing coefficients of the LSJ basis.

Z	Key	Conf	LSJ	$jj^{a,b,c}$	J^π	Energy		Mixing coefficients
						NIST ^d	MBPT ^e	
26	1	$2s^22p^6$	1S_0	$2p + 4(0)0$	0^e	0.000000E+00	0.000000E+00	-1.00(1)
26	2	$2s^22p^53s$	3P_2	$2p + 3(3)3\ 3s + 1(1)4$	2^o	7.249150E+02	7.252443E+02	-1.00(2)
26	3	$2s^22p^53s$	1P_1	$2p + 3(3)3\ 3s + 1(1)2$	1^o	7.267839E+02	7.271388E+02	-0.74(3) - 0.67(5)
26	4	$2s^22p^53s$	3P_0	$2p - 1(1)1\ 3s + 1(1)0$	0^o	7.375376E+02	7.378560E+02	-1.00(4)
26	5	$2s^22p^53s$	3P_1	$2p - 1(1)1\ 3s + 1(1)2$	1^o	7.387243E+02	7.390537E+02	-0.74(5)0.67(3)
26	6	$2s^22p^53p$	3S_1	$2p + 3(3)3\ 3p - 1(1)2$	1^e	7.552334E+02	7.554915E+02	-0.90(6)0.42(13)
26	7	$2s^22p^53p$	3D_2	$2p + 3(3)3\ 3p - 1(1)4$	2^e	7.586933E+02	7.589928E+02	-0.76(7) - 0.55(14)
26	8	$2s^22p^53p$	3D_3	$2p + 3(3)3\ 3p + 1(3)6$	3^e	7.603239E+02	7.606096E+02	1.00(8)
26	9	$2s^22p^53p$	1P_1	$2p + 3(3)3\ 3p + 1(3)2$	1^e	7.614395E+02	7.617403E+02	-0.71(9)0.50(12) - 0.44(13)
26	10	$2s^22p^53p$	3P_2	$2p + 3(3)3\ 3p + 1(3)4$	2^e	7.632480E+02	7.635530E+02	-0.82(10) - 0.57(14)
26	11	$2s^22p^53p$	3P_0	$2p + 3(3)3\ 3p + 1(3)0$	0^e	7.686848E+02	7.689810E+02	-0.96(11)
26	12	$2s^22p^53p$	3D_1	$2p - 1(1)1\ 3p - 1(1)2$	1^e	7.707739E+02	7.710614E+02	0.82(12)0.56(9)
26	13	$2s^22p^53p$	3P_1	$2p - 1(1)1\ 3p + 1(3)2$	1^e	7.740263E+02	7.743073E+02	0.79(13) - 0.41(9)
26	14	$2s^22p^53p$	1D_2	$2p - 1(1)1\ 3p + 1(3)4$	2^e	7.743944E+02	7.746855E+02	0.64(7) - 0.61(14)0.46(10)
26	15	$2s^22p^53p$	1S_0	$2p - 1(1)1\ 3p - 1(1)0$	0^e	7.869916E+02	7.877224E+02	0.96(15)
26	16	$2s^22p^53d$	3P_0	$2p + 3(3)3\ 3d - 1(3)0$	0^o	8.010749E+02	8.014314E+02	1.00(16)
26	17	$2s^22p^53d$	3P_1	$2p + 3(3)3\ 3d - 1(3)2$	1^o	8.020304E+02	8.024010E+02	-0.96(17)
26	18	$2s^22p^53d$	3P_2	$2p + 3(3)3\ 3d + 1(5)4$	2^o	8.038389E+02	8.042110E+02	0.85(18) - 0.43(25)
26	19	$2s^22p^53d$	3F_4	$2p + 3(3)3\ 3d + 1(5)8$	4^o	8.039104E+02	8.042644E+02	-1.00(19)
26	20	$2s^22p^53d$	3F_3	$2p + 3(3)3\ 3d - 1(3)6$	3^o	8.046339E+02	8.050331E+02	0.80(20)0.55(26)
26	21	$2s^22p^53d$	1D_2	$2p + 3(3)3\ 3d - 1(3)4$	2^o	8.063541E+02	8.067280E+02	-0.64(21)0.59(24) - 0.49(25)
26	22	$2s^22p^53d$	3D_3	$2p + 3(3)3\ 3d + 1(5)6$	3^o	8.074260E+02	8.078004E+02	-0.80(22) - 0.58(26)
26	23	$2s^22p^53d$	3D_1	$2p + 3(3)3\ 3d + 1(5)2$	1^o	8.120439E+02	8.123690E+02	-0.86(23)0.47(27)
26	24	$2s^22p^53d$	3F_2	$2p - 1(1)1\ 3d - 1(3)4$	2^o	8.172299E+02	8.175964E+02	-0.79(24) - 0.54(21)
26	25	$2s^22p^53d$	3D_2	$2p - 1(1)1\ 3d + 1(5)4$	2^o	8.180443E+02	8.184135E+02	0.71(25)0.52(18) - 0.46(21)
26	26	$2s^22p^53d$	1F_3	$2p - 1(1)1\ 3d + 1(5)6$	3^o	8.185583E+02	8.189342E+02	0.60(26) - 0.57(20) - 0.55(22)
26	27	$2s^22p^53d$	1P_1	$2p - 1(1)1\ 3d - 1(3)2$	1^o	8.253914E+02	8.257000E+02	-0.88(27) - 0.44(23)
26	28	$2s2p^63s$	3S_1	$2s + 1(1)1\ 3s + 1(1)2$	1^e	8.589874E+02	...	0.99(28)
26	29	$2s2p^63s$	1S_0	$2s + 1(1)1\ 3s + 1(1)0$	0^e	8.648332E+02	8.691000E+02	1.00(29)
26	30	$2s2p^63p$	3P_0	$2s + 1(1)1\ 3p - 1(1)0$	0^o	8.917391E+02	...	1.00(30)
26	31	$2s2p^63p$	3P_1	$2s + 1(1)1\ 3p - 1(1)2$	1^o	8.922064E+02	8.925500E+02	-0.94(31)
26	32	$2s2p^63p$	3P_2	$2s + 1(1)1\ 3p + 1(3)4$	2^o	8.945275E+02	...	-1.00(32)
26	33	$2s2p^63p$	1P_1	$2s + 1(1)1\ 3p + 1(3)2$	1^o	8.964628E+02	8.969390E+02	-0.94(33)
26	34	$2s2p^63d$	3D_1	$2s + 1(1)1\ 3d - 1(3)2$	1^e	9.364837E+02	...	1.00(34)
26	35	$2s2p^63d$	3D_2	$2s + 1(1)1\ 3d - 1(3)4$	2^e	9.366273E+02	...	1.00(35)
26	36	$2s2p^63d$	3D_3	$2s + 1(1)1\ 3d + 1(5)6$	3^e	9.369023E+02	...	1.00(36)
26	37	$2s2p^63d$	1D_2	$2s + 1(1)1\ 3d + 1(5)4$	2^e	9.417026E+02	...	-1.00(37)
26	38	$2s^22p^54s$	3P_2	$2p + 3(3)3\ 4s + 1(1)4$	2^o	9.765650E+02	9.768700E+02	1.00(38)
26	39	$2s^22p^54s$	1P_1	$2p + 3(3)3\ 4s + 1(1)2$	1^o	9.771869E+02	9.777150E+02	0.79(39)0.61(42)

Table 1 continued

Table 1 (*continued*)

Z	Key	Conf	<i>LSJ</i>	<i>jj</i> ^{a,b,c}	<i>J</i> ^π	Energy		<i>LSJ</i> ^f
						NIST ^d	MBPT ^e	
26	40	$2s^2 2p^5 4p$	3S_1	$2p + 3(3)3\ 4p - 1(1)2$	1^e	9.891387E+02	...	-0.83(40)0.54(49)
26	41	$2s^2 2p^5 4s$	3P_0	$2p - 1(1)1\ 4s + 1(1)0$	0^o	9.892215E+02	...	1.00(41)
26	42	$2s^2 2p^5 4s$	3P_1	$2p - 1(1)1\ 4s + 1(1)2$	1^o	9.895691E+02	9.897700E+02	0.80(42) - 0.61(39)
26	43	$2s^2 2p^5 4p$	3D_2	$2p + 3(3)3\ 4p - 1(1)4$	2^e	9.900391E+02	...	0.73(43)0.58(50)
26	44	$2s^2 2p^5 4p$	3D_3	$2p + 3(3)3\ 4p + 1(3)6$	3^e	9.907127E+02	...	-1.00(44)
26	45	$2s^2 2p^5 4p$	1P_1	$2p + 3(3)3\ 4p + 1(3)2$	1^e	9.911078E+02	...	0.78(45) - 0.42(48)
26	46	$2s^2 2p^5 4p$	3P_2	$2p + 3(3)3\ 4p + 1(3)4$	2^e	9.917199E+02	...	-0.83(46) - 0.56(50)
26	47	$2s^2 2p^5 4p$	3P_0	$2p + 3(3)3\ 4p + 1(3)0$	0^e	9.951565E+02	...	-0.78(47)0.62(53)
26	48	$2s^2 2p^5 4p$	3D_1	$2p - 1(1)1\ 4p - 1(1)2$	1^e	1.002430E+03	...	0.85(48)0.50(45)
26	49	$2s^2 2p^5 4p$	3P_1	$2p - 1(1)1\ 4p + 1(3)2$	1^e	1.003619E+03	...	0.75(49)0.47(40)
26	50	$2s^2 2p^5 4p$	1D_2	$2p - 1(1)1\ 4p + 1(3)4$	2^e	1.003847E+03	...	0.68(43) - 0.59(50)0.43(46)
26	51	$2s^2 2p^5 4d$	3P_0	$2p + 3(3)3\ 4d - 1(3)0$	0^o	1.005846E+03	...	-1.00(51)
26	52	$2s^2 2p^5 4d$	3P_1	$2p + 3(3)3\ 4d - 1(3)2$	1^o	1.006284E+03	1.006260E+03	0.92(52)
26	53	$2s^2 2p^5 4p$	1S_0	$2p - 1(1)1\ 4p - 1(1)0$	0^e	1.006331E+03	...	0.78(53)0.62(47)
26	54	$2s^2 2p^5 4d$	3F_4	$2p + 3(3)3\ 4d + 1(5)8$	4^o	1.006822E+03	1.007198E+03	-1.00(54)
26	55	$2s^2 2p^5 4d$	3P_2	$2p + 3(3)3\ 4d + 1(5)4$	2^o	1.007000E+03	...	-0.76(55)0.54(69)
26	56	$2s^2 2p^5 4d$	3F_3	$2p + 3(3)3\ 4d - 1(3)6$	3^o	1.007104E+03	1.007471E+03	0.76(56)0.58(70)
26	57	$2s^2 2p^5 4d$	1D_2	$2p + 3(3)3\ 4d - 1(3)4$	2^o	1.007727E+03	1.010682E+03	-0.70(57)0.51(68) - 0.50(69)
26	58	$2s^2 2p^5 4d$	3D_3	$2p + 3(3)3\ 4d + 1(5)6$	3^o	1.008117E+03	...	0.82(58)0.56(70)
26	59	$2s^2 2p^5 4d$	3D_1	$2p + 3(3)3\ 4d + 1(5)2$	1^o	1.010525E+03	1.010970E+03	0.69(59) - 0.69(71)
26	60	$2s^2 2p^5 4f$	1G_4	$2p + 3(3)3\ 4f - 1(5)8$	4^e	1.014685E+03	1.015800E+03	-0.72(60) - 0.69(73)
26	61	$2s^2 2p^5 4f$	3D_1	$2p + 3(3)3\ 4f - 1(5)2$	1^e	1.014689E+03	...	-1.00(61)
26	62	$2s^2 2p^5 4f$	3G_5	$2p + 3(3)3\ 4f + 1(7)10$	5^e	1.014716E+03	1.015180E+03	1.00(62)
26	63	$2s^2 2p^5 4f$	3D_2	$2p + 3(3)3\ 4f + 1(7)4$	2^e	1.014816E+03	...	0.86(63) - 0.48(65)
26	64	$2s^2 2p^5 4f$	3F_3	$2p + 3(3)3\ 4f + 1(7)6$	3^e	1.015172E+03	1.015680E+03	0.68(75) - 0.65(64)
26	65	$2s^2 2p^5 4f$	1D_2	$2p + 3(3)3\ 4f - 1(5)4$	2^e	1.015195E+03	1.015180E+03	0.71(74) - 0.67(65)
26	66	$2s^2 2p^5 4f$	1F_3	$2p + 3(3)3\ 4f - 1(5)6$	3^e	1.015255E+03	1.017170E+03	0.73(66) - 0.51(72)0.44(64)
26	67	$2s^2 2p^5 4f$	3F_4	$2p + 3(3)3\ 4f + 1(7)8$	4^e	1.015338E+03	1.017900E+03	-0.85(67)
26	68	$2s^2 2p^5 4d$	3F_2	$2p - 1(1)1\ 4d - 1(3)4$	2^o	1.019637E+03	...	0.84(68)0.48(57)
26	69	$2s^2 2p^5 4d$	3D_2	$2p - 1(1)1\ 4d + 1(5)4$	2^o	1.019899E+03	...	-0.64(69) - 0.63(55)0.40(57)
26	70	$2s^2 2p^5 4d$	1F_3	$2p - 1(1)1\ 4d + 1(5)6$	3^o	1.020196E+03	...	-0.63(56)0.59(70) - 0.50(58)
26	71	$2s^2 2p^5 4d$	1P_1	$2p - 1(1)1\ 4d - 1(3)2$	1^o	1.022167E+03	1.022750E+03	-0.72(71) - 0.62(59)
26	72	$2s^2 2p^5 4f$	3G_3	$2p - 1(1)1\ 4f - 1(5)6$	3^e	1.027549E+03	1.027710E+03	-0.85(72) - 0.42(66)
26	73	$2s^2 2p^5 4f$	3G_4	$2p - 1(1)1\ 4f + 1(7)8$	4^e	1.027657E+03	1.014200E+03	-0.63(73)0.57(60) - 0.52(67)
26	74	$2s^2 2p^5 4f$	3F_2	$2p - 1(1)1\ 4f - 1(5)4$	2^e	1.027779E+03	...	-0.69(74) - 0.57(65) - 0.45(63)
26	75	$2s^2 2p^5 4f$	3D_3	$2p - 1(1)1\ 4f + 1(7)6$	3^e	1.027786E+03	1.027710E+03	-0.72(75) - 0.54(64)0.43(66)
26	76	$2s^2 2p^5 5s$	3P_2	$2p + 3(3)3\ 5s + 1(1)4$	2^o	1.084748E+03	...	1.00(76)
26	77	$2s^2 2p^5 5s$	1P_1	$2p + 3(3)3\ 5s + 1(1)2$	1^o	1.085063E+03	1.085730E+03	0.81(77)0.59(85)
26	78	$2s^2 2p^5 5p$	3S_1	$2p + 3(3)3\ 5p - 1(1)2$	1^e	1.090937E+03	...	-0.82(78)0.56(111)
26	79	$2s^2 2p^5 5p$	3D_2	$2p + 3(3)3\ 5p - 1(1)4$	2^e	1.091448E+03	...	0.72(79)0.59(112)
26	80	$2s^2 2p^5 5p$	3D_3	$2p + 3(3)3\ 5p + 1(3)6$	3^e	1.091783E+03	...	1.00(80)
26	81	$2s^2 2p^5 5p$	1P_1	$2p + 3(3)3\ 5p + 1(3)2$	1^e	1.091979E+03	...	-0.79(81)0.41(103)

Table 1 continued

Table 1 (*continued*)

Z	Key	Conf	<i>LSJ</i>	<i>jj</i> ^{a,b,c}	<i>J</i> ^π	Energy		<i>LSJ</i> ^f
						NIST ^d	MBPT ^e	
26	82	$2s^22p^55p$	3P_2	$2p + 3(3)3\ 5p + 1(3)4$	2^e	1.092280E+03	...	-0.83(82) - 0.55(112)
26	83	$2s^22p^55p$	1S_0	$2p + 3(3)3\ 5p + 1(3)0$	0^e	1.094073E+03	...	-0.74(83)0.67(113)
26	84	$2s^22p^55s$	3P_0	$2p - 1(1)1\ 5s + 1(1)0$	0^o	1.097393E+03	...	-1.00(84)
26	85	$2s^22p^55s$	3P_1	$2p - 1(1)1\ 5s + 1(1)2$	1^o	1.097588E+03	1.098500E+03	-0.80(85)0.59(77)
26	86	$2s^22p^55d$	3P_0	$2p + 3(3)3\ 5d - 1(3)0$	0^o	1.099155E+03	...	-1.00(86)
26	87	$2s^22p^55d$	3P_1	$2p + 3(3)3\ 5d - 1(3)2$	1^o	1.099383E+03	1.098500E+03	0.90(87) - 0.42(119)
26	88	$2s^22p^55d$	3F_4	$2p + 3(3)3\ 5d + 1(5)8$	4^o	1.099625E+03	...	1.00(88)
26	89	$2s^22p^55d$	3P_2	$2p + 3(3)3\ 5d + 1(5)4$	2^o	1.099728E+03	...	-0.73(89)0.58(117)
26	90	$2s^22p^55d$	3F_3	$2p + 3(3)3\ 5d - 1(3)6$	3^o	1.099759E+03	...	-0.75(90) - 0.59(118)
26	91	$2s^22p^55d$	1D_2	$2p + 3(3)3\ 5d - 1(3)4$	2^o	1.100054E+03	...	-0.72(91) - 0.49(117)0.49(116)
26	92	$2s^22p^55d$	3D_3	$2p + 3(3)3\ 5d + 1(5)6$	3^o	1.100243E+03	...	-0.83(92) - 0.55(118)
26	93	$2s^22p^55d$	1P_1	$2p + 3(3)3\ 5d + 1(5)2$	1^o	1.101529E+03	1.101850E+03	0.76(93) - 0.61(119)
26	94	$2s^22p^55f$	3D_1	$2p + 3(3)3\ 5f - 1(5)2$	1^e	1.103417E+03	...	-0.98(94)
26	95	$2s^22p^55f$	3D_2	$2p + 3(3)3\ 5f + 1(7)4$	2^e	1.103526E+03	...	-0.88(95)0.41(99)
26	96	$2s^22p^55f$	1G_4	$2p + 3(3)3\ 5f - 1(5)8$	4^e	1.103541E+03	...	0.72(96)0.70(121)
26	97	$2s^22p^55f$	3G_5	$2p + 3(3)3\ 5f + 1(7)10$	5^e	1.103548E+03	1.103830E+03	-1.00(97)
26	98	$2s^22p^55f$	3F_3	$2p + 3(3)3\ 5f + 1(7)6$	3^e	1.103736E+03	...	-0.68(122)0.60(98) - 0.42(100)
26	99	$2s^22p^55f$	1D_2	$2p + 3(3)3\ 5f - 1(5)4$	2^e	1.103798E+03	...	0.71(99) - 0.69(123)
26	100	$2s^22p^55f$	1F_3	$2p + 3(3)3\ 5f - 1(5)6$	3^e	1.103818E+03	...	-0.69(100)0.51(120) - 0.51(98)
26	101	$2s^22p^55f$	3F_4	$2p + 3(3)3\ 5f + 1(7)8$	4^e	1.103865E+03	...	-0.86(101)
26	102	$2s^22p^55g$	3F_2	$2p + 3(3)3\ 5g - 1(7)4$	2^o	1.103950E+03	...	-1.00(102)
26	103	$2s^22p^55p$	3D_1	$2p - 1(1)1\ 5p - 1(1)2$	1^e	1.103975E+03	...	0.78(103)0.54(81)
26	104	$2s^22p^55g$	3F_3	$2p + 3(3)3\ 5g + 1(9)6$	3^o	1.103975E+03	...	0.78(104) - 0.63(124)
26	105	$2s^22p^55g$	1H_5	$2p + 3(3)3\ 5g - 1(7)10$	5^o	1.104048E+03	...	-0.73(105) - 0.68(127)
26	106	$2s^22p^55g$	3H_6	$2p + 3(3)3\ 5g + 1(9)12$	6^o	1.104072E+03	...	1.00(106)
26	107	$2s^22p^55g$	3G_3	$2p + 3(3)3\ 5g - 1(7)6$	3^o	1.104132E+03	...	0.75(107) - 0.53(124)
26	108	$2s^22p^55g$	3G_4	$2p + 3(3)3\ 5g + 1(9)8$	4^o	1.104150E+03	...	0.65(125) - 0.62(108)0.44(109)
26	109	$2s^22p^55g$	1G_4	$2p + 3(3)3\ 5g - 1(7)8$	4^o	1.104204E+03	...	-0.68(109)0.52(126) - 0.51(108)
26	110	$2s^22p^55g$	3G_5	$2p + 3(3)3\ 5g + 1(9)10$	5^o	1.104226E+03	...	-0.85(110)
26	111	$2s^22p^55p$	3P_1	$2p - 1(1)1\ 5p + 1(3)2$	1^e	1.104375E+03	...	-0.73(111) - 0.46(103) - 0.44(78)
26	112	$2s^22p^55p$	1D_2	$2p - 1(1)1\ 5p + 1(3)4$	2^e	1.104692E+03	...	-0.69(79)0.58(112) - 0.42(82)
26	113	$2s^22p^55p$	3P_0	$2p - 1(1)1\ 5p - 1(1)0$	0^e	1.105511E+03	...	0.74(113)0.66(83)
26	114	$2s2p^64s$	3S_1	$2s + 1(1)1\ 4s + 1(1)2$	1^e	1.109417E+03	...	0.97(114)
26	115	$2s2p^64s$	1S_0	$2s + 1(1)1\ 4s + 1(1)0$	0^e	1.111182E+03	...	0.99(115)
26	116	$2s^22p^55d$	3F_2	$2p - 1(1)1\ 5d - 1(3)4$	2^o	1.112357E+03	...	-0.85(116) - 0.48(91)
26	117	$2s^22p^55d$	3D_2	$2p - 1(1)1\ 5d + 1(5)4$	2^o	1.112464E+03	...	0.66(89)0.63(117)
26	118	$2s^22p^55d$	1F_3	$2p - 1(1)1\ 5d + 1(5)6$	3^o	1.112637E+03	...	-0.65(90)0.59(118) - 0.48(92)
26	119	$2s^22p^55d$	3D_1	$2p - 1(1)1\ 5d - 1(3)2$	1^o	1.113443E+03	1.113630E+03	0.67(119)0.65(93)
26	120	$2s^22p^55f$	3G_3	$2p - 1(1)1\ 5f - 1(5)6$	3^e	1.116308E+03	...	-0.85(120) - 0.44(100)
26	121	$2s^22p^55f$	3G_4	$2p - 1(1)1\ 5f + 1(7)8$	4^e	1.116369E+03	...	-0.64(121)0.57(96) - 0.51(101)
26	122	$2s^22p^55f$	3D_3	$2p - 1(1)1\ 5f + 1(7)6$	3^e	1.116374E+03	...	-0.73(122) - 0.55(98)
26	123	$2s^22p^55f$	3F_2	$2p - 1(1)1\ 5f - 1(5)4$	2^e	1.116412E+03	...	0.68(123)0.57(99)0.46(95)

Table 1 continued

Table 1 (*continued*)

Z	Key	Conf	<i>LSJ</i>	<i>jj</i> ^{a,b,c}	<i>J</i> ^π	Energy		Mixing coefficients <i>LSJ</i> ^f
						NIST ^d	MBPT ^e	
26	124	$2s^22p^55g$	1F_3	$2p - 1(1)1\ 5g - 1(7)6$	3^o	1.116761E+03	...	0.66(107)0.57(124)0.49(104)
26	125	$2s^22p^55g$	3F_4	$2p - 1(1)1\ 5g + 1(9)8$	4^o	1.116781E+03	...	0.75(125) - 0.49(109)0.43(108)
26	126	$2s^22p^55g$	3H_4	$2p - 1(1)1\ 5g - 1(7)8$	4^o	1.116800E+03	...	-0.84(126) - 0.42(108)
26	127	$2s^22p^55g$	3H_5	$2p - 1(1)1\ 5g + 1(9)10$	5^o	1.116824E+03	...	-0.63(127)0.57(105) - 0.52(110)
26	128	$2s2p^64p$	3P_0	$2s + 1(1)1\ 4p - 1(1)0$	0^o	1.122371E+03	...	-1.00(128)
26	129	$2s2p^64p$	3P_1	$2s + 1(1)1\ 4p - 1(1)2$	1^o	1.122541E+03	1.122800E+03	-0.93(129)
26	130	$2s2p^64p$	3P_2	$2s + 1(1)1\ 4p + 1(3)4$	2^o	1.123451E+03	...	1.00(130)
26	131	$2s2p^64p$	1P_1	$2s + 1(1)1\ 4p + 1(3)2$	1^o	1.124112E+03	1.124780E+03	-0.93(131)
26	132	$2s2p^64d$	3D_1	$2s + 1(1)1\ 4d - 1(3)2$	1^e	1.139075E+03	...	1.00(132)
26	133	$2s2p^64d$	3D_2	$2s + 1(1)1\ 4d - 1(3)4$	2^e	1.139135E+03	...	-0.99(133)
26	134	$2s2p^64d$	3D_3	$2s + 1(1)1\ 4d + 1(5)6$	3^e	1.139259E+03	...	-0.99(134)
26	135	$2s2p^64d$	1D_2	$2s + 1(1)1\ 4d + 1(5)4$	2^e	1.141022E+03	...	-0.99(135)
26	136	$2s^22p^56s$	3P_2	$2p + 3(3)3\ 6s + 1(1)4$	2^o	1.141273E+03	...	1.00(136)
26	137	$2s^22p^56s$	1P_1	$2p + 3(3)3\ 6s + 1(1)2$	1^o	1.141421E+03	1.142640E+03	-0.81(137) - 0.58(181)
26	138	$2s^22p^56p$	3S_1	$2p + 3(3)3\ 6p - 1(1)2$	1^e	1.144840E+03	...	-0.78(138)0.60(183)
26	139	$2s^22p^56p$	3D_2	$2p + 3(3)3\ 6p - 1(1)4$	2^e	1.145071E+03	...	0.71(139)0.56(184) - 0.41(142)
26	140	$2s^22p^56p$	3D_3	$2p + 3(3)3\ 6p + 1(3)6$	3^e	1.145269E+03	...	-1.00(140)
26	141	$2s^22p^56p$	1P_1	$2p + 3(3)3\ 6p + 1(3)2$	1^e	1.145332E+03	...	-0.81(141)
26	142	$2s^22p^56p$	3P_2	$2p + 3(3)3\ 6p + 1(3)4$	2^e	1.145501E+03	...	-0.81(142) - 0.58(184)
26	143	$2s^22p^56p$	1S_0	$2p + 3(3)3\ 6p + 1(3)0$	0^e	1.146513E+03	...	0.78(143) - 0.63(185)
26	144	$2s2p^64f$	3F_2	$2s + 1(1)1\ 4f - 1(5)4$	2^o	1.146719E+03	...	-0.98(144)
26	145	$2s2p^64f$	3F_3	$2s + 1(1)1\ 4f + 1(7)6$	3^o	1.146795E+03	...	0.98(145)
26	146	$2s2p^64f$	3F_4	$2s + 1(1)1\ 4f + 1(7)8$	4^o	1.146908E+03	...	-0.99(146)
26	147	$2s2p^64f$	1F_3	$2s + 1(1)1\ 4f - 1(5)6$	3^o	1.146974E+03	...	-0.98(147)
26	148	$2s^22p^56d$	3P_0	$2p + 3(3)3\ 6d - 1(3)0$	0^o	1.149352E+03	...	1.00(148)
26	149	$2s^22p^56d$	3P_1	$2p + 3(3)3\ 6d - 1(3)2$	1^o	1.149483E+03	...	-0.90(149)0.43(189)
26	150	$2s^22p^56d$	3F_4	$2p + 3(3)3\ 6d + 1(5)8$	4^o	1.149609E+03	...	1.00(150)
26	151	$2s^22p^56d$	3P_2	$2p + 3(3)3\ 6d + 1(5)4$	2^o	1.149677E+03	...	0.72(151) - 0.60(187)
26	152	$2s^22p^56d$	3F_3	$2p + 3(3)3\ 6d - 1(3)6$	3^o	1.149688E+03	...	-0.75(152) - 0.59(188)
26	153	$2s^22p^56d$	1D_2	$2p + 3(3)3\ 6d - 1(3)4$	2^o	1.149846E+03	...	-0.73(153) - 0.49(187)0.48(186)
26	154	$2s^22p^56d$	3D_3	$2p + 3(3)3\ 6d + 1(5)6$	3^o	1.149957E+03	...	0.82(154)0.56(188)
26	155	$2s^22p^56d$	1P_1	$2p + 3(3)3\ 6d + 1(5)2$	1^o	1.150688E+03	1.151190E+03	0.78(155) - 0.58(189)
26	156	$2s^22p^56f$	1G_4	$2p + 3(3)3\ 6f - 1(5)8$	4^e	1.151840E+03	...	0.71(156)0.70(191)
26	157	$2s^22p^56f$	3G_5	$2p + 3(3)3\ 6f + 1(7)10$	5^e	1.151841E+03	...	-1.00(157)
26	158	$2s^22p^56f$	3D_1	$2p + 3(3)3\ 6f - 1(5)2$	1^e	1.151866E+03	...	1.00(158)
26	159	$2s^22p^56f$	3D_2	$2p + 3(3)3\ 6f + 1(7)4$	2^e	1.151906E+03	...	-0.87(159)0.41(162)
26	160	$2s^22p^56f$	3F_3	$2p + 3(3)3\ 6f - 1(5)6$	3^e	1.151987E+03	...	0.77(160) - 0.58(192)
26	161	$2s^22p^56f$	1F_3	$2p + 3(3)3\ 6f + 1(7)6$	3^e	1.151996E+03	...	0.81(161) - 0.44(190)
26	162	$2s^22p^56f$	1D_2	$2p + 3(3)3\ 6f - 1(5)4$	2^e	1.152004E+03	...	0.70(162) - 0.70(193)
26	163	$2s^22p^56f$	3F_4	$2p + 3(3)3\ 6f + 1(7)8$	4^e	1.152023E+03	...	-0.86(163)
26	164	$2s^22p^56g$	1H_5	$2p + 3(3)3\ 6g - 1(7)10$	5^o	1.152158E+03	...	0.73(164)0.69(195)
26	165	$2s^22p^56g$	3H_6	$2p + 3(3)3\ 6g + 1(9)12$	6^o	1.152171E+03	...	1.00(165)

Table 1 continued

Table 1 (*continued*)

Z	Key	Conf	<i>LSJ</i>	<i>jj</i> ^{a,b,c}	<i>J</i> ^π	Energy		<i>LSJ</i> ^f
						NIST ^d	MBPT ^e	
26	166	$2s^22p^56h$	3G_3	$2p + 3(3)3\ 6h - 1(9)6$	3^e	1.152197E+03	...	1.00(166)
26	167	$2s^22p^56h$	3G_4	$2p + 3(3)3\ 6h + 1(11)8$	4^e	1.152206E+03	...	0.76(167) - 0.65(196)
26	168	$2s^22p^56h$	1I_6	$2p + 3(3)3\ 6h - 1(9)12$	6^e	1.152211E+03	...	0.72(168)0.69(200)
26	169	$2s^22p^56h$	3I_7	$2p + 3(3)3\ 6h + 1(11)14$	7^e	1.152221E+03	...	1.00(169)
26	170	$2s^22p^56h$	3H_4	$2p + 3(3)3\ 6h - 1(9)8$	4^e	1.152247E+03	...	-0.77(170)0.50(196)
26	171	$2s^22p^56g$	1G_4	$2p + 3(3)3\ 6g - 1(7)8$	4^o	1.152247E+03	...	0.62(171)0.59(177) - 0.52(194)
26	172	$2s^22p^56h$	3H_5	$2p + 3(3)3\ 6h + 1(11)10$	5^e	1.152255E+03	...	-0.70(172)0.61(199)
26	173	$2s^22p^56g$	3G_5	$2p + 3(3)3\ 6g + 1(9)10$	5^o	1.152260E+03	...	-0.85(173)
26	174	$2s^22p^56h$	1H_5	$2p + 3(3)3\ 6h - 1(9)10$	5^e	1.152261E+03	...	-0.74(174)0.51(197)
26	175	$2s^22p^56h$	3H_6	$2p + 3(3)3\ 6h + 1(11)12$	6^e	1.152270E+03	...	0.85(175)
26	176	$2s^22p^56g$	3G_3	$2p + 3(3)3\ 6g - 1(7)6$	3^o	1.152324E+03	...	0.76(176) - 0.46(198) - 0.45(179)
26	177	$2s^22p^56g$	3G_4	$2p + 3(3)3\ 6g + 1(9)8$	4^o	1.152338E+03	...	0.64(201) - 0.55(177)0.53(171)
26	178	$2s^22p^56g$	3F_2	$2p + 3(3)3\ 6g - 1(7)4$	2^o	1.152384E+03	...	-0.98(178)
26	179	$2s^22p^56g$	3F_3	$2p + 3(3)3\ 6g + 1(9)6$	3^o	1.152400E+03	...	-0.72(179)0.66(198)
26	180	$2s^22p^56s$	3P_0	$2p - 1(1)1\ 6s + 1(1)0$	0^o	1.153941E+03	...	1.00(180)
26	181	$2s^22p^56s$	3P_1	$2p - 1(1)1\ 6s + 1(1)2$	1^o	1.154050E+03	...	-0.81(181)0.58(137)
26	182	$2s^22p^56p$	3D_1	$2p - 1(1)1\ 6p - 1(1)2$	1^e	1.157641E+03	...	-0.85(182) - 0.48(141)
26	183	$2s^22p^56p$	3P_1	$2p - 1(1)1\ 6p + 1(3)2$	1^e	1.157955E+03	...	-0.72(183) - 0.52(138)
26	184	$2s^22p^56p$	1D_2	$2p - 1(1)1\ 6p + 1(3)4$	2^e	1.158034E+03	...	0.70(139) - 0.58(184)0.41(142)
26	185	$2s^22p^56p$	3P_0	$2p - 1(1)1\ 6p - 1(1)0$	0^e	1.158419E+03	...	-0.78(185) - 0.63(143)
26	186	$2s^22p^56d$	3F_2	$2p - 1(1)1\ 6d - 1(3)4$	2^o	1.162320E+03	...	0.86(186)0.46(153)
26	187	$2s^22p^56d$	3D_2	$2p - 1(1)1\ 6d + 1(5)4$	2^o	1.162387E+03	...	-0.68(151) - 0.61(187)
26	188	$2s^22p^56d$	1F_3	$2p - 1(1)1\ 6d + 1(5)6$	3^o	1.162480E+03	...	0.66(152) - 0.58(188)0.48(154)
26	189	$2s^22p^56d$	3D_1	$2p - 1(1)1\ 6d - 1(3)2$	1^o	1.162906E+03	1.163340E+03	-0.69(189) - 0.62(155)
26	190	$2s^22p^56f$	3G_3	$2p - 1(1)1\ 6f - 1(5)6$	3^e	1.164571E+03	...	0.86(190)0.41(161)
26	191	$2s^22p^56f$	3G_4	$2p - 1(1)1\ 6f + 1(7)8$	4^e	1.164609E+03	...	0.64(191) - 0.58(156)0.51(163)
26	192	$2s^22p^56f$	3D_3	$2p - 1(1)1\ 6f + 1(7)6$	3^e	1.164641E+03	...	-0.74(192) - 0.53(160)0.41(161)
26	193	$2s^22p^56f$	3F_2	$2p - 1(1)1\ 6f - 1(5)4$	2^e	1.164653E+03	...	-0.67(193) - 0.58(162) - 0.47(159)
26	194	$2s^22p^56g$	3H_4	$2p - 1(1)1\ 6g - 1(7)8$	4^o	1.164885E+03	...	0.85(194)
26	195	$2s^22p^56g$	3H_5	$2p - 1(1)1\ 6g + 1(9)10$	5^o	1.164899E+03	...	0.63(195) - 0.58(164)0.52(173)
26	196	$2s^22p^56h$	1G_4	$2p - 1(1)1\ 6h - 1(9)8$	4^e	1.164923E+03	...	0.63(170)0.58(196)0.51(167)
26	197	$2s^22p^56h$	3I_5	$2p - 1(1)1\ 6h - 1(9)10$	5^e	1.164925E+03	...	-0.84(197) - 0.44(174)
26	198	$2s^22p^56g$	1F_3	$2p - 1(1)1\ 6g - 1(7)6$	3^o	1.164931E+03	...	0.65(176)0.58(198)0.50(179)
26	199	$2s^22p^56h$	3G_5	$2p - 1(1)1\ 6h + 1(11)10$	5^e	1.164932E+03	...	0.77(199)0.51(172)
26	200	$2s^22p^56h$	3I_6	$2p - 1(1)1\ 6h + 1(11)12$	6^e	1.164934E+03	...	0.62(200) - 0.58(168)0.53(175)
26	201	$2s^22p^56g$	3F_4	$2p - 1(1)1\ 6g + 1(9)8$	4^o	1.164944E+03	...	0.76(201)0.49(177) - 0.42(171)

Table 1 continued

Table 1 (*continued*)

Z	Key	Conf	<i>LSJ</i>	<i>jj</i> ^{a,b,c}	<i>J</i> ^π	Energy		Mixing coefficients
						NIST ^d	MBPT ^e	

^aThe number at the end or inside of the bracket is $2J$.

^b $s+ = s_{1/2}$, $p- = p_{1/2}$, $p+ = p_{3/2}$, $d- = d_{3/2}$, $d+ = d_{5/2}$, $f- = f_{5/2}$, $f+ = f_{7/2}$, $g- = g_{7/2}$, $g+ = g_{9/2}$, $h- = h_{9/2}$, and $h+ = h_{11/2}$.

^cThe number after \pm is the occupation number of the corresponding sub-shell. For example, the jj configuration of level 2 is $2s_{1/2}^2 2p_{1/2}^2 2p_{3/2}^3 3s_{1/2}$.

^dThe observed energies from the NIST ASD ([Kramida et al. 2015](#)).

^eThe present MBPT results.

^fThe mixing coefficient of the LSJ basis of the state indicated by the key in parenthesis.

NOTE—Only the 201 levels in Ne-like Fe are shown here. Table 1 is available online in its entirety in the home page of *ApJS*. A portion is shown here for guidance regarding its form and content.

Table 2. Wavelengths(λ , in Å), line strengths(S , in atomic units), weighted oscillator strengths (gf , dimensionless) and transition rates(A , in s^{-1}) for the transitions in Ne-like ions from Cr XV to Kr XXVII.

Z	$j - i$	Type	λ	S	gf	A
26	2 – 1	M2	1.7103E+01	1.013E–01	4.525E–08	2.063E+05
26	3 – 1	E1	1.7059E+01	6.862E–03	1.222E–01	9.335E+11
26	3 – 2	M1	6.6341E+03	1.118E+00	6.816E–07	3.443E+01
26	4 – 3	M1	1.1529E+03	8.879E–01	3.114E–06	1.563E+04
26	5 – 1	E1	1.6784E+01	5.518E–03	9.986E–02	7.882E+11
26	5 – 2	M1	8.9783E+02	1.347E+00	6.069E–06	1.674E+04
26	5 – 3	M1	1.0384E+03	3.670E–01	1.429E–06	2.948E+03
26	5 – 4	M1	1.0448E+04	1.089E+00	4.214E–07	8.582E+00
26	6 – 2	E1	4.0894E+02	3.317E–01	2.464E–01	3.276E+09
26	6 – 2	M2	4.0894E+02	2.073E+00	6.775E–11	9.008E–01
26	6 – 3	E1	4.3580E+02	1.450E–02	1.010E–02	1.183E+08
26	6 – 3	M2	4.3580E+02	8.995E–02	2.429E–12	2.844E–02
26	6 – 4	E1	7.0064E+02	5.001E–03	2.168E–03	9.820E+06
26	6 – 5	E1	7.5101E+02	6.879E–03	2.782E–03	1.097E+07
26	6 – 5	M2	7.5101E+02	3.746E–01	1.977E–12	7.793E–03
26	7 – 1	E2	1.6342E+01	2.650E–03	1.019E–04	5.092E+08
26	7 – 2	E1	3.6705E+02	2.948E–01	2.440E–01	2.416E+09
26	7 – 2	M2	3.6705E+02	1.516E–02	6.852E–13	6.785E–03
26	7 – 3	E1	3.8855E+02	3.486E–01	2.726E–01	2.408E+09
26	7 – 4	M2	5.8606E+02	3.748E–02	4.162E–13	1.616E–03
26	7 – 5	M2	6.2089E+02	5.741E–02	5.361E–13	1.855E–03
26	7 – 6	M1	3.5835E+03	1.363E–01	1.538E–07	1.598E+01
26	7 – 6	E2	3.5835E+03	2.679E–02	9.775E–11	1.015E–02
26	8 – 2	E1	3.5015E+02	9.000E–01	7.808E–01	6.068E+09
26	8 – 2	M2	3.5015E+02	5.908E+00	3.076E–10	2.391E+00
26	8 – 3	M2	3.6966E+02	8.564E+00	3.790E–10	2.643E+00
26	8 – 5	M2	5.7401E+02	1.152E–01	1.361E–12	3.936E–03
26	8 – 6	E2	2.4356E+03	1.768E–01	2.054E–09	3.300E–01
26	8 – 7	M1	7.6035E+03	2.688E+00	1.430E–06	2.356E+01
26	8 – 7	E2	7.6035E+03	1.070E–01	4.089E–11	6.739E–04

Table 2 continued

Table 2 (*continued*)

<i>Z</i>	<i>j - i</i>	Type	λ	<i>S</i>	<i>gf</i>	<i>A</i>
26	9 - 2	E1	3.3946E+02	1.857E-02	1.662E-02	3.207E+08
26	9 - 2	M2	3.3946E+02	3.717E+00	2.124E-10	4.098E+00
26	9 - 3	E1	3.5776E+02	3.643E-01	3.093E-01	5.373E+09
26	9 - 3	M2	3.5776E+02	3.901E-01	1.904E-11	3.308E-01
26	9 - 5	M2	5.4582E+02	2.865E-02	3.938E-13	2.939E-03
26	9 - 6	M1	1.9978E+03	8.962E-02	1.814E-07	1.011E+02
26	9 - 7	M1	4.5148E+03	1.088E+00	9.749E-07	1.063E+02
26	9 - 7	E2	4.5148E+03	9.070E-02	1.655E-10	1.805E-02
26	9 - 8	E2	1.1114E+04	1.424E-02	1.742E-12	3.135E-05
26	10 - 1	E2	1.6244E+01	2.742E-03	1.074E-04	5.430E+08
26	10 - 2	E1	3.2344E+02	3.549E-01	3.333E-01	4.250E+09
26	10 - 2	M2	3.2344E+02	6.818E+00	4.504E-10	5.743E+00
26	10 - 3	E1	3.4002E+02	2.972E-01	2.655E-01	3.064E+09
26	10 - 3	M2	3.4002E+02	3.018E+00	1.716E-10	1.980E+00
26	10 - 5	E1	5.0557E+02	6.891E-03	4.140E-03	2.161E+07
26	10 - 5	M2	5.0557E+02	1.632E-02	2.822E-13	1.473E-03
26	10 - 6	M1	1.5470E+03	2.945E-01	7.699E-07	4.292E+02
26	10 - 7	M1	2.7221E+03	6.209E-01	9.223E-07	1.660E+02
26	10 - 7	E2	2.7221E+03	1.547E-01	1.288E-09	2.319E-01
26	10 - 8	E2	4.2401E+03	1.664E-01	3.665E-10	2.720E-02
26	10 - 9	M1	6.8557E+03	3.783E-01	2.232E-07	6.334E+00
26	10 - 9	E2	6.8557E+03	1.190E-01	6.199E-11	1.760E-03
26	11 - 2	M2	2.8326E+02	1.239E+00	1.219E-10	1.013E+01
26	11 - 3	E1	2.9590E+02	9.723E-02	9.981E-02	7.604E+09
26	11 - 5	E1	4.1383E+02	3.585E-02	2.632E-02	1.025E+09
26	11 - 6	M1	9.2172E+02	3.200E-01	1.404E-06	1.102E+04
26	11 - 7	E2	1.2409E+03	4.363E-02	3.834E-09	1.661E+01
26	11 - 9	M1	1.7112E+03	3.481E-01	8.225E-07	1.874E+03
26	11 - 10	E2	2.2804E+03	1.724E-02	2.441E-10	3.131E-01
26	12 - 2	E1	2.7036E+02	3.794E-04	4.263E-04	1.297E+07
26	12 - 2	M2	2.7036E+02	1.096E-01	1.239E-11	3.770E-01
26	12 - 3	E1	2.8185E+02	1.106E-03	1.192E-03	3.335E+07
26	12 - 3	M2	2.8185E+02	1.375E-02	1.373E-12	3.844E-02

Table 2 *continued*

Table 2 (*continued*)

<i>Z</i>	<i>j – i</i>	Type	λ	<i>S</i>	<i>gf</i>	<i>A</i>
26	12 – 4	E1	3.7304E+02	1.485E–01	1.209E–01	1.932E+09
26	12 – 5	E1	3.8685E+02	2.310E–01	1.814E–01	2.695E+09
26	12 – 5	M2	3.8685E+02	3.336E–02	1.288E–12	1.913E–02
26	12 – 6	M1	7.9781E+02	9.948E–02	5.042E–07	1.761E+03
26	12 – 7	M1	1.0263E+03	1.642E+00	6.469E–06	1.366E+04
26	12 – 9	M1	1.3282E+03	2.443E–01	7.438E–07	9.373E+02
26	13 – 2	E1	2.5246E+02	1.902E–02	2.289E–02	7.984E+08
26	13 – 2	M2	2.5246E+02	9.527E–02	1.323E–11	4.617E–01
26	13 – 3	M2	2.6244E+02	2.115E–01	2.615E–11	8.442E–01
26	13 – 4	E1	3.3979E+02	2.283E–01	2.041E–01	3.930E+09
26	13 – 5	E1	3.5121E+02	1.387E–01	1.200E–01	2.162E+09
26	13 – 5	M2	3.5121E+02	5.608E+00	2.894E–10	5.216E+00
26	13 – 6	M1	6.5974E+02	1.383E–01	8.478E–07	4.331E+03
26	13 – 8	E2	9.0484E+02	2.065E–02	4.680E–09	1.271E+01
26	13 – 9	M1	9.8503E+02	5.868E–01	2.409E–06	5.521E+03
26	13 – 10	M1	1.1503E+03	9.983E–01	3.509E–06	5.897E+03
26	13 – 11	M1	2.3212E+03	1.154E+00	2.011E–06	8.299E+02
26	13 – 12	M1	3.8121E+03	7.044E–02	7.472E–08	1.143E+01
26	13 – 12	E2	3.8121E+03	1.357E–01	4.114E–10	6.294E–02
26	14 – 1	E2	1.6010E+01	3.062E–03	1.253E–04	6.519E+08
26	14 – 2	E1	2.5058E+02	4.105E–03	4.976E–03	1.057E+08
26	14 – 3	E1	2.6041E+02	3.269E–03	3.813E–03	7.501E+07
26	14 – 3	M2	2.6041E+02	6.802E–02	8.609E–12	1.694E–01
26	14 – 4	M2	3.3640E+02	4.071E+00	2.391E–10	2.818E+00
26	14 – 5	E1	3.4759E+02	6.433E–01	5.622E–01	6.207E+09
26	14 – 5	M2	3.4759E+02	6.036E+00	3.213E–10	3.548E+00
26	14 – 6	M1	6.4707E+02	2.958E–02	1.849E–07	5.891E+02
26	14 – 8	M1	8.8117E+02	1.899E+00	8.715E–06	1.497E+04
26	14 – 9	M1	9.5705E+02	1.356E–01	5.729E–07	8.345E+02
26	14 – 10	M1	1.1123E+03	9.925E–01	3.608E–06	3.890E+03
26	14 – 11	E2	2.1715E+03	3.689E–02	6.049E–10	1.711E–01
26	14 – 12	M1	3.4246E+03	1.346E+00	1.589E–06	1.808E+02
26	14 – 12	E2	3.4246E+03	1.242E–01	5.194E–10	5.908E–02

Table 2 continued

Table 2 (*continued*)

<i>Z</i>	<i>j – i</i>	Type	λ	<i>S</i>	<i>gf</i>	<i>A</i>
26	14 – 13	M1	3.3685E+04	8.485E–01	1.019E–07	1.198E–01
26	14 – 13	E2	3.3685E+04	7.639E–02	3.356E–13	3.946E–07
26	15 – 2	M2	1.9973E+02	9.379E–01	2.631E–10	4.400E+01
26	15 – 3	E1	2.0593E+02	4.535E–02	6.690E–02	1.052E+10
26	15 – 5	E1	2.5687E+02	1.043E–01	1.234E–01	1.247E+10
26	15 – 6	M1	3.9040E+02	2.317E–02	2.400E–07	1.050E+04
26	15 – 9	M1	4.8522E+02	2.693E–02	2.245E–07	6.359E+03
26	15 – 10	E2	5.2218E+02	1.519E–02	1.791E–08	4.381E+02
26	15 – 13	M1	9.5627E+02	8.644E–02	3.655E–07	2.666E+03
26	15 – 14	E2	9.8421E+02	4.991E–02	8.789E–09	6.052E+01
26	16 – 2	E2	1.6279E+02	3.402E–02	1.324E–06	3.332E+05
26	16 – 6	E1	2.7046E+02	1.054E–01	1.184E–01	1.080E+10
26	16 – 7	M2	2.9254E+02	3.942E–02	3.519E–12	2.743E–01
26	16 – 9	E1	3.1281E+02	4.262E–03	4.138E–03	2.821E+08
26	16 – 13	E1	4.5838E+02	5.990E–03	3.969E–03	1.260E+08
26	17 – 1	E1	1.5459E+01	4.946E–04	9.718E–03	9.042E+10
26	17 – 2	E2	1.6078E+02	9.551E–02	3.858E–06	3.319E+05
26	17 – 6	E1	2.6494E+02	2.507E–01	2.874E–01	9.105E+09
26	17 – 6	M2	2.6494E+02	8.937E–01	1.074E–10	3.402E+00
26	17 – 7	E1	2.8609E+02	2.730E–02	2.898E–02	7.874E+08
26	17 – 7	M2	2.8609E+02	3.174E–01	3.030E–11	8.230E–01
26	17 – 8	M2	2.9728E+02	2.598E–02	2.211E–12	5.562E–02
26	17 – 9	M2	3.0545E+02	3.244E–01	2.544E–11	6.064E–01
26	17 – 10	E1	3.1969E+02	5.022E–02	4.772E–02	1.038E+09
26	17 – 10	M2	3.1969E+02	5.803E–01	3.970E–11	8.637E–01
26	17 – 11	E1	3.7182E+02	1.196E–02	9.768E–03	1.571E+08
26	17 – 13	M2	4.4274E+02	7.413E–02	1.909E–12	2.166E–02
26	17 – 16	M1	1.2975E+04	1.800E+00	5.612E–07	7.411E+00
26	18 – 1	M2	1.5424E+01	1.809E+00	1.102E–06	6.180E+06
26	18 – 2	E2	1.5709E+02	1.189E–01	5.149E–06	2.784E+05
26	18 – 3	E2	1.6090E+02	4.405E–02	1.775E–06	9.149E+04
26	18 – 6	E1	2.5508E+02	2.107E–01	2.509E–01	5.143E+09
26	18 – 6	M2	2.5508E+02	1.195E+00	1.610E–10	3.301E+00

Table 2 *continued*

Table 2 (*continued*)

<i>Z</i>	<i>j – i</i>	Type	λ	<i>S</i>	<i>gf</i>	<i>A</i>
26	18 – 7	E1	2.7463E+02	4.082E–02	4.515E–02	7.985E+08
26	18 – 7	M2	2.7463E+02	6.015E–01	6.491E–11	1.148E+00
26	18 – 8	E1	2.8492E+02	1.970E–02	2.100E–02	3.452E+08
26	18 – 8	M2	2.8492E+02	1.595E+00	1.541E–10	2.532E+00
26	18 – 9	E1	2.9242E+02	6.291E–02	6.535E–02	1.019E+09
26	18 – 9	M2	2.9242E+02	6.929E–02	6.194E–12	9.663E–02
26	18 – 10	E1	3.0545E+02	2.492E–01	2.478E–01	3.543E+09
26	18 – 10	M2	3.0545E+02	5.621E+00	4.409E–10	6.304E+00
26	18 – 11	M2	3.5269E+02	1.215E+00	6.191E–11	6.639E–01
26	18 – 12	E1	3.7497E+02	1.596E–03	1.293E–03	1.226E+07
26	18 – 12	M2	3.7497E+02	3.048E–02	1.292E–12	1.226E–02
26	18 – 13	E1	4.1588E+02	2.105E–03	1.537E–03	1.186E+07
26	18 – 13	M2	4.1588E+02	2.038E–01	6.332E–12	4.884E–02
26	18 – 14	E1	4.2108E+02	6.991E–03	5.043E–03	3.795E+07
26	18 – 14	M2	4.2108E+02	3.107E–01	9.302E–12	6.998E–02
26	18 – 15	M2	7.3593E+02	1.448E+00	8.122E–12	2.000E–02
26	18 – 16	E2	4.4857E+03	2.353E–02	4.378E–11	2.903E–03
26	18 – 17	M1	6.8559E+03	2.325E+00	1.371E–06	3.892E+01
26	18 – 17	E2	6.8559E+03	2.711E–02	1.412E–11	4.009E–04
26	19 – 2	E2	1.5695E+02	3.026E–01	1.314E–05	3.954E+05
26	19 – 7	M2	2.7420E+02	4.498E+00	4.877E–10	4.808E+00
26	19 – 8	E1	2.8446E+02	1.092E+00	1.167E+00	1.069E+10
26	19 – 8	M2	2.8446E+02	1.612E+01	1.565E–09	1.433E+01
26	19 – 10	M2	3.0491E+02	5.975E+00	4.711E–10	3.756E+00
26	19 – 14	M2	4.2006E+02	1.037E–02	3.128E–13	1.314E–03
26	20 – 2	E2	1.5553E+02	1.006E–01	4.492E–06	1.769E+05
26	20 – 3	E2	1.5926E+02	1.357E–01	5.639E–06	2.119E+05
26	20 – 6	M2	2.5098E+02	1.640E–01	2.319E–11	3.509E–01
26	20 – 7	E1	2.6988E+02	7.168E–01	8.068E–01	1.056E+10
26	20 – 7	M2	2.6988E+02	2.594E–01	2.950E–11	3.860E–01
26	20 – 8	E1	2.7981E+02	1.233E–01	1.338E–01	1.628E+09
26	20 – 9	M2	2.8704E+02	3.221E–02	3.044E–12	3.521E–02
26	20 – 10	E1	2.9958E+02	1.072E–02	1.087E–02	1.154E+08

Table 2 continued

Table 2 (*continued*)

<i>Z</i>	<i>j – i</i>	Type	λ	<i>S</i>	<i>gf</i>	<i>A</i>
26	20 – 12	M2	3.6617E+02	4.711E–02	2.145E–12	1.524E–02
26	20 – 13	M2	4.0508E+02	5.938E–02	1.997E–12	1.160E–02
26	20 – 14	M2	4.1001E+02	1.313E–01	4.257E–12	2.413E–02
26	20 – 18	M1	1.5594E+04	7.385E–02	1.915E–08	7.504E–02
26	20 – 19	M1	1.7136E+04	4.277E+00	1.009E–06	3.275E+00
26	20 – 19	E2	1.7136E+04	5.502E–02	1.836E–12	5.957E–06
26	21 – 1	M2	1.5376E+01	3.140E–01	1.931E–07	1.089E+06
26	21 – 2	E2	1.5224E+02	4.216E–02	2.006E–06	1.155E+05
26	21 – 3	E2	1.5582E+02	1.221E–01	5.420E–06	2.978E+05
26	21 – 6	E1	2.4253E+02	1.266E–02	1.585E–02	3.596E+08
26	21 – 6	M2	2.4253E+02	5.508E–01	8.630E–11	1.957E+00
26	21 – 7	E1	2.6014E+02	2.071E–01	2.418E–01	4.767E+09
26	21 – 8	E1	2.6935E+02	1.089E–02	1.228E–02	2.259E+08
26	21 – 8	M2	2.6935E+02	3.896E–01	4.456E–11	8.193E–01
26	21 – 9	E1	2.7604E+02	3.882E–01	4.272E–01	7.479E+09
26	21 – 9	M2	2.7604E+02	1.381E–01	1.467E–11	2.568E–01
26	21 – 10	M2	2.8763E+02	1.284E+00	1.206E–10	1.945E+00
26	21 – 11	M2	3.2914E+02	4.904E–01	3.074E–11	3.786E–01
26	21 – 13	M2	3.8352E+02	3.936E–02	1.560E–12	1.415E–02
26	21 – 15	M2	6.4033E+02	2.234E–01	1.902E–12	6.188E–03
26	21 – 17	M1	2.8676E+03	4.945E–02	6.974E–08	1.131E+01
26	21 – 18	E2	4.9294E+03	2.232E–02	3.129E–11	1.718E–03
26	21 – 19	E2	5.0738E+03	1.044E–02	1.343E–11	6.958E–04
26	21 – 20	M1	7.2079E+03	2.145E+00	1.203E–06	3.090E+01
26	21 – 20	E2	7.2079E+03	1.015E–01	4.550E–11	1.168E–03
26	22 – 2	E2	1.5026E+02	1.306E–01	6.463E–06	2.727E+05
26	22 – 3	E2	1.5375E+02	1.010E–01	4.666E–06	1.881E+05
26	22 – 6	M2	2.3755E+02	2.461E–01	4.103E–11	6.929E–01
26	22 – 7	E1	2.5442E+02	4.043E–03	4.827E–03	7.107E+07
26	22 – 7	M2	2.5442E+02	1.743E+00	2.365E–10	3.482E+00
26	22 – 8	E1	2.6322E+02	1.651E–01	1.906E–01	2.621E+09
26	22 – 8	M2	2.6322E+02	7.893E+00	9.674E–10	1.330E+01
26	22 – 9	M2	2.6961E+02	7.397E+00	8.437E–10	1.106E+01

Table 2 *continued*

Table 2 (*continued*)

Z	$j - i$	Type	λ	S	gf	A
26	22 – 10	E1	2.8065E+02	7.031E–01	7.610E–01	9.207E+09
26	22 – 10	M2	2.8065E+02	3.165E+00	3.200E–10	3.872E+00
26	22 – 12	M2	3.3827E+02	8.395E–02	4.848E–12	4.037E–02
26	22 – 13	M2	3.7121E+02	1.045E–01	4.568E–12	3.159E–02
26	22 – 17	E2	2.2979E+03	2.353E–02	3.256E–10	5.876E–02
26	22 – 18	M1	3.4563E+03	5.538E–01	6.480E–07	5.168E+01
26	22 – 18	E2	3.4563E+03	9.194E–02	3.739E–10	2.982E–02
26	22 – 19	M1	3.5267E+03	1.645E–01	1.886E–07	1.445E+01
26	22 – 19	E2	3.5267E+03	1.039E–01	3.977E–10	3.047E–02
26	22 – 20	M1	4.4406E+03	4.487E–01	4.086E–07	1.975E+01
26	22 – 20	E2	4.4406E+03	2.812E–02	5.392E–11	2.606E–03
26	22 – 21	M1	1.1566E+04	1.178E+00	4.119E–07	2.934E+00
26	23 – 1	E1	1.5268E+01	3.206E–02	6.379E–01	6.084E+12
26	23 – 3	E2	1.4542E+02	9.079E–02	4.957E–06	5.212E+05
26	23 – 6	M2	2.1824E+02	2.776E+00	5.969E–10	2.786E+01
26	23 – 7	E1	2.3239E+02	1.246E–02	1.629E–02	6.707E+08
26	23 – 8	M2	2.3972E+02	4.434E–02	7.194E–12	2.783E–01
26	23 – 9	E1	2.4501E+02	1.533E–01	1.900E–01	7.039E+09
26	23 – 9	M2	2.4501E+02	6.331E–01	9.622E–11	3.564E+00
26	23 – 10	M2	2.5409E+02	1.589E+00	2.165E–10	7.455E+00
26	23 – 11	E1	2.8595E+02	1.832E–01	1.946E–01	5.291E+09
26	23 – 13	M2	3.2612E+02	1.845E–01	1.189E–11	2.485E–01
26	23 – 16	M1	1.1303E+03	9.470E–02	3.388E–07	5.896E+02
26	23 – 17	M1	1.2382E+03	2.964E–01	9.681E–07	1.404E+03
26	23 – 18	M1	1.5111E+03	2.390E–01	6.395E–07	6.228E+02
26	23 – 20	E2	1.6732E+03	1.214E–02	4.351E–10	3.456E–01
26	23 – 21	M1	2.1790E+03	7.866E–01	1.460E–06	6.836E+02
26	23 – 21	E2	2.1790E+03	6.950E–02	1.128E–09	5.281E–01
26	24 – 1	M2	1.5171E+01	1.033E–01	6.616E–08	3.834E+05
26	24 – 4	E2	1.5558E+02	7.371E–02	3.286E–06	1.811E+05
26	24 – 5	E2	1.5793E+02	9.190E–02	3.917E–06	2.095E+05
26	24 – 6	E1	1.9999E+02	5.253E–04	7.979E–04	2.662E+07
26	24 – 6	M2	1.9999E+02	2.146E–02	5.997E–12	2.000E–01

Table 2 *continued*

Table 2 (*continued*)

<i>Z</i>	<i>j - i</i>	Type	λ	<i>S</i>	<i>gf</i>	<i>A</i>
26	24 - 7	E1	2.1181E+02	1.766E-03	2.532E-03	7.531E+07
26	24 - 8	M2	2.1788E+02	1.634E-02	3.532E-12	9.925E-02
26	24 - 9	M2	2.2223E+02	1.354E-02	2.758E-12	7.449E-02
26	24 - 10	E1	2.2968E+02	5.758E-04	7.615E-04	1.926E+07
26	24 - 10	M2	2.2968E+02	5.167E-02	9.533E-12	2.411E-01
26	24 - 11	M2	2.5540E+02	1.475E-02	1.979E-12	4.047E-02
26	24 - 12	E1	2.6689E+02	5.150E-01	5.861E-01	1.098E+10
26	24 - 12	M2	2.6689E+02	1.479E-01	1.739E-11	3.258E-01
26	24 - 13	E1	2.8698E+02	9.934E-03	1.051E-02	1.703E+08
26	24 - 13	M2	2.8698E+02	1.055E-02	9.980E-13	1.617E-02
26	24 - 14	E1	2.8944E+02	8.416E-02	8.832E-02	1.406E+09
26	24 - 14	M2	2.8944E+02	1.164E-02	1.073E-12	1.709E-02
26	24 - 15	M2	4.1002E+02	1.867E-01	6.056E-12	4.805E-02
26	24 - 17	M1	8.1572E+02	7.618E-02	3.777E-07	7.572E+02
26	24 - 18	M1	9.2588E+02	1.069E-01	4.667E-07	7.263E+02
26	24 - 20	M1	9.8432E+02	2.230E+00	9.162E-06	1.262E+04
26	24 - 21	M1	1.1400E+03	9.341E-01	3.313E-06	3.401E+03
26	24 - 22	M1	1.2646E+03	2.019E-02	6.456E-08	5.385E+01
26	24 - 23	M1	2.3908E+03	2.155E-01	3.646E-07	8.509E+01
26	25 - 1	M2	1.5156E+01	9.133E-02	5.864E-08	3.405E+05
26	25 - 4	E2	1.5400E+02	8.818E-02	4.053E-06	2.280E+05
26	25 - 5	E2	1.5631E+02	7.257E-02	3.191E-06	1.742E+05
26	25 - 6	E1	1.9739E+02	1.398E-03	2.151E-03	7.364E+07
26	25 - 6	M2	1.9739E+02	1.965E-01	5.709E-11	1.955E+00
26	25 - 7	E1	2.0890E+02	5.017E-03	7.295E-03	2.230E+08
26	25 - 7	M2	2.0890E+02	1.304E-01	3.197E-11	9.772E-01
26	25 - 8	E1	2.1480E+02	3.985E-03	5.635E-03	1.629E+08
26	25 - 8	M2	2.1480E+02	6.540E-02	1.475E-11	4.264E-01
26	25 - 9	E1	2.1903E+02	5.969E-04	8.277E-04	2.302E+07
26	25 - 9	M2	2.1903E+02	9.521E-02	2.025E-11	5.631E-01
26	25 - 10	E1	2.2626E+02	1.685E-02	2.262E-02	5.894E+08
26	25 - 10	M2	2.2626E+02	2.708E-01	5.225E-11	1.362E+00
26	25 - 11	M2	2.5119E+02	1.102E+00	1.555E-10	3.288E+00

Table 2 *continued*

Table 2 (*continued*)

<i>Z</i>	<i>j - i</i>	Type	λ	<i>S</i>	<i>gf</i>	<i>A</i>
26	25 - 12	M2	2.6229E+02	5.727E-01	7.094E-11	1.376E+00
26	25 - 13	E1	2.8167E+02	5.269E-01	5.683E-01	9.556E+09
26	25 - 13	M2	2.8167E+02	8.366E+00	8.368E-10	1.407E+01
26	25 - 14	E1	2.8404E+02	5.979E-02	6.394E-02	1.057E+09
26	25 - 14	M2	2.8404E+02	3.413E+00	3.329E-10	5.504E+00
26	25 - 15	M2	3.9927E+02	3.455E-01	1.213E-11	1.015E-01
26	25 - 17	M1	7.7423E+02	1.362E-01	7.115E-07	1.583E+03
26	25 - 18	M1	8.7280E+02	8.419E-01	3.901E-06	6.831E+03
26	25 - 20	M1	9.2454E+02	1.144E-02	5.006E-08	7.813E+01
26	25 - 21	M1	1.0606E+03	2.490E-01	9.495E-07	1.126E+03
26	25 - 22	M1	1.1677E+03	1.351E+00	4.680E-06	4.579E+03
26	25 - 22	E2	1.1677E+03	1.618E-02	1.706E-09	1.670E+00
26	25 - 23	M1	2.0663E+03	2.111E+00	4.131E-06	1.291E+03
26	25 - 24	M1	1.5224E+04	1.221E-02	3.244E-09	1.867E-02
26	25 - 24	E2	1.5224E+04	1.170E-02	5.568E-13	3.205E-06
26	26 - 5	E2	1.5530E+02	2.324E-01	1.042E-05	4.116E+05
26	26 - 6	M2	1.9579E+02	7.920E-02	2.359E-11	5.863E-01
26	26 - 7	M2	2.0711E+02	3.636E-02	9.149E-12	2.033E-01
26	26 - 8	E1	2.1291E+02	4.811E-03	6.863E-03	1.443E+08
26	26 - 8	M2	2.1291E+02	3.136E-02	7.262E-12	1.527E-01
26	26 - 10	E1	2.2416E+02	6.167E-04	8.357E-04	1.585E+07
26	26 - 12	M2	2.5947E+02	3.548E+00	4.541E-10	6.427E+00
26	26 - 13	M2	2.7842E+02	2.045E+00	2.118E-10	2.603E+00
26	26 - 14	E1	2.8074E+02	8.565E-01	9.267E-01	1.120E+10
26	26 - 14	M2	2.8074E+02	1.482E+01	1.497E-09	1.810E+01
26	26 - 18	M1	8.4232E+02	2.172E-01	1.043E-06	1.400E+03
26	26 - 19	M1	8.4643E+02	2.192E+00	1.047E-05	1.393E+04
26	26 - 21	M1	1.0159E+03	8.983E-02	3.576E-07	3.301E+02
26	26 - 22	M1	1.1137E+03	1.606E+00	5.831E-06	4.479E+03
26	26 - 24	M1	9.3332E+03	2.228E+00	9.651E-07	1.056E+01
26	26 - 24	E2	9.3332E+03	4.968E-02	1.026E-11	1.122E-04
26	26 - 25	M1	2.4121E+04	1.043E+00	1.749E-07	2.865E-01
26	26 - 25	E2	2.4121E+04	3.504E-02	4.193E-13	6.867E-07

Table 2 *continued*

Table 2 (*continued*)

<i>Z</i>	<i>j</i> – <i>i</i>	Type	λ	<i>S</i>	<i>gf</i>	<i>A</i>
26	27 – 1	E1	1.5021E+01	1.098E–01	2.220E+00	2.188E+13
26	27 – 3	E2	1.2574E+02	1.544E–02	1.304E–06	1.834E+05
26	27 – 5	E2	1.4306E+02	9.829E–02	5.636E–06	6.124E+05
26	27 – 6	M2	1.7672E+02	8.332E–01	3.375E–10	2.403E+01
26	27 – 9	E1	1.9387E+02	1.775E–02	2.781E–02	1.645E+09
26	27 – 9	M2	1.9387E+02	1.942E–01	5.958E–11	3.524E+00
26	27 – 10	M2	1.9951E+02	6.364E–01	1.791E–10	1.001E+01
26	27 – 11	E1	2.1864E+02	1.056E–02	1.467E–02	6.823E+08
26	27 – 12	E1	2.2700E+02	9.444E–02	1.264E–01	5.453E+09
26	27 – 12	M2	2.2700E+02	2.626E–01	5.019E–11	2.165E+00
26	27 – 13	E1	2.4138E+02	5.846E–02	7.357E–02	2.808E+09
26	27 – 13	M2	2.4138E+02	8.358E–02	1.328E–11	5.069E–01
26	27 – 15	E1	3.2288E+02	1.817E–01	1.710E–01	3.647E+09
26	27 – 16	M1	5.0988E+02	6.400E–02	5.076E–07	4.341E+03
26	27 – 17	M1	5.3073E+02	1.273E–01	9.701E–07	7.658E+03
26	27 – 18	M1	5.7527E+02	2.331E–02	1.639E–07	1.101E+03
26	27 – 21	M1	6.5127E+02	2.127E–01	1.321E–06	6.923E+03
26	27 – 23	M1	9.2890E+02	1.650E–01	7.183E–07	1.851E+03
26	27 – 24	M1	1.5191E+03	5.432E–02	1.446E–07	1.393E+02
26	27 – 24	E2	1.5191E+03	3.909E–02	1.872E–09	1.804E+00
26	27 – 25	M1	1.6875E+03	6.404E–01	1.535E–06	1.198E+03
26	27 – 25	E2	1.6875E+03	3.196E–02	1.117E–09	8.718E–01

Note: Only transitions among the lowest 27 states of $2s^22p^6$ and $2s^22p^53l$ configurations in Fe XVII are shown here. Table 2 is available online in its entirety in the home page of *ApJS*. A portion is shown here for guidance regarding its form and content.

Table 3. Comparisons of the experimental and theoretical energies in Fe XVII.

Key	Config.	LSJ	Energy					
			Exp.			Cal.		
			NIST ^a	CHAINTI ^b	MBPT ^c	MCDHF/RCI ^d	MCDHF/RCI2 ^e	MR-MP ^f
1	$2s^22p^6$	1S_0	0.0000	0.000	0.0000	0.0000	0.0000	0.0000
2	$2s^22p^53s$	3P_2	725.2443	725.223	724.9150	725.1672	725.1969	725.170
3	$2s^22p^53s$	1P_1	727.1388	727.138	726.7839	727.0773	727.1015	727.060
4	$2s^22p^53s$	3P_0	737.8560	737.889	737.5376	737.8046	737.8303	737.815
5	$2s^22p^53s$	3P_1	739.0537	739.073	738.7243	739.0032	739.0243	738.997
6	$2s^22p^53p$	3S_1	755.4915	755.485	755.2334	755.2505	755.5067	755.462
7	$2s^22p^53p$	3D_2	758.9928	758.980	758.6933	758.7627	759.0026	758.939
8	$2s^22p^53p$	3D_3	760.6096	760.599	760.3239	760.3758	760.6175	760.564
9	$2s^22p^53p$	1P_1	761.7403	761.746	761.4395	761.5072	761.7462	761.688
10	$2s^22p^53p$	3P_2	763.5530	763.550	763.2480	763.3194	763.5543	763.496
11	$2s^22p^53p$	3P_0	768.9810	769.027	768.6848	768.7880	769.0172	768.979
12	$2s^22p^53p$	3D_1	771.0614	771.091	770.7739	770.8451	771.0806	771.032
13	$2s^22p^53p$	3P_1	774.3073	774.342	774.0263	774.0890	774.3242	774.284
14	$2s^22p^53p$	1D_2	774.6855	774.719	774.3944	774.4695	774.7016	774.656
15	$2s^22p^53p$	1S_0	787.7224	787.716	786.9916	787.5283	787.7466	787.440
16	$2s^22p^53d$	3P_0	801.4314	801.425	801.0749	801.3651	801.4230	801.386
17	$2s^22p^53d$	3P_1	802.401	802.331	802.0304	802.3185	802.3661	802.341
18	$2s^22p^53d$	3P_2	804.211	804.195	803.8389	804.1375	804.1821	804.159
19	$2s^22p^53d$	3F_4	804.2644	804.264	803.9104	804.2131	804.2538	804.225
20	$2s^22p^53d$	3F_3	805.0331	804.999	804.6339	804.9542	804.9908	804.953
21	$2s^22p^53d$	1D_2	806.728	806.741	806.3541	806.6746	806.7107	806.675
22	$2s^22p^53d$	3D_3	807.8004	807.799	807.4260	807.7571	807.7912	807.749
23	$2s^22p^53d$	3D_1	812.369	812.372	812.0439	812.3944	812.4308	812.405
24	$2s^22p^53d$	3F_2	817.5964	817.628	817.2299	817.5516	817.5840	817.564
25	$2s^22p^53d$	3D_2	818.4135	818.446	818.0443	818.3668	818.4017	818.381
26	$2s^22p^53d$	1F_3	818.9342	818.974	818.5583	818.8942	818.9253	818.898
27	$2s^22p^53d$	1P_1	825.7	825.846	825.3914	825.8280	825.8712	825.763
28	$2s2p^63s$	3S_1	858.9874	859.2394	...	859.206

Table 3 continued

Table 3 (*continued*)

Key	Config.	LSJ	Energy					
			Exp.			Cal.		
			NIST ^a	CHAINTI ^b	MBPT ^c	MCDHF/RCI ^d	MCDHF/RCI2 ^e	MR-MP ^f
29	$2s2p^63s$	1S_0	869.1	865.266	864.8332	865.2301	...	865.146
30	$2s2p^63p$	3P_0	891.7391	892.2437	...	891.959
31	$2s2p^63p$	3P_1	892.550	892.615	892.2064	892.6962	...	892.412
32	$2s2p^63p$	3P_2	894.5275	895.0184	...	894.748
33	$2s2p^63p$	1P_1	896.939	896.812	896.4628	896.9897	...	896.674
34	$2s2p^63d$	3D_1	936.4837	936.7598	...	936.837
35	$2s2p^63d$	3D_2	936.6273	936.9026	...	936.979
36	$2s2p^63d$	3D_3	936.9023	937.1768	...	937.251
37	$2s2p^63d$	1D_2	...	942.169	941.7026	942.0337	...	942.003
38	$2s^22p^54s$	3P_2	976.87	976.901	976.5650	976.9351
39	$2s^22p^54s$	1P_1	977.715	977.793	977.1869	977.5662
40	$2s^22p^54p$	3S_1	989.1387	989.3138
41	$2s^22p^54s$	3P_0	989.2215	989.6100
42	$2s^22p^54s$	3P_1	989.77	990.210	989.5691	989.9321
43	$2s^22p^54p$	3D_2	990.0391	990.2135
44	$2s^22p^54p$	3D_3	...	992.430	990.7127	990.8853
45	$2s^22p^54p$	1P_1	991.1078	991.2819
46	$2s^22p^54p$	3P_2	991.7199	991.8914
47	$2s^22p^54p$	3P_0	...	994.922	995.1565	995.3967
48	$2s^22p^54p$	3D_1	1002.430	1002.616
49	$2s^22p^54p$	3P_1	1003.619	1003.804
50	$2s^22p^54p$	1D_2	1003.847	1004.032
51	$2s^22p^54d$	3P_0	1005.846	1006.220
52	$2s^22p^54d$	3P_1	1006.26	1006.20	1006.284	1006.654
53	$2s^22p^54p$	1S_0	...	1006.82	1006.331	1006.629
54	$2s^22p^54d$	3F_4	1007.198	1007.28	1006.822	1007.199
55	$2s^22p^54d$	3P_2	1007.000	1007.373
56	$2s^22p^54d$	3F_3	1007.471	1007.59	1007.104	1007.482
57	$2s^22p^54d$	1D_2	1010.682	...	1007.727	1008.102
58	$2s^22p^54d$	3D_3	1008.117	1008.493

Table 3 continued

Table 3 (*continued*)

Key	Config.	LSJ	Energy					
			Exp.			Cal.		
			NIST ^a	CHAINI ^b	MBPT ^c	MCDHF/RCI ^d	MCDHF/RCI2 ^e	MR-MP ^f
59	$2s^22p^54d$	3D_1	1010.97	1010.96	1010.525	1010.912
60	$2s^22p^54f$	1G_4	1017.9	1015.86	1014.685	1014.893
61	$2s^22p^54f$	3D_1	1014.689	1014.887
62	$2s^22p^54f$	3G_5	1015.18	1015.26	1014.716	1014.920
63	$2s^22p^54f$	3D_2	1014.816	1015.019
64	$2s^22p^54f$	3F_3	1015.68	1015.70	1015.172	1015.373
65	$2s^22p^54f$	1D_2	1015.18	...	1015.195	1015.406
66	$2s^22p^54f$	1F_3	1017.17	1015.96	1015.255	1015.461
67	$2s^22p^54f$	3F_4	1015.80	1015.21	1015.338	1015.543
68	$2s^22p^54d$	3F_2	1019.637	1020.024
69	$2s^22p^54d$	3D_2	1019.899	1020.285
70	$2s^22p^54d$	1F_3	1020.196	1020.586
71	$2s^22p^54d$	1P_1	1022.75	1022.62	1022.167	1022.570
72	$2s^22p^54f$	3G_3	1027.71	1028.66	1027.549	1027.767
73	$2s^22p^54f$	3G_4	1014.2	1028.20	1027.657	1027.877
74	$2s^22p^54f$	3F_2	1027.779	1028.000
75	$2s^22p^54f$	3D_3	1027.71	1028.66	1027.786	1028.002
76	$2s^22p^55s$	3P_2	1084.748	1085.132
77	$2s^22p^55s$	1P_1	1085.73	1085.68	1085.063	1085.456
78	$2s^22p^55p$	3S_1	1090.937	1091.126
79	$2s^22p^55p$	3D_2	1091.448	1091.637
80	$2s^22p^55p$	3D_3	1091.783	1091.970
81	$2s^22p^55p$	1P_1	1091.979	1092.168
82	$2s^22p^55p$	3P_2	1092.280	1092.468
83	$2s^22p^55p$	1S_0	1094.073	1094.349
84	$2s^22p^55s$	3P_0	1097.393	1097.798
85	$2s^22p^55s$	3P_1	1098.5	1098.47	1097.588	1097.948
86	$2s^22p^55d$	3P_0	1099.155	1099.539
87	$2s^22p^55d$	3P_1	1098.5	...	1099.383	1099.765
88	$2s^22p^55d$	3F_4	1099.625	1100.010

Table 3 continued

Table 3 (*continued*)

Key	Config.	LSJ	Energy					
			Exp.			Cal.		
			NIST ^a	CHAINI ^b	MBPT ^c	MCDHF/RCI ^d	MCDHF/RCI2 ^e	MR-MP ^f
89	$2s^22p^55d$	3P_2	1099.728	1100.113
90	$2s^22p^55d$	3F_3	1099.759	1100.146
91	$2s^22p^55d$	1D_2	1100.054	1100.441
92	$2s^22p^55d$	3D_3	1100.243	1100.630
93	$2s^22p^55d$	1P_1	1101.85	1102.08	1101.529	1101.936
94	$2s^22p^55f$	3D_1	1103.417	1103.607
95	$2s^22p^55f$	3D_2	1103.527	1103.718
96	$2s^22p^55f$	1G_4	1103.541	1103.739
97	$2s^22p^55f$	3G_5	1103.83	1103.96	1103.548	1103.743
98	$2s^22p^55f$	3F_3	1103.736	1103.927
99	$2s^22p^55f$	1D_2	1103.798	1103.996
100	$2s^22p^55f$	1F_3	1103.818	1104.013
101	$2s^22p^55f$	3F_4	1103.865	1104.059
102	$2s^22p^55g$	3F_2	1103.950	1104.336
103	$2s^22p^55p$	3D_1	1103.975	1104.177
104	$2s^22p^55g$	3F_3	1103.975	1104.362
105	$2s^22p^55g$	1H_5	1104.048	1104.441
106	$2s^22p^55g$	3H_6	1104.072	1104.464
107	$2s^22p^55g$	3G_3	1104.132	1104.521
108	$2s^22p^55g$	3G_4	1104.150	1104.539
109	$2s^22p^55g$	1G_4	1104.204	1104.595
110	$2s^22p^55g$	3G_5	1104.226	1104.617
111	$2s^22p^55p$	3P_1	1104.375	1104.580
112	$2s^22p^55p$	1D_2	1104.692	1104.893
113	$2s^22p^55p$	3P_0	1105.511	1105.787
114	$2s2p^64s$	3S_1	1109.417	1109.751
115	$2s2p^64s$	1S_0	...	1111.65	1111.182	1111.538
116	$2s^22p^55d$	3F_2	1112.357	1112.755
117	$2s^22p^55d$	3D_2	1112.464	1112.864
118	$2s^22p^55d$	1F_3	1112.637	1113.037

Table 3 *continued*

Table 3 (*continued*)

Key	Config.	LSJ	Energy					
			Exp.			Cal.		
			NIST ^a	CHAINI ^b	MBPT ^c	MCDHF/RCI ^d	MCDHF/RCI2 ^e	MR-MP ^f
119	$2s^22p^55d$	3D_1	1113.63	1114.06	1113.443	1113.862
120	$2s^22p^55f$	3G_3	1116.308	1116.516
121	$2s^22p^55f$	3G_4	1116.369	1116.579
122	$2s^22p^55f$	3D_3	1116.374	1116.579
123	$2s^22p^55f$	3F_2	1116.412	1116.621
124	$2s^22p^55g$	1F_3	1116.761	1117.163
125	$2s^22p^55g$	3F_4	1116.781	1117.183
126	$2s^22p^55g$	3H_4	1116.800	1117.206
127	$2s^22p^55g$	3H_5	1116.824	1117.230
128	$2s2p^64p$	3P_0	1122.371	1122.935
129	$2s2p^64p$	3P_1	1122.80	1122.74	1122.541	1123.083
130	$2s2p^64p$	3P_2	1123.451	1124.004
131	$2s2p^64p$	1P_1	1124.78	1124.78	1124.112	1124.659
132	$2s2p^64d$	3D_1	1139.075	1139.420
133	$2s2p^64d$	3D_2	1139.135	1139.478
134	$2s2p^64d$	3D_3	1139.259	1139.600
135	$2s2p^64d$	1D_2	1141.022	1141.362
136	$2s^22p^56s$	3P_2	...	1141.40	1141.273	1141.666
137	$2s^22p^56s$	1P_1	1142.64	...	1141.421	1141.824
138	$2s^22p^56p$	3S_1	1144.840	1145.042
139	$2s^22p^56p$	3D_2	1145.071	1145.283
140	$2s^22p^56p$	3D_3	1145.269	1145.474
141	$2s^22p^56p$	1P_1	1145.332	1145.541
142	$2s^22p^56p$	3P_2	1145.501	1145.713
143	$2s^22p^56p$	1S_0	1146.513	1146.880
144	$2s2p^64f$	3F_2	1146.719	1147.273
145	$2s2p^64f$	3F_3	1146.795	1147.352
146	$2s2p^64f$	3F_4	1146.908	1147.469
147	$2s2p^64f$	1F_3	1146.974	1147.538
148	$2s^22p^56d$	3P_0	1149.352	1149.743

Table 3 continued

Table 3 (*continued*)

Key	Config.	LSJ	Energy					
			Exp.			Cal.		
			NIST ^a	CHAINTI ^b	MBPT ^c	MCDHF/RCI ^d	MCDHF/RCI2 ^e	MR-MP ^f
149	$2s^22p^56d$	3P_1	1149.483	1149.875
150	$2s^22p^56d$	3F_4	1149.609	1150.004
151	$2s^22p^56d$	3P_2	1149.677	1150.075
152	$2s^22p^56d$	3F_3	1149.688	1150.089
153	$2s^22p^56d$	1D_2	1149.846	1150.251
154	$2s^22p^56d$	3D_3	1149.957	1150.364
155	$2s^22p^56d$	1P_1	1151.19	1151.20	1150.688	1151.154
156	$2s^22p^56f$	1G_4	1151.840	1152.033
157	$2s^22p^56f$	3G_5	1151.841	1152.033
158	$2s^22p^56f$	3D_1	1151.866	1152.056
159	$2s^22p^56f$	3D_2	1151.906	1152.098
160	$2s^22p^56f$	3F_3	1151.987	1152.178
161	$2s^22p^56f$	1F_3	1151.996	1152.189
162	$2s^22p^56f$	1D_2	1152.004	1152.199
163	$2s^22p^56f$	3F_4	1152.023	1152.215
164	$2s^22p^56g$	1H_5	1152.158	1152.548
165	$2s^22p^56g$	3H_6	1152.171	1152.561
166	$2s^22p^56h$	3G_3	1152.197	1152.384
167	$2s^22p^56h$	3G_4	1152.206	1152.393
168	$2s^22p^56h$	1I_6	1152.211	1152.399
169	$2s^22p^56h$	3I_7	1152.221	1152.408
170	$2s^22p^56h$	3H_4	1152.247	1152.433
171	$2s^22p^56g$	1G_4	1152.247	1152.636
172	$2s^22p^56h$	3H_5	1152.255	1152.441
173	$2s^22p^56g$	3G_5	1152.260	1152.650
174	$2s^22p^56h$	1H_5	1152.261	1152.448
175	$2s^22p^56h$	3H_6	1152.270	1152.457
176	$2s^22p^56g$	3G_3	1152.324	1152.720
177	$2s^22p^56g$	3G_4	1152.338	1152.733
178	$2s^22p^56g$	3F_2	1152.384	1152.787

Table 3 *continued*

Table 3 (*continued*)

Key	Config.	LSJ	Energy					
			Exp.			Cal.		
			NIST ^a	CHIANTI ^b	MBPT ^c	MCDHF/RCI ^d	MCDHF/RCI2 ^e	MR-MP ^f
179	$2s^22p^56g$	3F_3	1152.400	1152.803
180	$2s^22p^56s$	3P_0	1153.941	1154.352
181	$2s^22p^56s$	3P_1	1154.050	1154.444
182	$2s^22p^56p$	3D_1	1157.642	1157.860
183	$2s^22p^56p$	3P_1	1157.955	1158.177
184	$2s^22p^56p$	1D_2	1158.034	1158.255
185	$2s^22p^56p$	3P_0	1158.419	1158.768
186	$2s^22p^56d$	3F_2	1162.320	1162.731
187	$2s^22p^56d$	3D_2	1162.387	1162.801
188	$2s^22p^56d$	1F_3	1162.480	1162.895
189	$2s^22p^56d$	3D_1	1163.34	1163.41	1162.906	1163.377
190	$2s^22p^56f$	3G_3	1164.571	1164.778
191	$2s^22p^56f$	3G_4	1164.609	1164.816
192	$2s^22p^56f$	3D_3	1164.641	1164.846
193	$2s^22p^56f$	3F_2	1164.653	1164.861
194	$2s^22p^56g$	3H_4	1164.885	1165.288
195	$2s^22p^56g$	3H_5	1164.899	1165.303
196	$2s^22p^56h$	1G_4	1164.923	1165.125
197	$2s^22p^56h$	3I_5	1164.925	1165.127
198	$2s^22p^56g$	1F_3	1164.931	1165.335
199	$2s^22p^56h$	3G_5	1164.932	1165.134
200	$2s^22p^56h$	3I_6	1164.934	1165.136
201	$2s^22p^56g$	3F_4	1164.944	1165.348

^aThe observed energies from the NIST ASD (Kramida et al. 2015).

^bThe observed energies from the Chianti database (Del Zanna et al. 2015; Dere et al. 1997).

^cThe present MBPT energies.

^dThe present MCDHF/RCI energies.

^eThe MCDHF/RCI2 energies calculated by Jönsson et al. (2014).

^fThe MR-MP energies calculated by Ishikawa et al. (2009).

Table 4. Level Energies (in eV) for the states which the NIST experimental values differ from the MBPT results by more than 0.2%.

Z	Key ^a	State	Energy		Difference (%)
			MBPT ^b	NIST ^c	
24	29	$2s2p^63s\ ^1S_0$	707.2378	712.822	-0.78
24	87	$2s^22p^55d\ ^3P_1$	884.1274	886.24	-0.24
26	29	$2s2p^63s\ ^1S_0$	864.8332	869.1	-0.49
26	57	$2s^22p^54d\ ^1D_2$	1007.727	1010.682	-0.29
26	67	$2s^22p^54f\ ^3F_4$	1015.338	1017.9	-0.25
26	73	$2s^22p^54f\ ^3G_4$	1027.657	1014.2	1.33
28	28	$2s2p^63s\ ^3S_1$	1031.886	1036.26	-0.42
28	29	$2s2p^63s\ ^1S_0$	1038.504	1043.45	-0.47
30	27	$2s^22p^53d\ ^1P_1$	1185.086	1188.26	-0.27
31	97	$2s2p^64p\ ^1P_1$	1742.279	1768.63	-1.49
32	87	$2s2p^64p\ ^3P_1$	1878.827	1883.07	-0.23
32	89	$2s2p^64p\ ^1P_1$	1882.237	1886.79	-0.24
34	47	$2s^22p^54s\ ^3P_1$	1986.773	1961.1820	1.30
35	71	$2s^22p^54d\ ^3D_1$	2189.996	2194.7682	-0.22
35	83	$2s2p^64p\ ^1P_1$	2337.637	2342.8053	-0.22
35	97	$2s^22p^55d\ ^1P_1$	2355.808	2361.1550	-0.23
35	131	$2s^22p^55d\ ^3D_1$	2402.879	2408.3929	-0.23
35	155	$2s^22p^56d\ ^1P_1$	2470.301	2477.2042	-0.28

^aThe index number of the level given in Table 1.

^bThe present MBPT energies.

^cThe NIST recommended energies (Kramida et al. 2015).

Table 5. Comparisons of the oscillator strengths (gf) for the transitions among the $n \leq 3$ levels in Fe XVII. The MBPT and MCDHF/RCI values, as well as the MCDHF/RCI2 and NIST results, are listed for comparison.

$j - i$	Transition	Type	gf			
			MBPT ^a	MCDHF/RCI ^b	MCDHF/RCI2 ^c	NIST ^d
2 - 1	$2s^2 2p^5 3s \ 3P_2 - 2s^2 2p^6 \ 1S_0$	M2	4.525E-08	4.599E-08	4.559E-08	...
3 - 1	$2s^2 2p^5 3s \ 1P_1 - 2s^2 2p^6 \ 1S_0$	E1	1.222E-01	1.232E-01	1.219E-01	1.22E-01
5 - 1	$2s^2 2p^5 3s \ 3P_1 - 2s^2 2p^6 \ 1S_0$	E1	9.986E-02	1.028E-01	1.013E-01	1.05E-01
7 - 1	$2s^2 2p^5 3p \ 3D_2 - 2s^2 2p^6 \ 1S_0$	E2	1.019E-04	1.023E-04	1.023E-04	...
10 - 1	$2s^2 2p^5 3p \ 3P_2 - 2s^2 2p^6 \ 1S_0$	E2	1.074E-04	1.087E-04	1.085E-04	...
14 - 1	$2s^2 2p^5 3p \ 1D_2 - 2s^2 2p^6 \ 1S_0$	E2	1.253E-04	1.270E-04	1.267E-04	...
17 - 1	$2s^2 2p^5 3d \ 3P_1 - 2s^2 2p^6 \ 1S_0$	E1	9.718E-03	1.018E-02	9.864E-03	9.70E-03
18 - 1	$2s^2 2p^5 3d \ 3P_2 - 2s^2 2p^6 \ 1S_0$	M2	1.102E-06	1.120E-06	1.109E-06	...
21 - 1	$2s^2 2p^5 3d \ 1D_2 - 2s^2 2p^6 \ 1S_0$	M2	1.931E-07	1.978E-07	1.961E-07	...
23 - 1	$2s^2 2p^5 3d \ 3D_1 - 2s^2 2p^6 \ 1S_0$	E1	6.379E-01	6.456E-01	6.367E-01	6.30E-01
24 - 1	$2s^2 2p^5 3d \ 3F_2 - 2s^2 2p^6 \ 1S_0$	M2	6.616E-08	6.892E-08	6.816E-08	...
25 - 1	$2s^2 2p^5 3d \ 3D_2 - 2s^2 2p^6 \ 1S_0$	M2	5.864E-08	5.773E-08	5.761E-08	...
27 - 1	$2s^2 2p^5 3d \ 1P_1 - 2s^2 2p^6 \ 1S_0$	E1	2.220E+00	2.288E+00	2.269E+00	2.31E+00
31 - 1	$2s 2p^6 3p \ 3P_1 - 2s^2 2p^6 \ 1S_0$	E1	3.674E-02	3.589E-02	...	3.00E-02
32 - 1	$2s 2p^6 3p \ 3P_2 - 2s^2 2p^6 \ 1S_0$	M2	1.199E-07	1.208E-07
33 - 1	$2s 2p^6 3p \ 1P_1 - 2s^2 2p^6 \ 1S_0$	E1	2.865E-01	2.905E-01	...	2.80E-01
37 - 1	$2s 2p^6 3d \ 1D_2 - 2s^2 2p^6 \ 1S_0$	E2	1.390E-03	1.398E-03
3 - 2	$2s^2 2p^5 3s \ 1P_1 - 2s^2 2p^5 3s \ 3P_2$	M1	6.816E-07	7.120E-07	7.094E-07	...
5 - 2	$2s^2 2p^5 3s \ 3P_1 - 2s^2 2p^5 3s \ 3P_2$	M1	6.069E-06	6.119E-06	6.119E-06	...
6 - 2	$2s^2 2p^5 3p \ 3S_1 - 2s^2 2p^5 3s \ 3P_2$	E1	2.464E-01	2.486E-01	2.502E-01	2.50E-01
6 - 2	$2s^2 2p^5 3p \ 3S_1 - 2s^2 2p^5 3s \ 3P_2$	M2	6.775E-11	6.766E-11	6.874E-11	...
7 - 2	$2s^2 2p^5 3p \ 3D_2 - 2s^2 2p^5 3s \ 3P_2$	E1	2.440E-01	2.488E-01	2.495E-01	...
7 - 2	$2s^2 2p^5 3p \ 3D_2 - 2s^2 2p^5 3s \ 3P_2$	M2	6.852E-13	6.132E-13
8 - 2	$2s^2 2p^5 3p \ 3D_3 - 2s^2 2p^5 3s \ 3P_2$	E1	7.808E-01	7.921E-01	7.947E-01	8.50E-01
8 - 2	$2s^2 2p^5 3p \ 3D_3 - 2s^2 2p^5 3s \ 3P_2$	M2	3.076E-10	3.075E-10	3.121E-10	...
9 - 2	$2s^2 2p^5 3p \ 1P_1 - 2s^2 2p^5 3s \ 3P_2$	E1	1.662E-02	1.726E-02	1.719E-02	...

Table 5 continued

Table 5 (*continued*)

$j - i$	Transition	Type	gf			
			MBPT ^a	MCDHF/RCI ^b	MCDHF/RCI2 ^c	NIST ^d
9 - 2	$2s^2 2p^5 3p \ ^1P_1 - 2s^2 2p^5 3s \ ^3P_2$	M2	2.124E-10	2.114E-10	2.145E-10	...
10 - 2	$2s^2 2p^5 3p \ ^3P_2 - 2s^2 2p^5 3s \ ^3P_2$	E1	3.333E-01	3.376E-01	3.384E-01	...
10 - 2	$2s^2 2p^5 3p \ ^3P_2 - 2s^2 2p^5 3s \ ^3P_2$	M2	4.504E-10	4.512E-10	4.573E-10	...
11 - 2	$2s^2 2p^5 3p \ ^3P_0 - 2s^2 2p^5 3s \ ^3P_2$	M2	1.219E-10	1.213E-10	1.226E-10	...
12 - 2	$2s^2 2p^5 3p \ ^3D_1 - 2s^2 2p^5 3s \ ^3P_2$	E1	4.263E-04	4.255E-04	4.231E-04	...
12 - 2	$2s^2 2p^5 3p \ ^3D_1 - 2s^2 2p^5 3s \ ^3P_2$	M2	1.239E-11	1.258E-11	1.266E-11	...
13 - 2	$2s^2 2p^5 3p \ ^3P_1 - 2s^2 2p^5 3s \ ^3P_2$	E1	2.289E-02	2.363E-02	2.345E-02	...
13 - 2	$2s^2 2p^5 3p \ ^3P_1 - 2s^2 2p^5 3s \ ^3P_2$	M2	1.323E-11	1.353E-11	1.364E-11	...
14 - 2	$2s^2 2p^5 3p \ ^1D_2 - 2s^2 2p^5 3s \ ^3P_2$	E1	4.976E-03	5.088E-03	5.056E-03	...
15 - 2	$2s^2 2p^5 3p \ ^1S_0 - 2s^2 2p^5 3s \ ^3P_2$	M2	2.631E-10	2.765E-10	2.778E-10	...
16 - 2	$2s^2 2p^5 3d \ ^3P_0 - 2s^2 2p^5 3s \ ^3P_2$	E2	1.324E-06	1.346E-06	1.350E-06	...
17 - 2	$2s^2 2p^5 3d \ ^3P_1 - 2s^2 2p^5 3s \ ^3P_2$	E2	3.858E-06	3.923E-06	3.933E-06	...
18 - 2	$2s^2 2p^5 3d \ ^3P_2 - 2s^2 2p^5 3s \ ^3P_2$	E2	5.149E-06	5.239E-06	5.252E-06	...
19 - 2	$2s^2 2p^5 3d \ ^3F_4 - 2s^2 2p^5 3s \ ^3P_2$	E2	1.314E-05	1.335E-05	1.337E-05	...
20 - 2	$2s^2 2p^5 3d \ ^3F_3 - 2s^2 2p^5 3s \ ^3P_2$	E2	4.492E-06	4.618E-06	4.618E-06	...
21 - 2	$2s^2 2p^5 3d \ ^1D_2 - 2s^2 2p^5 3s \ ^3P_2$	E2	2.006E-06	2.032E-06	2.030E-06	...
22 - 2	$2s^2 2p^5 3d \ ^3D_3 - 2s^2 2p^5 3s \ ^3P_2$	E2	6.463E-06	6.516E-06	6.522E-06	...
28 - 2	$2s 2p^6 3s \ ^3S_1 - 2s^2 2p^5 3s \ ^3P_2$	E1	2.938E-01	3.072E-01
28 - 2	$2s 2p^6 3s \ ^3S_1 - 2s^2 2p^5 3s \ ^3P_2$	M2	2.116E-09	2.138E-09
29 - 2	$2s 2p^6 3s \ ^1S_0 - 2s^2 2p^5 3s \ ^3P_2$	M2	1.374E-09	1.384E-09
4 - 3	$2s^2 2p^5 3s \ ^3P_0 - 2s^2 2p^5 3s \ ^1P_1$	M1	3.114E-06	3.176E-06	3.174E-06	...
5 - 3	$2s^2 2p^5 3s \ ^3P_1 - 2s^2 2p^5 3s \ ^1P_1$	M1	1.429E-06	1.443E-06	1.443E-06	...
6 - 3	$2s^2 2p^5 3p \ ^3S_1 - 2s^2 2p^5 3s \ ^1P_1$	E1	1.010E-02	1.042E-02	1.042E-02	...
6 - 3	$2s^2 2p^5 3p \ ^3S_1 - 2s^2 2p^5 3s \ ^1P_1$	M2	2.429E-12	2.369E-12
7 - 3	$2s^2 2p^5 3p \ ^3D_2 - 2s^2 2p^5 3s \ ^1P_1$	E1	2.726E-01	2.753E-01	2.764E-01	...
8 - 3	$2s^2 2p^5 3p \ ^3D_3 - 2s^2 2p^5 3s \ ^1P_1$	M2	3.790E-10	3.761E-10	3.822E-10	...
9 - 3	$2s^2 2p^5 3p \ ^1P_1 - 2s^2 2p^5 3s \ ^1P_1$	E1	3.093E-01	3.134E-01	3.146E-01	...
9 - 3	$2s^2 2p^5 3p \ ^1P_1 - 2s^2 2p^5 3s \ ^1P_1$	M2	1.904E-11	1.881E-11	1.911E-11	...

Table 5 *continued*

Table 5 (*continued*)

$j - i$	Transition	Type	gf			
			MBPT ^a	MCDHF/RCI ^b	MCDHF/RCI2 ^c	NIST ^d
10 - 3	$2s^2 2p^5 3p \ 3P_2 - 2s^2 2p^5 3s \ 1P_1$	E1	2.655E-01	2.707E-01	2.712E-01	...
10 - 3	$2s^2 2p^5 3p \ 3P_2 - 2s^2 2p^5 3s \ 1P_1$	M2	1.716E-10	1.707E-10	1.732E-10	...
11 - 3	$2s^2 2p^5 3p \ 3P_0 - 2s^2 2p^5 3s \ 1P_1$	E1	9.981E-02	1.013E-01	1.013E-01	...
12 - 3	$2s^2 2p^5 3p \ 3D_1 - 2s^2 2p^5 3s \ 1P_1$	E1	1.192E-03	1.166E-03	1.160E-03	...
12 - 3	$2s^2 2p^5 3p \ 3D_1 - 2s^2 2p^5 3s \ 1P_1$	M2	1.373E-12	1.362E-12
13 - 3	$2s^2 2p^5 3p \ 3P_1 - 2s^2 2p^5 3s \ 1P_1$	M2	2.615E-11	2.731E-11	2.739E-11	...
14 - 3	$2s^2 2p^5 3p \ 1D_2 - 2s^2 2p^5 3s \ 1P_1$	E1	3.813E-03	4.091E-03	4.087E-03	...
14 - 3	$2s^2 2p^5 3p \ 1D_2 - 2s^2 2p^5 3s \ 1P_1$	M2	8.609E-12	9.353E-12	9.381E-12	...
15 - 3	$2s^2 2p^5 3p \ 1S_0 - 2s^2 2p^5 3s \ 1P_1$	E1	6.690E-02	6.977E-02	6.968E-02	...
18 - 3	$2s^2 2p^5 3d \ 3P_2 - 2s^2 2p^5 3s \ 1P_1$	E2	1.775E-06	1.798E-06	1.798E-06	...
20 - 3	$2s^2 2p^5 3d \ 3F_3 - 2s^2 2p^5 3s \ 1P_1$	E2	5.639E-06	5.678E-06	5.687E-06	...
21 - 3	$2s^2 2p^5 3d \ 1D_2 - 2s^2 2p^5 3s \ 1P_1$	E2	5.420E-06	5.508E-06	5.513E-06	...
22 - 3	$2s^2 2p^5 3d \ 3D_3 - 2s^2 2p^5 3s \ 1P_1$	E2	4.666E-06	4.792E-06	4.787E-06	...
23 - 3	$2s^2 2p^5 3d \ 3D_1 - 2s^2 2p^5 3s \ 1P_1$	E2	4.957E-06	5.032E-06	5.024E-06	...
27 - 3	$2s^2 2p^5 3d \ 1P_1 - 2s^2 2p^5 3s \ 1P_1$	E2	1.304E-06	1.335E-06	1.331E-06	...
28 - 3	$2s 2p^6 3s \ 3S_1 - 2s^2 2p^5 3s \ 1P_1$	E1	7.934E-02	8.363E-02
28 - 3	$2s 2p^6 3s \ 3S_1 - 2s^2 2p^5 3s \ 1P_1$	M2	2.563E-09	2.594E-09
29 - 3	$2s 2p^6 3s \ 1S_0 - 2s^2 2p^5 3s \ 1P_1$	E1	6.424E-02	6.631E-02	...	7.80E-02
37 - 3	$2s 2p^6 3d \ 1D_2 - 2s^2 2p^5 3s \ 1P_1$	E1	1.216E-03	1.217E-03
5 - 4	$2s^2 2p^5 3s \ 3P_1 - 2s^2 2p^5 3s \ 3P_0$	M1	4.214E-07	4.282E-07	4.268E-07	...
6 - 4	$2s^2 2p^5 3p \ 3S_1 - 2s^2 2p^5 3s \ 3P_0$	E1	2.168E-03	2.176E-03	2.199E-03	2.40E-03
7 - 4	$2s^2 2p^5 3p \ 3D_2 - 2s^2 2p^5 3s \ 3P_0$	M2	4.162E-13	4.205E-13
12 - 4	$2s^2 2p^5 3p \ 3D_1 - 2s^2 2p^5 3s \ 3P_0$	E1	1.209E-01	1.232E-01	1.237E-01	...
13 - 4	$2s^2 2p^5 3p \ 3P_1 - 2s^2 2p^5 3s \ 3P_0$	E1	2.041E-01	2.068E-01	2.074E-01	...
14 - 4	$2s^2 2p^5 3p \ 1D_2 - 2s^2 2p^5 3s \ 3P_0$	M2	2.391E-10	2.390E-10	2.423E-10	...
24 - 4	$2s^2 2p^5 3d \ 3F_2 - 2s^2 2p^5 3s \ 3P_0$	E2	3.286E-06	3.393E-06	3.396E-06	...
25 - 4	$2s^2 2p^5 3d \ 3D_2 - 2s^2 2p^5 3s \ 3P_0$	E2	4.053E-06	4.070E-06	4.075E-06	...
28 - 4	$2s 2p^6 3s \ 3S_1 - 2s^2 2p^5 3s \ 3P_0$	E1	5.449E-02	5.697E-02

Table 5 *continued*

Table 5 (*continued*)

$j - i$	Transition	Type	gf			
			MBPT ^a	MCDHF/RCI ^b	MCDHF/RCI2 ^c	NIST ^d
6 - 5	$2s^2 2p^5 3p \ ^3S_1 - 2s^2 2p^5 3s \ ^3P_1$	E1	2.782E-03	2.760E-03	2.792E-03	...
6 - 5	$2s^2 2p^5 3p \ ^3S_1 - 2s^2 2p^5 3s \ ^3P_1$	M2	1.977E-12	1.939E-12
7 - 5	$2s^2 2p^5 3p \ ^3D_2 - 2s^2 2p^5 3s \ ^3P_1$	M2	5.361E-13	5.378E-13
8 - 5	$2s^2 2p^5 3p \ ^3D_3 - 2s^2 2p^5 3s \ ^3P_1$	M2	1.361E-12	1.431E-12
9 - 5	$2s^2 2p^5 3p \ ^1P_1 - 2s^2 2p^5 3s \ ^3P_1$	M2	3.938E-13	4.053E-13
10 - 5	$2s^2 2p^5 3p \ ^3P_2 - 2s^2 2p^5 3s \ ^3P_1$	E1	4.140E-03	4.356E-03	4.367E-03	...
10 - 5	$2s^2 2p^5 3p \ ^3P_2 - 2s^2 2p^5 3s \ ^3P_1$	M2	2.822E-13	3.238E-13
11 - 5	$2s^2 2p^5 3p \ ^3P_0 - 2s^2 2p^5 3s \ ^3P_1$	E1	2.632E-02	2.684E-02	2.699E-02	...
12 - 5	$2s^2 2p^5 3p \ ^3D_1 - 2s^2 2p^5 3s \ ^3P_1$	E1	1.814E-01	1.834E-01	1.842E-01	...
12 - 5	$2s^2 2p^5 3p \ ^3D_1 - 2s^2 2p^5 3s \ ^3P_1$	M2	1.288E-12	1.353E-12
13 - 5	$2s^2 2p^5 3p \ ^3P_1 - 2s^2 2p^5 3s \ ^3P_1$	E1	1.200E-01	1.221E-01	1.225E-01	...
13 - 5	$2s^2 2p^5 3p \ ^3P_1 - 2s^2 2p^5 3s \ ^3P_1$	M2	2.894E-10	2.874E-10	2.920E-10	...
14 - 5	$2s^2 2p^5 3p \ ^1D_2 - 2s^2 2p^5 3s \ ^3P_1$	E1	5.622E-01	5.701E-01	5.718E-01	...
14 - 5	$2s^2 2p^5 3p \ ^1D_2 - 2s^2 2p^5 3s \ ^3P_1$	M2	3.213E-10	3.200E-10	3.248E-10	...
15 - 5	$2s^2 2p^5 3p \ ^1S_0 - 2s^2 2p^5 3s \ ^3P_1$	E1	1.234E-01	1.271E-01	1.270E-01	...
24 - 5	$2s^2 2p^5 3d \ ^3F_2 - 2s^2 2p^5 3s \ ^3P_1$	E2	3.917E-06	3.926E-06	3.929E-06	...
25 - 5	$2s^2 2p^5 3d \ ^3D_2 - 2s^2 2p^5 3s \ ^3P_1$	E2	3.191E-06	3.289E-06	3.292E-06	...
26 - 5	$2s^2 2p^5 3d \ ^1F_3 - 2s^2 2p^5 3s \ ^3P_1$	E2	1.042E-05	1.058E-05	1.058E-05	...
27 - 5	$2s^2 2p^5 3d \ ^1P_1 - 2s^2 2p^5 3s \ ^3P_1$	E2	5.636E-06	5.753E-06	5.740E-06	...
28 - 5	$2s2p^6 3s \ ^3S_1 - 2s^2 2p^5 3s \ ^3P_1$	E1	8.824E-02	9.149E-02
28 - 5	$2s2p^6 3s \ ^3S_1 - 2s^2 2p^5 3s \ ^3P_1$	M2	1.018E-10	1.086E-10
29 - 5	$2s2p^6 3s \ ^1S_0 - 2s^2 2p^5 3s \ ^3P_1$	E1	4.618E-02	4.839E-02	...	5.70E-02
37 - 5	$2s2p^6 3d \ ^1D_2 - 2s^2 2p^5 3s \ ^3P_1$	E1	9.608E-04	9.894E-04
7 - 6	$2s^2 2p^5 3p \ ^3D_2 - 2s^2 2p^5 3p \ ^3S_1$	M1	1.538E-07	1.568E-07	1.568E-07	...
7 - 6	$2s^2 2p^5 3p \ ^3D_2 - 2s^2 2p^5 3p \ ^3S_1$	E2	9.775E-11	1.043E-10
8 - 6	$2s^2 2p^5 3p \ ^3D_3 - 2s^2 2p^5 3p \ ^3S_1$	E2	2.054E-09	2.119E-09	2.100E-09	...
9 - 6	$2s^2 2p^5 3p \ ^1P_1 - 2s^2 2p^5 3p \ ^3S_1$	M1	1.814E-07	1.809E-07	1.818E-07	...
10 - 6	$2s^2 2p^5 3p \ ^3P_2 - 2s^2 2p^5 3p \ ^3S_1$	M1	7.699E-07	7.774E-07	7.777E-07	...

Table 5 *continued*

Table 5 (*continued*)

$j - i$	Transition	Type	gf			
			MBPT ^a	MCDHF/RCI ^b	MCDHF/RCI2 ^c	NIST ^d
11 - 6	$2s^22p^53p\ ^3P_0 - 2s^22p^53p\ ^3S_1$	M1	1.404E-06	1.425E-06	1.426E-06	...
12 - 6	$2s^22p^53p\ ^3D_1 - 2s^22p^53p\ ^3S_1$	M1	5.042E-07	5.038E-07	5.059E-07	...
13 - 6	$2s^22p^53p\ ^3P_1 - 2s^22p^53p\ ^3S_1$	M1	8.478E-07	8.614E-07	8.598E-07	...
14 - 6	$2s^22p^53p\ ^1D_2 - 2s^22p^53p\ ^3S_1$	M1	1.849E-07	1.883E-07	1.877E-07	...
15 - 6	$2s^22p^53p\ ^1S_0 - 2s^22p^53p\ ^3S_1$	M1	2.400E-07	2.335E-07	2.341E-07	...
16 - 6	$2s^22p^53d\ ^3P_0 - 2s^22p^53p\ ^3S_1$	E1	1.184E-01	1.213E-01	1.207E-01	1.20E-01
17 - 6	$2s^22p^53d\ ^3P_1 - 2s^22p^53p\ ^3S_1$	E1	2.874E-01	2.946E-01	2.926E-01	3.00E-01
17 - 6	$2s^22p^53d\ ^3P_1 - 2s^22p^53p\ ^3S_1$	M2	1.074E-10	1.113E-10	1.093E-10	...
18 - 6	$2s^22p^53d\ ^3P_2 - 2s^22p^53p\ ^3S_1$	E1	2.509E-01	2.580E-01	2.559E-01	2.61E-01
18 - 6	$2s^22p^53d\ ^3P_2 - 2s^22p^53p\ ^3S_1$	M2	1.610E-10	1.665E-10	1.635E-10	...
20 - 6	$2s^22p^53d\ ^3F_3 - 2s^22p^53p\ ^3S_1$	M2	2.319E-11	2.415E-11	2.376E-11	...
21 - 6	$2s^22p^53d\ ^1D_2 - 2s^22p^53p\ ^3S_1$	E1	1.585E-02	1.575E-02	1.569E-02	...
21 - 6	$2s^22p^53d\ ^1D_2 - 2s^22p^53p\ ^3S_1$	M2	8.630E-11	8.913E-11	8.790E-11	...
22 - 6	$2s^22p^53d\ ^3D_3 - 2s^22p^53p\ ^3S_1$	M2	4.103E-11	4.293E-11	4.199E-11	...
23 - 6	$2s^22p^53d\ ^3D_1 - 2s^22p^53p\ ^3S_1$	M2	5.969E-10	6.138E-10	6.039E-10	...
24 - 6	$2s^22p^53d\ ^3F_2 - 2s^22p^53p\ ^3S_1$	E1	7.979E-04	8.035E-04	7.935E-04	...
24 - 6	$2s^22p^53d\ ^3F_2 - 2s^22p^53p\ ^3S_1$	M2	5.997E-12	6.516E-12	6.403E-12	...
25 - 6	$2s^22p^53d\ ^3D_2 - 2s^22p^53p\ ^3S_1$	E1	2.151E-03	2.224E-03	2.230E-03	...
25 - 6	$2s^22p^53d\ ^3D_2 - 2s^22p^53p\ ^3S_1$	M2	5.709E-11	5.915E-11	5.811E-11	...
26 - 6	$2s^22p^53d\ ^1F_3 - 2s^22p^53p\ ^3S_1$	M2	2.359E-11	2.435E-11	2.399E-11	...
27 - 6	$2s^22p^53d\ ^1P_1 - 2s^22p^53p\ ^3S_1$	M2	3.375E-10	3.541E-10	3.497E-10	...
30 - 6	$2s2p^63p\ ^3P_0 - 2s^22p^53p\ ^3S_1$	E1	4.881E-02	5.097E-02
31 - 6	$2s2p^63p\ ^3P_1 - 2s^22p^53p\ ^3S_1$	E1	4.247E-02	4.504E-02	...	5.10E-02
31 - 6	$2s2p^63p\ ^3P_1 - 2s^22p^53p\ ^3S_1$	M2	1.514E-09	1.537E-09
32 - 6	$2s2p^63p\ ^3P_2 - 2s^22p^53p\ ^3S_1$	E1	1.507E-02	1.617E-02
32 - 6	$2s2p^63p\ ^3P_2 - 2s^22p^53p\ ^3S_1$	M2	1.101E-09	1.133E-09
33 - 6	$2s2p^63p\ ^1P_1 - 2s^22p^53p\ ^3S_1$	M2	2.915E-10	3.109E-10
8 - 7	$2s^22p^53p\ ^3D_3 - 2s^22p^53p\ ^3D_2$	M1	1.430E-06	1.435E-06	1.436E-06	...

Table 5 *continued*

Table 5 (*continued*)

$j - i$	Transition	Type	gf			
			MBPT ^a	MCDHF/RCI ^b	MCDHF/RCI2 ^c	NIST ^d
8 - 7	$2s^2 2p^5 3p \ ^3D_3 - 2s^2 2p^5 3p \ ^3D_2$	E2	4.089E-11	4.029E-11
9 - 7	$2s^2 2p^5 3p \ ^1P_1 - 2s^2 2p^5 3p \ ^3D_2$	M1	9.749E-07	9.950E-07	9.931E-07	...
9 - 7	$2s^2 2p^5 3p \ ^1P_1 - 2s^2 2p^5 3p \ ^3D_2$	E2	1.655E-10	1.662E-10
10 - 7	$2s^2 2p^5 3p \ ^3P_2 - 2s^2 2p^5 3p \ ^3D_2$	M1	9.223E-07	9.367E-07	9.357E-07	...
10 - 7	$2s^2 2p^5 3p \ ^3P_2 - 2s^2 2p^5 3p \ ^3D_2$	E2	1.288E-09	1.308E-09	1.304E-09	...
11 - 7	$2s^2 2p^5 3p \ ^3P_0 - 2s^2 2p^5 3p \ ^3D_2$	E2	3.834E-09	3.908E-09	3.899E-09	...
12 - 7	$2s^2 2p^5 3p \ ^3D_1 - 2s^2 2p^5 3p \ ^3D_2$	M1	6.469E-06	6.552E-06	6.551E-06	...
16 - 7	$2s^2 2p^5 3d \ ^3P_0 - 2s^2 2p^5 3p \ ^3D_2$	M2	3.519E-12	3.616E-12	3.638E-12	...
17 - 7	$2s^2 2p^5 3d \ ^3P_1 - 2s^2 2p^5 3p \ ^3D_2$	E1	2.898E-02	2.960E-02	2.932E-02	...
17 - 7	$2s^2 2p^5 3d \ ^3P_1 - 2s^2 2p^5 3p \ ^3D_2$	M2	3.030E-11	3.141E-11	3.073E-11	...
18 - 7	$2s^2 2p^5 3d \ ^3P_2 - 2s^2 2p^5 3p \ ^3D_2$	E1	4.515E-02	4.705E-02	4.693E-02	...
18 - 7	$2s^2 2p^5 3d \ ^3P_2 - 2s^2 2p^5 3p \ ^3D_2$	M2	6.491E-11	6.764E-11	6.671E-11	...
19 - 7	$2s^2 2p^5 3d \ ^3F_4 - 2s^2 2p^5 3p \ ^3D_2$	M2	4.877E-10	5.003E-10	4.925E-10	...
20 - 7	$2s^2 2p^5 3d \ ^3F_3 - 2s^2 2p^5 3p \ ^3D_2$	E1	8.068E-01	8.273E-01	8.207E-01	...
20 - 7	$2s^2 2p^5 3d \ ^3F_3 - 2s^2 2p^5 3p \ ^3D_2$	M2	2.950E-11	3.160E-11	3.092E-11	...
21 - 7	$2s^2 2p^5 3d \ ^1D_2 - 2s^2 2p^5 3p \ ^3D_2$	E1	2.418E-01	2.481E-01	2.462E-01	...
22 - 7	$2s^2 2p^5 3d \ ^3D_3 - 2s^2 2p^5 3p \ ^3D_2$	E1	4.827E-03	5.407E-03	5.328E-03	...
22 - 7	$2s^2 2p^5 3d \ ^3D_3 - 2s^2 2p^5 3p \ ^3D_2$	M2	2.365E-10	2.440E-10	2.402E-10	...
23 - 7	$2s^2 2p^5 3d \ ^3D_1 - 2s^2 2p^5 3p \ ^3D_2$	E1	1.629E-02	1.679E-02	1.661E-02	...
24 - 7	$2s^2 2p^5 3d \ ^3F_2 - 2s^2 2p^5 3p \ ^3D_2$	E1	2.532E-03	2.707E-03	2.694E-03	...
25 - 7	$2s^2 2p^5 3d \ ^3D_2 - 2s^2 2p^5 3p \ ^3D_2$	E1	7.295E-03	7.473E-03	7.376E-03	...
25 - 7	$2s^2 2p^5 3d \ ^3D_2 - 2s^2 2p^5 3p \ ^3D_2$	M2	3.197E-11	3.342E-11	3.290E-11	...
26 - 7	$2s^2 2p^5 3d \ ^1F_3 - 2s^2 2p^5 3p \ ^3D_2$	M2	9.149E-12	9.805E-12	9.637E-12	...
30 - 7	$2s2p^6 3p \ ^3P_0 - 2s^2 2p^5 3p \ ^3D_2$	M2	1.638E-09	1.677E-09
31 - 7	$2s2p^6 3p \ ^3P_1 - 2s^2 2p^5 3p \ ^3D_2$	E1	2.573E-01	2.705E-01
31 - 7	$2s2p^6 3p \ ^3P_1 - 2s^2 2p^5 3p \ ^3D_2$	M2	2.254E-09	2.297E-09
32 - 7	$2s2p^6 3p \ ^3P_2 - 2s^2 2p^5 3p \ ^3D_2$	E1	3.923E-03	4.158E-03
33 - 7	$2s2p^6 3p \ ^1P_1 - 2s^2 2p^5 3p \ ^3D_2$	E1	1.449E-02	1.583E-02

Table 5 *continued*

Table 5 (*continued*)

$j - i$	Transition	Type	gf			
			MBPT ^a	MCDHF/RCI ^b	MCDHF/RCI2 ^c	NIST ^d
33 - 7	$2s2p^63p\ ^1P_1 - 2s^22p^53p\ ^3D_2$	M2	1.943E-10	2.122E-10
9 - 8	$2s^22p^53p\ ^1P_1 - 2s^22p^53p\ ^3D_3$	E2	1.742E-12	1.876E-12
10 - 8	$2s^22p^53p\ ^3P_2 - 2s^22p^53p\ ^3D_3$	E2	3.665E-10	3.782E-10
13 - 8	$2s^22p^53p\ ^3P_1 - 2s^22p^53p\ ^3D_3$	E2	4.680E-09	4.793E-09	4.803E-09	...
14 - 8	$2s^22p^53p\ ^1D_2 - 2s^22p^53p\ ^3D_3$	M1	8.715E-06	8.827E-06	8.825E-06	...
17 - 8	$2s^22p^53d\ ^3P_1 - 2s^22p^53p\ ^3D_3$	M2	2.211E-12	2.281E-12
18 - 8	$2s^22p^53d\ ^3P_2 - 2s^22p^53p\ ^3D_3$	E1	2.100E-02	2.131E-02	2.107E-02	2.80E-02
18 - 8	$2s^22p^53d\ ^3P_2 - 2s^22p^53p\ ^3D_3$	M2	1.541E-10	1.588E-10	1.550E-10	...
19 - 8	$2s^22p^53d\ ^3F_4 - 2s^22p^53p\ ^3D_3$	E1	1.167E+00	1.197E+00	1.188E+00	1.19E+00
19 - 8	$2s^22p^53d\ ^3F_4 - 2s^22p^53p\ ^3D_3$	M2	1.565E-09	1.619E-09	1.590E-09	...
20 - 8	$2s^22p^53d\ ^3F_3 - 2s^22p^53p\ ^3D_3$	E1	1.338E-01	1.390E-01	1.378E-01	...
21 - 8	$2s^22p^53d\ ^1D_2 - 2s^22p^53p\ ^3D_3$	E1	1.228E-02	1.259E-02	1.249E-02	...
21 - 8	$2s^22p^53d\ ^1D_2 - 2s^22p^53p\ ^3D_3$	M2	4.456E-11	4.618E-11	4.542E-11	...
22 - 8	$2s^22p^53d\ ^3D_3 - 2s^22p^53p\ ^3D_3$	E1	1.906E-01	1.944E-01	1.929E-01	...
22 - 8	$2s^22p^53d\ ^3D_3 - 2s^22p^53p\ ^3D_3$	M2	9.674E-10	1.000E-09	9.853E-10	...
23 - 8	$2s^22p^53d\ ^3D_1 - 2s^22p^53p\ ^3D_3$	M2	7.194E-12	7.329E-12	7.195E-12	...
24 - 8	$2s^22p^53d\ ^3F_2 - 2s^22p^53p\ ^3D_3$	M2	3.532E-12	3.592E-12
25 - 8	$2s^22p^53d\ ^3D_2 - 2s^22p^53p\ ^3D_3$	E1	5.635E-03	5.913E-03	5.861E-03	...
25 - 8	$2s^22p^53d\ ^3D_2 - 2s^22p^53p\ ^3D_3$	M2	1.475E-11	1.548E-11	1.554E-11	...
26 - 8	$2s^22p^53d\ ^1F_3 - 2s^22p^53p\ ^3D_3$	E1	6.863E-03	7.070E-03	7.029E-03	...
26 - 8	$2s^22p^53d\ ^1F_3 - 2s^22p^53p\ ^3D_3$	M2	7.262E-12	7.216E-12	7.320E-12	...
31 - 8	$2s2p^63p\ ^3P_1 - 2s^22p^53p\ ^3D_3$	M2	1.779E-10	1.867E-10
32 - 8	$2s2p^63p\ ^3P_2 - 2s^22p^53p\ ^3D_3$	E1	4.079E-01	4.295E-01
32 - 8	$2s2p^63p\ ^3P_2 - 2s^22p^53p\ ^3D_3$	M2	2.075E-09	2.112E-09
33 - 8	$2s2p^63p\ ^1P_1 - 2s^22p^53p\ ^3D_3$	M2	3.409E-09	3.483E-09
10 - 9	$2s^22p^53p\ ^3P_2 - 2s^22p^53p\ ^1P_1$	M1	2.232E-07	2.261E-07	2.253E-07	...
10 - 9	$2s^22p^53p\ ^3P_2 - 2s^22p^53p\ ^1P_1$	E2	6.199E-11	6.350E-11
11 - 9	$2s^22p^53p\ ^3P_0 - 2s^22p^53p\ ^1P_1$	M1	8.225E-07	8.462E-07	8.434E-07	...

Table 5 *continued*

Table 5 (*continued*)

$j - i$	Transition	Type	gf			
			MBPT ^a	MCDHF/RCI ^b	MCDHF/RCI2 ^c	NIST ^d
12 - 9	$2s^2 2p^5 3p \ ^3D_1 - 2s^2 2p^5 3p \ ^1P_1$	M1	7.438E-07	7.636E-07	7.615E-07	...
13 - 9	$2s^2 2p^5 3p \ ^3P_1 - 2s^2 2p^5 3p \ ^1P_1$	M1	2.409E-06	2.434E-06	2.435E-06	...
14 - 9	$2s^2 2p^5 3p \ ^1D_2 - 2s^2 2p^5 3p \ ^1P_1$	M1	5.729E-07	5.813E-07	5.811E-07	...
15 - 9	$2s^2 2p^5 3p \ ^1S_0 - 2s^2 2p^5 3p \ ^1P_1$	M1	2.245E-07	2.222E-07	2.218E-07	...
16 - 9	$2s^2 2p^5 3d \ ^3P_0 - 2s^2 2p^5 3p \ ^1P_1$	E1	4.138E-03	4.315E-03	4.260E-03	...
17 - 9	$2s^2 2p^5 3d \ ^3P_1 - 2s^2 2p^5 3p \ ^1P_1$	M2	2.544E-11	2.605E-11	2.565E-11	...
18 - 9	$2s^2 2p^5 3d \ ^3P_2 - 2s^2 2p^5 3p \ ^1P_1$	E1	6.535E-02	6.617E-02	6.574E-02	...
18 - 9	$2s^2 2p^5 3d \ ^3P_2 - 2s^2 2p^5 3p \ ^1P_1$	M2	6.194E-12	6.404E-12
20 - 9	$2s^2 2p^5 3d \ ^3F_3 - 2s^2 2p^5 3p \ ^1P_1$	M2	3.044E-12	2.689E-12
21 - 9	$2s^2 2p^5 3d \ ^1D_2 - 2s^2 2p^5 3p \ ^1P_1$	E1	4.272E-01	4.394E-01	4.357E-01	...
21 - 9	$2s^2 2p^5 3d \ ^1D_2 - 2s^2 2p^5 3p \ ^1P_1$	M2	1.467E-11	1.519E-11	1.494E-11	...
22 - 9	$2s^2 2p^5 3d \ ^3D_3 - 2s^2 2p^5 3p \ ^1P_1$	M2	8.437E-10	8.701E-10	8.558E-10	...
23 - 9	$2s^2 2p^5 3d \ ^3D_1 - 2s^2 2p^5 3p \ ^1P_1$	E1	1.900E-01	1.947E-01	1.930E-01	...
23 - 9	$2s^2 2p^5 3d \ ^3D_1 - 2s^2 2p^5 3p \ ^1P_1$	M2	9.622E-11	9.784E-11	9.665E-11	...
24 - 9	$2s^2 2p^5 3d \ ^3F_2 - 2s^2 2p^5 3p \ ^1P_1$	M2	2.758E-12	2.781E-12
25 - 9	$2s^2 2p^5 3d \ ^3D_2 - 2s^2 2p^5 3p \ ^1P_1$	E1	8.277E-04	8.651E-04	8.524E-04	...
25 - 9	$2s^2 2p^5 3d \ ^3D_2 - 2s^2 2p^5 3p \ ^1P_1$	M2	2.025E-11	2.139E-11	2.091E-11	...
27 - 9	$2s^2 2p^5 3d \ ^1P_1 - 2s^2 2p^5 3p \ ^1P_1$	E1	2.781E-02	2.891E-02	2.888E-02	...
27 - 9	$2s^2 2p^5 3d \ ^1P_1 - 2s^2 2p^5 3p \ ^1P_1$	M2	5.958E-11	6.184E-11	6.110E-11	...
30 - 9	$2s 2p^6 3p \ ^3P_0 - 2s^2 2p^5 3p \ ^1P_1$	E1	5.211E-02	5.505E-02
31 - 9	$2s 2p^6 3p \ ^3P_1 - 2s^2 2p^5 3p \ ^1P_1$	M2	8.947E-10	9.218E-10
32 - 9	$2s 2p^6 3p \ ^3P_2 - 2s^2 2p^5 3p \ ^1P_1$	E1	1.451E-02	1.519E-02
32 - 9	$2s 2p^6 3p \ ^3P_2 - 2s^2 2p^5 3p \ ^1P_1$	M2	1.318E-09	1.337E-09
33 - 9	$2s 2p^6 3p \ ^1P_1 - 2s^2 2p^5 3p \ ^1P_1$	E1	9.517E-02	9.992E-02
11 - 10	$2s^2 2p^5 3p \ ^3P_0 - 2s^2 2p^5 3p \ ^3P_2$	E2	2.441E-10	2.511E-10	2.497E-10	...
13 - 10	$2s^2 2p^5 3p \ ^3P_1 - 2s^2 2p^5 3p \ ^3P_2$	M1	3.509E-06	3.560E-06	3.559E-06	...
14 - 10	$2s^2 2p^5 3p \ ^1D_2 - 2s^2 2p^5 3p \ ^3P_2$	M1	3.608E-06	3.655E-06	3.653E-06	...
15 - 10	$2s^2 2p^5 3p \ ^1S_0 - 2s^2 2p^5 3p \ ^3P_2$	E2	1.791E-08	1.963E-08	1.944E-08	...

Table 5 *continued*

Table 5 (*continued*)

$j - i$	Transition	Type	gf			
			MBPT ^a	MCDHF/RCI ^b	MCDHF/RCI2 ^c	NIST ^d
17 - 10	$2s^2 2p^5 3d \ 3P_1 - 2s^2 2p^5 3p \ 3P_2$	E1	4.772E-02	4.885E-02	4.853E-02	...
17 - 10	$2s^2 2p^5 3d \ 3P_1 - 2s^2 2p^5 3p \ 3P_2$	M2	3.970E-11	4.082E-11	4.005E-11	...
18 - 10	$2s^2 2p^5 3d \ 3P_2 - 2s^2 2p^5 3p \ 3P_2$	E1	2.478E-01	2.540E-01	2.522E-01	...
18 - 10	$2s^2 2p^5 3d \ 3P_2 - 2s^2 2p^5 3p \ 3P_2$	M2	4.409E-10	4.545E-10	4.468E-10	...
19 - 10	$2s^2 2p^5 3d \ 3F_4 - 2s^2 2p^5 3p \ 3P_2$	M2	4.711E-10	4.880E-10	4.795E-10	...
20 - 10	$2s^2 2p^5 3d \ 3F_3 - 2s^2 2p^5 3p \ 3P_2$	E1	1.087E-02	1.062E-02	1.061E-02	...
21 - 10	$2s^2 2p^5 3d \ 1D_2 - 2s^2 2p^5 3p \ 3P_2$	M2	1.206E-10	1.249E-10	1.232E-10	...
22 - 10	$2s^2 2p^5 3d \ 3D_3 - 2s^2 2p^5 3p \ 3P_2$	E1	7.610E-01	7.827E-01	7.763E-01	...
22 - 10	$2s^2 2p^5 3d \ 3D_3 - 2s^2 2p^5 3p \ 3P_2$	M2	3.200E-10	3.302E-10	3.244E-10	...
23 - 10	$2s^2 2p^5 3d \ 3D_1 - 2s^2 2p^5 3p \ 3P_2$	M2	2.165E-10	2.223E-10	2.185E-10	...
24 - 10	$2s^2 2p^5 3d \ 3F_2 - 2s^2 2p^5 3p \ 3P_2$	E1	7.615E-04	7.362E-04	7.263E-04	...
24 - 10	$2s^2 2p^5 3d \ 3F_2 - 2s^2 2p^5 3p \ 3P_2$	M2	9.533E-12	9.699E-12	9.545E-12	...
25 - 10	$2s^2 2p^5 3d \ 3D_2 - 2s^2 2p^5 3p \ 3P_2$	E1	2.262E-02	2.333E-02	2.306E-02	...
25 - 10	$2s^2 2p^5 3d \ 3D_2 - 2s^2 2p^5 3p \ 3P_2$	M2	5.225E-11	5.419E-11	5.329E-11	...
26 - 10	$2s^2 2p^5 3d \ 1F_3 - 2s^2 2p^5 3p \ 3P_2$	E1	8.357E-04	8.332E-04	8.217E-04	...
27 - 10	$2s^2 2p^5 3d \ 1P_1 - 2s^2 2p^5 3p \ 3P_2$	M2	1.791E-10	1.878E-10	1.849E-10	...
31 - 10	$2s 2p^6 3p \ 3P_1 - 2s^2 2p^5 3p \ 3P_2$	E1	1.236E-02	1.302E-02
31 - 10	$2s 2p^6 3p \ 3P_1 - 2s^2 2p^5 3p \ 3P_2$	M2	1.073E-10	1.172E-10
32 - 10	$2s 2p^6 3p \ 3P_2 - 2s^2 2p^5 3p \ 3P_2$	E1	1.109E-01	1.161E-01
32 - 10	$2s 2p^6 3p \ 3P_2 - 2s^2 2p^5 3p \ 3P_2$	M2	2.797E-09	2.871E-09
33 - 10	$2s 2p^6 3p \ 1P_1 - 2s^2 2p^5 3p \ 3P_2$	E1	1.193E-01	1.248E-01
33 - 10	$2s 2p^6 3p \ 1P_1 - 2s^2 2p^5 3p \ 3P_2$	M2	1.385E-09	1.419E-09
13 - 11	$2s^2 2p^5 3p \ 3P_1 - 2s^2 2p^5 3p \ 3P_0$	M1	2.011E-06	2.029E-06	2.031E-06	...
14 - 11	$2s^2 2p^5 3p \ 1D_2 - 2s^2 2p^5 3p \ 3P_0$	E2	6.049E-10	6.106E-10	6.137E-10	...
17 - 11	$2s^2 2p^5 3d \ 3P_1 - 2s^2 2p^5 3p \ 3P_0$	E1	9.768E-03	1.013E-02	1.007E-02	9.90E-03
18 - 11	$2s^2 2p^5 3d \ 3P_2 - 2s^2 2p^5 3p \ 3P_0$	M2	6.191E-11	6.306E-11	6.191E-11	...
21 - 11	$2s^2 2p^5 3d \ 1D_2 - 2s^2 2p^5 3p \ 3P_0$	M2	3.074E-11	3.164E-11	3.109E-11	...
23 - 11	$2s^2 2p^5 3d \ 3D_1 - 2s^2 2p^5 3p \ 3P_0$	E1	1.946E-01	2.002E-01	1.986E-01	1.70E-01

Table 5 *continued*

Table 5 (*continued*)

$j - i$	Transition	Type	gf			
			MBPT ^a	MCDHF/RCI ^b	MCDHF/RCI2 ^c	NIST ^d
24 – 11	$2s^2 2p^5 3d \ ^3F_2 - 2s^2 2p^5 3p \ ^3P_0$	M2	1.979E–12	2.326E–12
25 – 11	$2s^2 2p^5 3d \ ^3D_2 - 2s^2 2p^5 3p \ ^3P_0$	M2	1.555E–10	1.612E–10	1.584E–10	...
27 – 11	$2s^2 2p^5 3d \ ^1P_1 - 2s^2 2p^5 3p \ ^3P_0$	E1	1.467E–02	1.500E–02	1.486E–02	...
31 – 11	$2s 2p^6 3p \ ^3P_1 - 2s^2 2p^5 3p \ ^3P_0$	E1	2.778E–02	2.945E–02
32 – 11	$2s 2p^6 3p \ ^3P_2 - 2s^2 2p^5 3p \ ^3P_0$	M2	6.038E–10	6.134E–10
33 – 11	$2s 2p^6 3p \ ^1P_1 - 2s^2 2p^5 3p \ ^3P_0$	E1	2.131E–02	2.128E–02
13 – 12	$2s^2 2p^5 3p \ ^3P_1 - 2s^2 2p^5 3p \ ^3D_1$	M1	7.472E–08	7.333E–08	7.363E–08	...
13 – 12	$2s^2 2p^5 3p \ ^3P_1 - 2s^2 2p^5 3p \ ^3D_1$	E2	4.114E–10	4.143E–10
14 – 12	$2s^2 2p^5 3p \ ^1D_2 - 2s^2 2p^5 3p \ ^3D_1$	M1	1.589E–06	1.611E–06	1.611E–06	...
14 – 12	$2s^2 2p^5 3p \ ^1D_2 - 2s^2 2p^5 3p \ ^3D_1$	E2	5.194E–10	5.275E–10
18 – 12	$2s^2 2p^5 3d \ ^3P_2 - 2s^2 2p^5 3p \ ^3D_1$	E1	1.293E–03	1.343E–03	1.319E–03	...
18 – 12	$2s^2 2p^5 3d \ ^3P_2 - 2s^2 2p^5 3p \ ^3D_1$	M2	1.292E–12	1.349E–12
20 – 12	$2s^2 2p^5 3d \ ^3F_3 - 2s^2 2p^5 3p \ ^3D_1$	M2	2.145E–12	2.273E–12
22 – 12	$2s^2 2p^5 3d \ ^3D_3 - 2s^2 2p^5 3p \ ^3D_1$	M2	4.848E–12	5.263E–12
24 – 12	$2s^2 2p^5 3d \ ^3F_2 - 2s^2 2p^5 3p \ ^3D_1$	E1	5.861E–01	6.020E–01	5.973E–01	...
24 – 12	$2s^2 2p^5 3d \ ^3F_2 - 2s^2 2p^5 3p \ ^3D_1$	M2	1.739E–11	1.749E–11	1.723E–11	...
25 – 12	$2s^2 2p^5 3d \ ^3D_2 - 2s^2 2p^5 3p \ ^3D_1$	M2	7.094E–11	7.265E–11	7.160E–11	...
26 – 12	$2s^2 2p^5 3d \ ^1F_3 - 2s^2 2p^5 3p \ ^3D_1$	M2	4.541E–10	4.693E–10	4.618E–10	...
27 – 12	$2s^2 2p^5 3d \ ^1P_1 - 2s^2 2p^5 3p \ ^3D_1$	E1	1.264E–01	1.295E–01	1.287E–01	...
27 – 12	$2s^2 2p^5 3d \ ^1P_1 - 2s^2 2p^5 3p \ ^3D_1$	M2	5.019E–11	5.215E–11	5.129E–11	...
30 – 12	$2s 2p^6 3p \ ^3P_0 - 2s^2 2p^5 3p \ ^3D_1$	E1	4.789E–02	5.021E–02
31 – 12	$2s 2p^6 3p \ ^3P_1 - 2s^2 2p^5 3p \ ^3D_1$	E1	8.800E–02	9.275E–02
32 – 12	$2s 2p^6 3p \ ^3P_2 - 2s^2 2p^5 3p \ ^3D_1$	E1	2.661E–03	2.869E–03
32 – 12	$2s 2p^6 3p \ ^3P_2 - 2s^2 2p^5 3p \ ^3D_1$	M2	3.746E–11	3.883E–11
33 – 12	$2s 2p^6 3p \ ^1P_1 - 2s^2 2p^5 3p \ ^3D_1$	E1	1.816E–02	1.939E–02
14 – 13	$2s^2 2p^5 3p \ ^1D_2 - 2s^2 2p^5 3p \ ^3P_1$	M1	1.019E–07	1.061E–07	1.053E–07	...
14 – 13	$2s^2 2p^5 3p \ ^1D_2 - 2s^2 2p^5 3p \ ^3P_1$	E2	3.356E–13	3.774E–13
15 – 13	$2s^2 2p^5 3p \ ^1S_0 - 2s^2 2p^5 3p \ ^3P_1$	M1	3.655E–07	3.658E–07	3.656E–07	...

Table 5 *continued*

Table 5 (*continued*)

$j - i$	Transition	Type	gf			
			MBPT ^a	MCDHF/RCI ^b	MCDHF/RCI2 ^c	NIST ^d
16 – 13	$2s^2 2p^5 3d \ 3P_0 - 2s^2 2p^5 3p \ 3P_1$	E1	3.969E–03	4.114E–03	4.133E–03	...
17 – 13	$2s^2 2p^5 3d \ 3P_1 - 2s^2 2p^5 3p \ 3P_1$	M2	1.909E–12	2.051E–12
18 – 13	$2s^2 2p^5 3d \ 3P_2 - 2s^2 2p^5 3p \ 3P_1$	E1	1.537E–03	1.563E–03	1.566E–03	...
18 – 13	$2s^2 2p^5 3d \ 3P_2 - 2s^2 2p^5 3p \ 3P_1$	M2	6.332E–12	6.664E–12
20 – 13	$2s^2 2p^5 3d \ 3F_3 - 2s^2 2p^5 3p \ 3P_1$	M2	1.997E–12	2.144E–12
21 – 13	$2s^2 2p^5 3d \ 1D_2 - 2s^2 2p^5 3p \ 3P_1$	M2	1.560E–12	1.598E–12
22 – 13	$2s^2 2p^5 3d \ 3D_3 - 2s^2 2p^5 3p \ 3P_1$	M2	4.568E–12	4.747E–12
23 – 13	$2s^2 2p^5 3d \ 3D_1 - 2s^2 2p^5 3p \ 3P_1$	M2	1.189E–11	1.253E–11	1.225E–11	...
24 – 13	$2s^2 2p^5 3d \ 3F_2 - 2s^2 2p^5 3p \ 3P_1$	E1	1.051E–02	1.165E–02	1.158E–02	...
24 – 13	$2s^2 2p^5 3d \ 3F_2 - 2s^2 2p^5 3p \ 3P_1$	M2	9.980E–13	1.477E–12
25 – 13	$2s^2 2p^5 3d \ 3D_2 - 2s^2 2p^5 3p \ 3P_1$	E1	5.683E–01	5.822E–01	5.779E–01	...
25 – 13	$2s^2 2p^5 3d \ 3D_2 - 2s^2 2p^5 3p \ 3P_1$	M2	8.368E–10	8.648E–10	8.505E–10	...
26 – 13	$2s^2 2p^5 3d \ 1F_3 - 2s^2 2p^5 3p \ 3P_1$	M2	2.118E–10	2.180E–10	2.145E–10	...
27 – 13	$2s^2 2p^5 3d \ 1P_1 - 2s^2 2p^5 3p \ 3P_1$	E1	7.357E–02	7.580E–02	7.522E–02	...
27 – 13	$2s^2 2p^5 3d \ 1P_1 - 2s^2 2p^5 3p \ 3P_1$	M2	1.328E–11	1.438E–11	1.413E–11	...
30 – 13	$2s 2p^6 3p \ 3P_0 - 2s^2 2p^5 3p \ 3P_1$	E1	3.046E–03	3.221E–03
31 – 13	$2s 2p^6 3p \ 3P_1 - 2s^2 2p^5 3p \ 3P_1$	E1	7.485E–03	7.828E–03
31 – 13	$2s 2p^6 3p \ 3P_1 - 2s^2 2p^5 3p \ 3P_1$	M2	5.550E–11	5.897E–11
32 – 13	$2s 2p^6 3p \ 3P_2 - 2s^2 2p^5 3p \ 3P_1$	E1	7.697E–02	8.061E–02
32 – 13	$2s 2p^6 3p \ 3P_2 - 2s^2 2p^5 3p \ 3P_1$	M2	4.342E–11	4.522E–11
33 – 13	$2s 2p^6 3p \ 1P_1 - 2s^2 2p^5 3p \ 3P_1$	E1	4.251E–02	4.427E–02
33 – 13	$2s 2p^6 3p \ 1P_1 - 2s^2 2p^5 3p \ 3P_1$	M2	5.851E–11	5.950E–11
15 – 14	$2s^2 2p^5 3p \ 1S_0 - 2s^2 2p^5 3p \ 1D_2$	E2	8.789E–09	9.868E–09	9.796E–09	...
18 – 14	$2s^2 2p^5 3d \ 3P_2 - 2s^2 2p^5 3p \ 1D_2$	E1	5.043E–03	5.137E–03	5.077E–03	...
18 – 14	$2s^2 2p^5 3d \ 3P_2 - 2s^2 2p^5 3p \ 1D_2$	M2	9.302E–12	9.664E–12
19 – 14	$2s^2 2p^5 3d \ 3F_4 - 2s^2 2p^5 3p \ 1D_2$	M2	3.128E–13	3.477E–13
20 – 14	$2s^2 2p^5 3d \ 3F_3 - 2s^2 2p^5 3p \ 1D_2$	M2	4.257E–12	4.571E–12
24 – 14	$2s^2 2p^5 3d \ 3F_2 - 2s^2 2p^5 3p \ 1D_2$	E1	8.832E–02	8.972E–02	8.898E–02	...

Table 5 *continued*

Table 5 (*continued*)

$j - i$	Transition	Type	gf			
			MBPT ^a	MCDHF/RCI ^b	MCDHF/RCI2 ^c	NIST ^d
24 – 14	$2s^2 2p^5 3d \ ^3F_2 - 2s^2 2p^5 3p \ ^1D_2$	M2	1.073E–12	1.375E–12
25 – 14	$2s^2 2p^5 3d \ ^3D_2 - 2s^2 2p^5 3p \ ^1D_2$	E1	6.394E–02	6.675E–02	6.638E–02	...
25 – 14	$2s^2 2p^5 3d \ ^3D_2 - 2s^2 2p^5 3p \ ^1D_2$	M2	3.329E–10	3.436E–10	3.382E–10	...
26 – 14	$2s^2 2p^5 3d \ ^1F_3 - 2s^2 2p^5 3p \ ^1D_2$	E1	9.267E–01	9.518E–01	9.444E–01	...
26 – 14	$2s^2 2p^5 3d \ ^1F_3 - 2s^2 2p^5 3p \ ^1D_2$	M2	1.497E–09	1.548E–09	1.522E–09	...
30 – 14	$2s 2p^6 3p \ ^3P_0 - 2s^2 2p^5 3p \ ^1D_2$	M2	3.477E–11	3.656E–11
31 – 14	$2s 2p^6 3p \ ^3P_1 - 2s^2 2p^5 3p \ ^1D_2$	E1	4.494E–03	5.189E–03
31 – 14	$2s 2p^6 3p \ ^3P_1 - 2s^2 2p^5 3p \ ^1D_2$	M2	2.070E–11	2.327E–11
32 – 14	$2s 2p^6 3p \ ^3P_2 - 2s^2 2p^5 3p \ ^1D_2$	E1	1.208E–01	1.265E–01
33 – 14	$2s 2p^6 3p \ ^1P_1 - 2s^2 2p^5 3p \ ^1D_2$	E1	1.142E–01	1.218E–01
18 – 15	$2s^2 2p^5 3d \ ^3P_2 - 2s^2 2p^5 3p \ ^1S_0$	M2	8.122E–12	8.102E–12
21 – 15	$2s^2 2p^5 3d \ ^1D_2 - 2s^2 2p^5 3p \ ^1S_0$	M2	1.902E–12	1.946E–12
24 – 15	$2s^2 2p^5 3d \ ^3F_2 - 2s^2 2p^5 3p \ ^1S_0$	M2	6.056E–12	6.218E–12
25 – 15	$2s^2 2p^5 3d \ ^3D_2 - 2s^2 2p^5 3p \ ^1S_0$	M2	1.213E–11	1.165E–11
27 – 15	$2s^2 2p^5 3d \ ^1P_1 - 2s^2 2p^5 3p \ ^1S_0$	E1	1.710E–01	1.765E–01	1.748E–01	...
31 – 15	$2s 2p^6 3p \ ^3P_1 - 2s^2 2p^5 3p \ ^1S_0$	E1	2.139E–02	2.163E–02
32 – 15	$2s 2p^6 3p \ ^3P_2 - 2s^2 2p^5 3p \ ^1S_0$	M2	4.237E–10	4.404E–10
33 – 15	$2s 2p^6 3p \ ^1P_1 - 2s^2 2p^5 3p \ ^1S_0$	E1	6.789E–02	7.272E–02
17 – 16	$2s^2 2p^5 3d \ ^3P_1 - 2s^2 2p^5 3d \ ^3P_0$	M1	5.612E–07	5.683E–07	5.621E–07	...
18 – 16	$2s^2 2p^5 3d \ ^3P_2 - 2s^2 2p^5 3d \ ^3P_0$	E2	4.378E–11	4.505E–11
23 – 16	$2s^2 2p^5 3d \ ^3D_1 - 2s^2 2p^5 3d \ ^3P_0$	M1	3.388E–07	3.473E–07	3.478E–07	...
27 – 16	$2s^2 2p^5 3d \ ^1P_1 - 2s^2 2p^5 3d \ ^3P_0$	M1	5.076E–07	5.101E–07	5.094E–07	...
34 – 16	$2s 2p^6 3d \ ^3D_1 - 2s^2 2p^5 3d \ ^3P_0$	E1	1.605E–02	1.729E–02
35 – 16	$2s 2p^6 3d \ ^3D_2 - 2s^2 2p^5 3d \ ^3P_0$	M2	6.494E–10	6.604E–10
37 – 16	$2s 2p^6 3d \ ^1D_2 - 2s^2 2p^5 3d \ ^3P_0$	M2	1.479E–10	1.506E–10
18 – 17	$2s^2 2p^5 3d \ ^3P_2 - 2s^2 2p^5 3d \ ^3P_1$	M1	1.371E–06	1.401E–06	1.399E–06	...
18 – 17	$2s^2 2p^5 3d \ ^3P_2 - 2s^2 2p^5 3d \ ^3P_1$	E2	1.412E–11	1.465E–11
21 – 17	$2s^2 2p^5 3d \ ^1D_2 - 2s^2 2p^5 3d \ ^3P_1$	M1	6.974E–08	6.958E–08	6.919E–08	...

Table 5 *continued*

Table 5 (*continued*)

$j - i$	Transition	Type	gf			
			MBPT ^a	MCDHF/RCI ^b	MCDHF/RCI2 ^c	NIST ^d
22 – 17	$2s^2 2p^5 3d \ ^3D_3 - 2s^2 2p^5 3d \ ^3P_1$	E2	3.256E–10	3.369E–10
23 – 17	$2s^2 2p^5 3d \ ^3D_1 - 2s^2 2p^5 3d \ ^3P_1$	M1	9.681E–07	9.931E–07	9.949E–07	...
24 – 17	$2s^2 2p^5 3d \ ^3F_2 - 2s^2 2p^5 3d \ ^3P_1$	M1	3.777E–07	3.755E–07	3.759E–07	...
25 – 17	$2s^2 2p^5 3d \ ^3D_2 - 2s^2 2p^5 3d \ ^3P_1$	M1	7.115E–07	7.293E–07	7.288E–07	...
27 – 17	$2s^2 2p^5 3d \ ^1P_1 - 2s^2 2p^5 3d \ ^3P_1$	M1	9.701E–07	9.716E–07	9.708E–07	...
34 – 17	$2s 2p^6 3d \ ^3D_1 - 2s^2 2p^5 3d \ ^3P_1$	E1	3.474E–02	3.698E–02
34 – 17	$2s 2p^6 3d \ ^3D_1 - 2s^2 2p^5 3d \ ^3P_1$	M2	1.018E–10	1.045E–10
35 – 17	$2s 2p^6 3d \ ^3D_2 - 2s^2 2p^5 3d \ ^3P_1$	E1	1.821E–02	1.975E–02
35 – 17	$2s 2p^6 3d \ ^3D_2 - 2s^2 2p^5 3d \ ^3P_1$	M2	1.579E–09	1.600E–09
36 – 17	$2s 2p^6 3d \ ^3D_3 - 2s^2 2p^5 3d \ ^3P_1$	M2	6.333E–10	6.462E–10
37 – 17	$2s 2p^6 3d \ ^1D_2 - 2s^2 2p^5 3d \ ^3P_1$	M2	4.398E–10	4.480E–10
20 – 18	$2s^2 2p^5 3d \ ^3F_3 - 2s^2 2p^5 3d \ ^3P_2$	M1	1.915E–08	2.057E–08
21 – 18	$2s^2 2p^5 3d \ ^1D_2 - 2s^2 2p^5 3d \ ^3P_2$	E2	3.129E–11	3.263E–11
22 – 18	$2s^2 2p^5 3d \ ^3D_3 - 2s^2 2p^5 3d \ ^3P_2$	M1	6.480E–07	6.621E–07	6.620E–07	...
22 – 18	$2s^2 2p^5 3d \ ^3D_3 - 2s^2 2p^5 3d \ ^3P_2$	E2	3.739E–10	3.892E–10
23 – 18	$2s^2 2p^5 3d \ ^3D_1 - 2s^2 2p^5 3d \ ^3P_2$	M1	6.395E–07	6.547E–07	6.555E–07	...
24 – 18	$2s^2 2p^5 3d \ ^3F_2 - 2s^2 2p^5 3d \ ^3P_2$	M1	4.667E–07	4.554E–07	4.570E–07	...
25 – 18	$2s^2 2p^5 3d \ ^3D_2 - 2s^2 2p^5 3d \ ^3P_2$	M1	3.901E–06	3.971E–06	3.969E–06	...
26 – 18	$2s^2 2p^5 3d \ ^1F_3 - 2s^2 2p^5 3d \ ^3P_2$	M1	1.043E–06	1.056E–06	1.055E–06	...
27 – 18	$2s^2 2p^5 3d \ ^1P_1 - 2s^2 2p^5 3d \ ^3P_2$	M1	1.639E–07	1.639E–07	1.642E–07	...
29 – 18	$2s 2p^6 3s \ ^1S_0 - 2s^2 2p^5 3d \ ^3P_2$	M2	5.790E–12	6.550E–12
34 – 18	$2s 2p^6 3d \ ^3D_1 - 2s^2 2p^5 3d \ ^3P_2$	E1	1.196E–02	1.272E–02
34 – 18	$2s 2p^6 3d \ ^3D_1 - 2s^2 2p^5 3d \ ^3P_2$	M2	2.046E–10	2.098E–10
35 – 18	$2s 2p^6 3d \ ^3D_2 - 2s^2 2p^5 3d \ ^3P_2$	E1	5.615E–02	5.961E–02
35 – 18	$2s 2p^6 3d \ ^3D_2 - 2s^2 2p^5 3d \ ^3P_2$	M2	2.111E–10	2.129E–10
36 – 18	$2s 2p^6 3d \ ^3D_3 - 2s^2 2p^5 3d \ ^3P_2$	E1	2.228E–02	2.422E–02
36 – 18	$2s 2p^6 3d \ ^3D_3 - 2s^2 2p^5 3d \ ^3P_2$	M2	4.533E–09	4.603E–09
37 – 18	$2s 2p^6 3d \ ^1D_2 - 2s^2 2p^5 3d \ ^3P_2$	E1	2.213E–02	2.314E–02

Table 5 *continued*

Table 5 (*continued*)

$j - i$	Transition	Type	gf			
			MBPT ^a	MCDHF/RCI ^b	MCDHF/RCI2 ^c	NIST ^d
37 - 18	$2s2p^63d\ ^1D_2 - 2s^22p^53d\ ^3P_2$	M2	6.272E-10	6.425E-10
20 - 19	$2s^22p^53d\ ^3F_3 - 2s^22p^53d\ ^3F_4$	M1	1.009E-06	1.053E-06	1.047E-06	...
20 - 19	$2s^22p^53d\ ^3F_3 - 2s^22p^53d\ ^3F_4$	E2	1.836E-12	2.035E-12
21 - 19	$2s^22p^53d\ ^1D_2 - 2s^22p^53d\ ^3F_4$	E2	1.343E-11	1.397E-11
22 - 19	$2s^22p^53d\ ^3D_3 - 2s^22p^53d\ ^3F_4$	M1	1.886E-07	1.813E-07	1.819E-07	...
22 - 19	$2s^22p^53d\ ^3D_3 - 2s^22p^53d\ ^3F_4$	E2	3.977E-10	4.124E-10
26 - 19	$2s^22p^53d\ ^1F_3 - 2s^22p^53d\ ^3F_4$	M1	1.047E-05	1.062E-05	1.061E-05	...
35 - 19	$2s2p^63d\ ^3D_2 - 2s^22p^53d\ ^3F_4$	M2	1.524E-09	1.549E-09
36 - 19	$2s2p^63d\ ^3D_3 - 2s^22p^53d\ ^3F_4$	E1	4.860E-01	5.128E-01
36 - 19	$2s2p^63d\ ^3D_3 - 2s^22p^53d\ ^3F_4$	M2	2.471E-09	2.472E-09
37 - 19	$2s2p^63d\ ^1D_2 - 2s^22p^53d\ ^3F_4$	M2	3.746E-09	3.829E-09
21 - 20	$2s^22p^53d\ ^1D_2 - 2s^22p^53d\ ^3F_3$	M1	1.203E-06	1.234E-06	1.232E-06	...
21 - 20	$2s^22p^53d\ ^1D_2 - 2s^22p^53d\ ^3F_3$	E2	4.550E-11	4.622E-11
22 - 20	$2s^22p^53d\ ^3D_3 - 2s^22p^53d\ ^3F_3$	M1	4.086E-07	4.214E-07	4.206E-07	...
22 - 20	$2s^22p^53d\ ^3D_3 - 2s^22p^53d\ ^3F_3$	E2	5.392E-11	5.553E-11
23 - 20	$2s^22p^53d\ ^3D_1 - 2s^22p^53d\ ^3F_3$	E2	4.351E-10	4.528E-10	4.525E-10	...
24 - 20	$2s^22p^53d\ ^3F_2 - 2s^22p^53d\ ^3F_3$	M1	9.162E-06	9.282E-06	9.279E-06	...
25 - 20	$2s^22p^53d\ ^3D_2 - 2s^22p^53d\ ^3F_3$	M1	5.006E-08	6.562E-08	6.512E-08	...
34 - 20	$2s2p^63d\ ^3D_1 - 2s^22p^53d\ ^3F_3$	M2	3.212E-09	3.258E-09
35 - 20	$2s2p^63d\ ^3D_2 - 2s^22p^53d\ ^3F_3$	E1	2.691E-01	2.848E-01
35 - 20	$2s2p^63d\ ^3D_2 - 2s^22p^53d\ ^3F_3$	M2	1.529E-09	1.531E-09
36 - 20	$2s2p^63d\ ^3D_3 - 2s^22p^53d\ ^3F_3$	E1	2.539E-03	2.512E-03
37 - 20	$2s2p^63d\ ^1D_2 - 2s^22p^53d\ ^3F_3$	E1	1.034E-01	1.067E-01
37 - 20	$2s2p^63d\ ^1D_2 - 2s^22p^53d\ ^3F_3$	M2	9.943E-10	1.024E-09
22 - 21	$2s^22p^53d\ ^3D_3 - 2s^22p^53d\ ^1D_2$	M1	4.119E-07	4.154E-07	4.149E-07	...
23 - 21	$2s^22p^53d\ ^3D_1 - 2s^22p^53d\ ^1D_2$	M1	1.460E-06	1.495E-06	1.495E-06	...
23 - 21	$2s^22p^53d\ ^3D_1 - 2s^22p^53d\ ^1D_2$	E2	1.128E-09	1.165E-09	1.163E-09	...
24 - 21	$2s^22p^53d\ ^3F_2 - 2s^22p^53d\ ^1D_2$	M1	3.313E-06	3.391E-06	3.388E-06	...

Table 5 *continued*

Table 5 (*continued*)

$j - i$	Transition	Type	gf			
			MBPT ^a	MCDHF/RCI ^b	MCDHF/RCI2 ^c	NIST ^d
25 – 21	$2s^2 2p^5 3d \ ^3D_2 - 2s^2 2p^5 3d \ ^1D_2$	M1	9.495E–07	9.443E–07	9.456E–07	...
26 – 21	$2s^2 2p^5 3d \ ^1F_3 - 2s^2 2p^5 3d \ ^1D_2$	M1	3.576E–07	3.659E–07	3.662E–07	...
27 – 21	$2s^2 2p^5 3d \ ^1P_1 - 2s^2 2p^5 3d \ ^1D_2$	M1	1.321E–06	1.326E–06	1.323E–06	...
34 – 21	$2s 2p^6 3d \ ^3D_1 - 2s^2 2p^5 3d \ ^1D_2$	E1	1.295E–01	1.366E–01
34 – 21	$2s 2p^6 3d \ ^3D_1 - 2s^2 2p^5 3d \ ^1D_2$	M2	7.327E–10	7.467E–10
35 – 21	$2s 2p^6 3d \ ^3D_2 - 2s^2 2p^5 3d \ ^1D_2$	E1	3.870E–03	4.006E–03
35 – 21	$2s 2p^6 3d \ ^3D_2 - 2s^2 2p^5 3d \ ^1D_2$	M2	1.976E–09	2.003E–09
36 – 21	$2s 2p^6 3d \ ^3D_3 - 2s^2 2p^5 3d \ ^1D_2$	E1	5.234E–03	5.584E–03
36 – 21	$2s 2p^6 3d \ ^3D_3 - 2s^2 2p^5 3d \ ^1D_2$	M2	5.654E–10	5.791E–10
37 – 21	$2s 2p^6 3d \ ^1D_2 - 2s^2 2p^5 3d \ ^1D_2$	E1	8.099E–02	8.535E–02
37 – 21	$2s 2p^6 3d \ ^1D_2 - 2s^2 2p^5 3d \ ^1D_2$	M2	4.900E–10	4.962E–10
24 – 22	$2s^2 2p^5 3d \ ^3F_2 - 2s^2 2p^5 3d \ ^3D_3$	M1	6.456E–08	8.380E–08	8.284E–08	...
25 – 22	$2s^2 2p^5 3d \ ^3D_2 - 2s^2 2p^5 3d \ ^3D_3$	M1	4.680E–06	4.741E–06	4.740E–06	...
25 – 22	$2s^2 2p^5 3d \ ^3D_2 - 2s^2 2p^5 3d \ ^3D_3$	E2	1.706E–09	1.740E–09	1.738E–09	...
26 – 22	$2s^2 2p^5 3d \ ^1F_3 - 2s^2 2p^5 3d \ ^3D_3$	M1	5.831E–06	5.908E–06	5.906E–06	...
35 – 22	$2s 2p^6 3d \ ^3D_2 - 2s^2 2p^5 3d \ ^3D_3$	E1	4.385E–02	4.497E–02
35 – 22	$2s 2p^6 3d \ ^3D_2 - 2s^2 2p^5 3d \ ^3D_3$	M2	7.420E–10	7.730E–10
36 – 22	$2s 2p^6 3d \ ^3D_3 - 2s^2 2p^5 3d \ ^3D_3$	E1	1.219E–01	1.288E–01
36 – 22	$2s 2p^6 3d \ ^3D_3 - 2s^2 2p^5 3d \ ^3D_3$	M2	4.684E–09	4.740E–09
37 – 22	$2s 2p^6 3d \ ^1D_2 - 2s^2 2p^5 3d \ ^3D_3$	E1	1.370E–01	1.446E–01
37 – 22	$2s 2p^6 3d \ ^1D_2 - 2s^2 2p^5 3d \ ^3D_3$	M2	1.169E–09	1.187E–09
24 – 23	$2s^2 2p^5 3d \ ^3F_2 - 2s^2 2p^5 3d \ ^3D_1$	M1	3.646E–07	3.874E–07	3.868E–07	...
25 – 23	$2s^2 2p^5 3d \ ^3D_2 - 2s^2 2p^5 3d \ ^3D_1$	M1	4.131E–06	4.172E–06	4.173E–06	...
27 – 23	$2s^2 2p^5 3d \ ^1P_1 - 2s^2 2p^5 3d \ ^3D_1$	M1	7.183E–07	7.291E–07	7.277E–07	...
29 – 23	$2s 2p^6 3s \ ^1S_0 - 2s^2 2p^5 3d \ ^3D_1$	E1	9.415E–04	1.058E–03
34 – 23	$2s 2p^6 3d \ ^3D_1 - 2s^2 2p^5 3d \ ^3D_1$	E1	4.737E–02	5.002E–02
34 – 23	$2s 2p^6 3d \ ^3D_1 - 2s^2 2p^5 3d \ ^3D_1$	M2	2.344E–11	2.417E–11
35 – 23	$2s 2p^6 3d \ ^3D_2 - 2s^2 2p^5 3d \ ^3D_1$	E1	2.999E–02	3.194E–02

Table 5 *continued*

Table 5 (*continued*)

$j - i$	Transition	Type	gf			
			MBPT ^a	MCDHF/RCI ^b	MCDHF/RCI2 ^c	NIST ^d
35 - 23	$2s2p^63d\ ^3D_2 - 2s^22p^53d\ ^3D_1$	M2	2.561E-10	2.612E-10
36 - 23	$2s2p^63d\ ^3D_3 - 2s^22p^53d\ ^3D_1$	M2	7.006E-10	7.130E-10
37 - 23	$2s2p^63d\ ^1D_2 - 2s^22p^53d\ ^3D_1$	E1	1.333E-02	1.415E-02
37 - 23	$2s2p^63d\ ^1D_2 - 2s^22p^53d\ ^3D_1$	M2	1.358E-10	1.373E-10
25 - 24	$2s^22p^53d\ ^3D_2 - 2s^22p^53d\ ^3F_2$	M1	3.244E-09	2.400E-09
25 - 24	$2s^22p^53d\ ^3D_2 - 2s^22p^53d\ ^3F_2$	E2	5.568E-13	5.683E-13
26 - 24	$2s^22p^53d\ ^1F_3 - 2s^22p^53d\ ^3F_2$	M1	9.651E-07	9.956E-07	9.949E-07	...
26 - 24	$2s^22p^53d\ ^1F_3 - 2s^22p^53d\ ^3F_2$	E2	1.026E-11	1.068E-11
27 - 24	$2s^22p^53d\ ^1P_1 - 2s^22p^53d\ ^3F_2$	M1	1.446E-07	1.539E-07	1.536E-07	...
27 - 24	$2s^22p^53d\ ^1P_1 - 2s^22p^53d\ ^3F_2$	E2	1.872E-09	1.961E-09	1.961E-09	...
34 - 24	$2s2p^63d\ ^3D_1 - 2s^22p^53d\ ^3F_2$	E1	9.611E-02	1.006E-01
35 - 24	$2s2p^63d\ ^3D_2 - 2s^22p^53d\ ^3F_2$	E1	6.989E-02	7.427E-02
35 - 24	$2s2p^63d\ ^3D_2 - 2s^22p^53d\ ^3F_2$	M2	5.634E-11	5.747E-11
36 - 24	$2s2p^63d\ ^3D_3 - 2s^22p^53d\ ^3F_2$	E1	2.604E-03	2.917E-03
37 - 24	$2s2p^63d\ ^1D_2 - 2s^22p^53d\ ^3F_2$	E1	4.830E-02	5.038E-02
26 - 25	$2s^22p^53d\ ^1F_3 - 2s^22p^53d\ ^3D_2$	M1	1.749E-07	1.781E-07	1.768E-07	...
26 - 25	$2s^22p^53d\ ^1F_3 - 2s^22p^53d\ ^3D_2$	E2	4.193E-13	4.692E-13
27 - 25	$2s^22p^53d\ ^1P_1 - 2s^22p^53d\ ^3D_2$	M1	1.535E-06	1.548E-06	1.547E-06	...
27 - 25	$2s^22p^53d\ ^1P_1 - 2s^22p^53d\ ^3D_2$	E2	1.117E-09	1.207E-09	1.206E-09	...
28 - 25	$2s2p^63s\ ^3S_1 - 2s^22p^53d\ ^3D_2$	M2	1.069E-12	1.107E-12
34 - 25	$2s2p^63d\ ^3D_1 - 2s^22p^53d\ ^3D_2$	E1	1.999E-03	2.294E-03
35 - 25	$2s2p^63d\ ^3D_2 - 2s^22p^53d\ ^3D_2$	E1	4.126E-02	4.258E-02
36 - 25	$2s2p^63d\ ^3D_3 - 2s^22p^53d\ ^3D_2$	E1	5.922E-02	6.290E-02
36 - 25	$2s2p^63d\ ^3D_3 - 2s^22p^53d\ ^3D_2$	M2	2.071E-11	1.947E-11
37 - 25	$2s2p^63d\ ^1D_2 - 2s^22p^53d\ ^3D_2$	E1	4.342E-02	4.661E-02
37 - 25	$2s2p^63d\ ^1D_2 - 2s^22p^53d\ ^3D_2$	M2	4.337E-11	4.472E-11
34 - 26	$2s2p^63d\ ^3D_1 - 2s^22p^53d\ ^1F_3$	M2	5.350E-11	5.599E-11
35 - 26	$2s2p^63d\ ^3D_2 - 2s^22p^53d\ ^1F_3$	E1	4.237E-02	4.447E-02

Table 5 *continued*

Table 5 (*continued*)

$j - i$	Transition	Type	gf			
			MBPT ^a	MCDHF/RCI ^b	MCDHF/RCI2 ^c	NIST ^d
36 - 26	$2s2p^63d\ ^3D_3 - 2s^22p^53d\ ^1F_3$	E1	1.310E-01	1.376E-01
36 - 26	$2s2p^63d\ ^3D_3 - 2s^22p^53d\ ^1F_3$	M2	9.183E-11	8.887E-11
37 - 26	$2s2p^63d\ ^1D_2 - 2s^22p^53d\ ^1F_3$	E1	1.355E-01	1.430E-01
29 - 27	$2s2p^63s\ ^1S_0 - 2s^22p^53d\ ^1P_1$	E1	3.290E-03	3.731E-03
34 - 27	$2s2p^63d\ ^3D_1 - 2s^22p^53d\ ^1P_1$	E1	1.001E-02	1.031E-02
35 - 27	$2s2p^63d\ ^3D_2 - 2s^22p^53d\ ^1P_1$	E1	1.086E-02	1.123E-02
36 - 27	$2s2p^63d\ ^3D_3 - 2s^22p^53d\ ^1P_1$	M2	2.020E-11	2.189E-11
37 - 27	$2s2p^63d\ ^1D_2 - 2s^22p^53d\ ^1P_1$	E1	3.066E-02	3.338E-02
37 - 27	$2s2p^63d\ ^1D_2 - 2s^22p^53d\ ^1P_1$	M2	2.221E-11	2.275E-11
30 - 28	$2s2p^63p\ ^3P_0 - 2s2p^63s\ ^3S_1$	E1	1.111E-01	1.149E-01
31 - 28	$2s2p^63p\ ^3P_1 - 2s2p^63s\ ^3S_1$	E1	3.020E-01	3.132E-01
31 - 28	$2s2p^63p\ ^3P_1 - 2s2p^63s\ ^3S_1$	M2	1.620E-11	1.746E-11
32 - 28	$2s2p^63p\ ^3P_2 - 2s2p^63s\ ^3S_1$	E1	6.100E-01	6.298E-01
32 - 28	$2s2p^63p\ ^3P_2 - 2s2p^63s\ ^3S_1$	M2	3.020E-10	3.132E-10
33 - 28	$2s2p^63p\ ^1P_1 - 2s2p^63s\ ^3S_1$	E1	4.248E-02	4.218E-02
33 - 28	$2s2p^63p\ ^1P_1 - 2s2p^63s\ ^3S_1$	M2	3.656E-10	3.790E-10
34 - 28	$2s2p^63d\ ^3D_1 - 2s2p^63s\ ^3S_1$	E2	4.058E-06	4.119E-06
35 - 28	$2s2p^63d\ ^3D_2 - 2s2p^63s\ ^3S_1$	E2	6.796E-06	6.899E-06
36 - 28	$2s2p^63d\ ^3D_3 - 2s2p^63s\ ^3S_1$	E2	9.655E-06	9.801E-06
31 - 29	$2s2p^63p\ ^3P_1 - 2s2p^63s\ ^1S_0$	E1	2.825E-02	2.824E-02
32 - 29	$2s2p^63p\ ^3P_2 - 2s2p^63s\ ^1S_0$	M2	1.274E-10	1.310E-10
33 - 29	$2s2p^63p\ ^1P_1 - 2s2p^63s\ ^1S_0$	E1	2.706E-01	2.802E-01
37 - 29	$2s2p^63d\ ^1D_2 - 2s2p^63s\ ^1S_0$	E2	7.019E-06	7.140E-06
31 - 30	$2s2p^63p\ ^3P_1 - 2s2p^63p\ ^3P_0$	M1	2.662E-07	2.628E-07
32 - 30	$2s2p^63p\ ^3P_2 - 2s2p^63p\ ^3P_0$	E2	1.671E-10	1.671E-10
33 - 30	$2s2p^63p\ ^1P_1 - 2s2p^63p\ ^3P_0$	M1	3.357E-07	3.291E-07
34 - 30	$2s2p^63d\ ^3D_1 - 2s2p^63p\ ^3P_0$	E1	2.337E-01	2.383E-01
35 - 30	$2s2p^63d\ ^3D_2 - 2s2p^63p\ ^3P_0$	M2	1.446E-11	1.449E-11

Table 5 *continued*

Table 5 (*continued*)

$j - i$	Transition	Type	gf			
			MBPT ^a	MCDHF/RCI ^b	MCDHF/RCI2 ^c	NIST ^d
37 - 30	$2s2p^63d\ ^1D_2 - 2s2p^63p\ ^3P_0$	M2	2.090E-10	2.103E-10
32 - 31	$2s2p^63p\ ^3P_2 - 2s2p^63p\ ^3P_1$	M1	1.655E-06	1.688E-06
32 - 31	$2s2p^63p\ ^3P_2 - 2s2p^63p\ ^3P_1$	E2	1.934E-10	1.973E-10
33 - 31	$2s2p^63p\ ^1P_1 - 2s2p^63p\ ^3P_1$	M1	2.087E-07	2.009E-07
33 - 31	$2s2p^63p\ ^1P_1 - 2s2p^63p\ ^3P_1$	E2	3.933E-10	3.991E-10
34 - 31	$2s2p^63d\ ^3D_1 - 2s2p^63p\ ^3P_1$	E1	1.541E-01	1.577E-01
34 - 31	$2s2p^63d\ ^3D_1 - 2s2p^63p\ ^3P_1$	M2	1.929E-11	1.934E-11
35 - 31	$2s2p^63d\ ^3D_2 - 2s2p^63p\ ^3P_1$	E1	4.829E-01	4.937E-01
35 - 31	$2s2p^63d\ ^3D_2 - 2s2p^63p\ ^3P_1$	M2	1.757E-10	1.784E-10
36 - 31	$2s2p^63d\ ^3D_3 - 2s2p^63p\ ^3P_1$	M2	1.661E-10	1.638E-10
37 - 31	$2s2p^63d\ ^1D_2 - 2s2p^63p\ ^3P_1$	E1	6.840E-02	6.784E-02
37 - 31	$2s2p^63d\ ^1D_2 - 2s2p^63p\ ^3P_1$	M2	2.040E-10	2.087E-10
33 - 32	$2s2p^63p\ ^1P_1 - 2s2p^63p\ ^3P_2$	M1	1.688E-07	1.678E-07
33 - 32	$2s2p^63p\ ^1P_1 - 2s2p^63p\ ^3P_2$	E2	1.416E-11	1.462E-11
34 - 32	$2s2p^63d\ ^3D_1 - 2s2p^63p\ ^3P_2$	E1	1.093E-02	1.113E-02
35 - 32	$2s2p^63d\ ^3D_2 - 2s2p^63p\ ^3P_2$	E1	1.646E-01	1.678E-01
35 - 32	$2s2p^63d\ ^3D_2 - 2s2p^63p\ ^3P_2$	M2	1.132E-10	1.136E-10
36 - 32	$2s2p^63d\ ^3D_3 - 2s2p^63p\ ^3P_2$	E1	9.346E-01	9.525E-01
36 - 32	$2s2p^63d\ ^3D_3 - 2s2p^63p\ ^3P_2$	M2	1.270E-09	1.273E-09
37 - 32	$2s2p^63d\ ^1D_2 - 2s2p^63p\ ^3P_2$	M2	3.199E-10	3.220E-10
34 - 33	$2s2p^63d\ ^3D_1 - 2s2p^63p\ ^1P_1$	E1	1.741E-02	1.702E-02
34 - 33	$2s2p^63d\ ^3D_1 - 2s2p^63p\ ^1P_1$	M2	1.105E-12	1.158E-12
35 - 33	$2s2p^63d\ ^3D_2 - 2s2p^63p\ ^1P_1$	E1	3.738E-02	3.635E-02
35 - 33	$2s2p^63d\ ^3D_2 - 2s2p^63p\ ^1P_1$	M2	1.591E-10	1.571E-10
36 - 33	$2s2p^63d\ ^3D_3 - 2s2p^63p\ ^1P_1$	M2	3.336E-10	3.363E-10
37 - 33	$2s2p^63d\ ^1D_2 - 2s2p^63p\ ^1P_1$	E1	6.654E-01	6.820E-01
37 - 33	$2s2p^63d\ ^1D_2 - 2s2p^63p\ ^1P_1$	M2	5.129E-10	5.112E-10
35 - 34	$2s2p^63d\ ^3D_2 - 2s2p^63d\ ^3D_1$	M1	2.061E-07	2.084E-07

Table 5 *continued*

Table 5 (*continued*)

$j - i$	Transition	Type	gf			
			MBPT ^a	MCDHF/RCI ^b	MCDHF/RCI2 ^c	NIST ^d
35 – 34	$2s2p^63d\ ^3D_2 - 2s2p^63d\ ^3D_1$	E2	1.875E–14	1.888E–14
36 – 35	$2s2p^63d\ ^3D_3 - 2s2p^63d\ ^3D_2$	M1	4.094E–07	4.148E–07
36 – 35	$2s2p^63d\ ^3D_3 - 2s2p^63d\ ^3D_2$	E2	1.512E–13	1.531E–13

^aThe present MBPT oscillator strengths.

^bThe present MCDHF/RCI oscillator strengths.

^cThe MCDHF/RCI oscillator strengths given by Jönsson et al. (2014).

^dThe oscillator strengths recommended by the NIST ASD.